

# **Finite Element Analysis to Study the Magnetic Normal Force in Ball End Type Magnetorheological Finishing Process**

*A Dissertation Submitted*  
In Partial Fulfillment of the Requirements  
for the Degree of

**Master of Engineering**  
in  
**Production and Industrial**

by

**Manpreet Sharma**



*to the*

**MECHANICAL ENGINEERING DEPARTMENT  
THAPAR UNIVERSITY, PATIALA**

July, 2015

# CERTIFICATE

I hereby declare that the thesis entitled “**Finite Element Analysis to Study the Magnetic Normal Force in Ball End Type Magnetorheological Finishing Process**” is an authentic record of my study carried out as requirements for the award of the degree of **Master of Engineering in Production and Industrial** at **Thapar University, Patiala** under the supervision of **Dr. Anant Kumar Singh**, Assistant Professor, Mechanical Engineering Department, Thapar University, Patiala during July, 2015. The matter embodied in this report has not been submitted in partial or full to any other university or institute for the award of any degree.

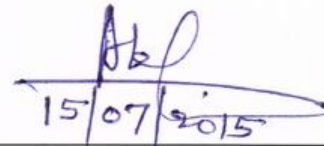
Date: 14/07/2015



**Manpreet Sharma**

Roll no. - 821182003

It is certified that the above statement made by the student is correct to the best of my/our knowledge and belief.



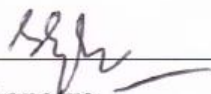
**Dr. Anant Kumar Singh**

Assistant Professor

Mechanical Engineering Department

Thapar University, Patiala - 14700

Countersigned by



**Dr. S. K. Mohapatra**

Sr. Professor & Head

Mechanical Engineering Department



**Dr. S.S. Bhatia**

Dean of Academic Affairs

Thapar University, Patiala - 147004

# Acknowledgements

I am highly grateful to the authorities of Thapar University, Patiala for providing this opportunity to carry out the report work.

I would like to express a deep sense of gratitude and thank profusely to my thesis guides **Dr. Anant Kumar Singh** for their sincere & invaluable guidance and suggestions which inspired me to submit thesis report in the present form.

I would also like to thank all the faculty members of Mechanical engineering department for their intellectual support and unyielding encouragement.

I am deeply indebted to all my friends who helped me with their encouragement, ample morale support and valuable suggestions.

Finally, I would like to extend my gratitude to all those persons who directly or indirectly helped me in the process and contributed towards this phase of my report work.

Manpreet Sharma

# Abstract

The developed ball end type magnetorheological finishing process has the advantage to finish a 3D complex shaped surface. The number of carbonyl iron particle chains per active abrasives on the surface of workpiece has been studied. The arrangement of carbonyl iron particles with active abrasives on the surface of workpiece along ball end type magnetorheological finishing tool with hollow core and solid core have been modeled using Maxwell Ansoft V13 (student version). Further, the finite element simulation to find the magnetic normal force on the active particles were carried out during ball end type magnetorheological finishing process having tool with hollow core and solid core. Effects of magnetically induced normal force on the active abrasive particles on workpiece surfaces for ball end type magnetorheological finishing tool with hollow core and solid core has been analyzed by varying the parameters like magnetizing current, working gap and position of electromagnet coil. The performance of both the cases such as tool with hollow core and solid core has been verified. It has been seen that in case of solid core tool the magnitude of magnetically induced normal force on the active abrasive particles with same parameters like working gap, magnetizing current and distance of coil from tool tip surface was found more as compared to hollow core tool. Therefore in case of tool with solid core, the better bonding between carbonyl iron particles along with active abrasives can be achieved even with low magnetizing current during the finishing of workpiece surfaces.

# Contents

<b>List of figures</b>	1
<b>List of tables</b>	5
<b>List of Nomenclature</b>	7
<b>1. Introduction</b>	8
1.1 Introduction	8
1.2 Traditional finishing processes	8
1.2.1 Grinding	8
1.2.2 Lapping	9
1.2.3 Honing	9
1.2.4 Polishing and buffing	10
1.2.5 Super finishing	10
1.3 Advanced finishing processes	11
1.3.1 Abrasive flow machining	11
1.3.2 Magnetorheological finishing	12
1.3.3 Magnetorheological abrasive flow finishing	13
1.3.4 Ball end magnetorheological finishing process	14
1.4 Applications of advance finishing process	14
<b>2. Literature Review</b>	15
2.1 Literature review	15
2.2 Research gap	17
2.3 Objective of the present work	17
2.4 Methodology	18
<b>3. Finite Element Analysis of for effect of CIP chain on the workpiece</b>	19
3.1 Maxwell Ansoft software	19
3.1.1 Maxwell - solution type	19
3.1.2 Setting up design	20
3.2 Formation of CIP chain	22
3.2.1 Number of CIP chains in working gap	23
3.2.2 Number of CIP chains per abrasive	24
3.3 Modeling of BEMRF hollow core tool by using Maxwell Ansoft V13	24
3.4 FE analysis for BEMRF hollow core tool	25

3.4.1 Coil distance 45 mm and gap is 0.66 mm, while varying the current	27
3.4.2 Coil distance 45 mm and gap is 1.5 mm, while varying the current	28
3.4.3 Coil distance 45 mm and gap is 2.34 mm, while varying the current	30
3.4.4 Coil distance 50 mm and gap is 0.66 mm, while varying the current	32
3.4.5 Coil distance 50 mm and gap is 1.5 mm, while varying the current	34
3.4.6 Coil distance 50 mm and gap is 2.34 mm, while varying the current	36
3.4.7 Coil distance 55 mm and gap is 0.66 mm, while varying the current	38
3.4.8 Coil distance 55 mm and gap is 1.5 mm, while varying the current	40
3.4.9 Coil distance 55 mm and gap is 2.34 mm, while varying the current	42
3.4.10 Coil distance 60 mm and gap is 0.66 mm, while varying the current	44
3.4.11 Coil distance 60 mm and gap is 1.5 mm, while varying the current	46
3.4.12 Coil distance 60 mm and gap is 2.34 mm, while varying the current	48
3.4.13 Coil distance 65 mm and gap is 0.66 mm, while varying the current	50
3.4.14 Coil distance 65 mm and gap is 1.5 mm, while varying the current	52
3.4.15 Coil distance 65 mm and gap is 2.34 mm, while varying the current	54
3.5 Modeling of BEMRF solid core tool by using Maxwell Ansoft V13	57
3.6 FE analysis for BEMRF solid core tool	58
3.6.1 Coil distance 45 mm and gap is 0.66 mm, while varying the current	59
3.6.2 Coil distance 45 mm and gap is 1.5 mm, while varying the current	60
3.6.3 Coil distance 45 mm and gap is 2.34 mm, while varying the current	62
3.6.4 Coil distance 50 mm and gap is 0.66 mm, while varying the current	64
3.6.5 Coil distance 50 mm and gap is 1.5 mm, while varying the current	66
3.6.6 Coil distance 50 mm and gap is 2.34 mm, while varying the current	68
3.7 Results and discussion	70
3.7.1 Effect of working gap variation	71
3.7.2 Effect of current variation	72
3.7.3 Effect of coil position variation	72
3.8 Validation of magnetic normal forces	77
<b>4. Conclusions and future scope</b>	<b>78</b>
4.1 Conclusions	78
4.2 Future scope	78
<b>References</b>	<b>79</b>

# List of Figures

Figure 1.1	Grinding process	8
Figure 1.2	Lapping process	9
Figure 1.3	Honing process	9
Figure 1.4	Buffing machine	10
Figure 1.5	Schematic diagram of the super finishing process	11
Figure 1.6	Experimental setup of abrasive flow machining	12
Figure 1.7	A Vertical MRF Machine	13
Figure 1.8	Magnetorheological Abrasive Flow Finishing Process	13
Figure 1.9	Photograph of (a) an experimental set-up and (b) MR polishing (MRP) fluid delivery system	14
Figure 3.1	Modeling of a ball end type magnetorheological tool	21
Figure 3.2	MRP fluid layer in working gap	23
Figure 3.3	Electromagnetic model of core with central hole	25
Figure 3.4	CIP chain arrangement	25
Figure 3.5	FE simulation of the BEMRF hollow core tool of 45 mm coil distance and 0.66 mm with varying Current	27
Figure 3.6	Result analysis of force v/s current at 0.66 mm gap and 45mm coil Distance	28
Figure 3.7	FE simulation of the BEMRF hollow core tool of 45 mm coil distance and 1.5 mm with varying Current	29
Figure 3.8	Result analysis of force v/s current at 1.5 mm gap and 45mm coil distance	30
Figure 3.9	FE simulation of the BEMRF hollow core tool of 45 mm coil distance and 2.34 mm with varying Current	31
Figure 3.10	Result analysis of force v/s current at 2.34 mm gap and 45mm coil Distance	32
Figure 3.11	FE simulation of the BEMRF hollow core tool of 50 mm coil distance and 0.66 mm with varying Current	33
Figure 3.12	Result analysis of force v/s current at 0.66 mm gap and 50 mm coil distance	34

Figure 3.13	FE simulation of the BEMRF hollow core tool of 50 mm coil distance and 1.5 mm with varying Current	35
Figure 3.14	Result analysis of force v/s current at 1.5 mm gap and 50 mm distance	36
Figure 3.15	FE simulation of the BEMRF hollow core tool of 50 mm coil distance and 2.34 mm with varying Current	37
Figure 3.16	Result analysis of force v/s current at 2.34 mm gap and 50 mm coil distance	38
Figure 3.17	FE simulation of the BEMRF hollow core tool of 55 mm coil distance and 0.66 mm with varying Current	39
Figure 3.18	Result analysis of force v/s current at 0.66 mm gap and 55 mm coil distance	40
Figure 3.19	FE simulation of the BEMRF hollow core tool of 55 mm coil distance and 1.5 mm with varying Current	41
Figure 3.20	Result analysis of force v/s current at 1.5 mm gap and 55 mm coil distance	42
Figure 3.21	FE simulation of the BEMRF hollow core tool of 55 mm coil distance and 2.34 mm with varying Current	43
Figure 3.22	Result analysis of force v/s current at 2.34 mm gap and 55 mm coil distance	44
Figure 3.23	FE simulation of the BEMRF hollow core tool of 60 mm coil distance and 0.66 mm with Current density (a) 1 amp (b) 2 amp (c) 3 amp (d) 4 amp (e) 5 amp	45
Figure 3.24	Result analysis of force v/s current at 0.66 mm gap and 60 mm coil distance	46
Figure 3.25	FE simulation of the BEMRF hollow core tool of 60 mm coil distance and 1.5 mm with varying Current	47
Figure 3.26	Result analysis of force v/s current at 1.5 mm gap and 60 mm coil distance	48
Figure 3.27	FE simulation of the BEMRF hollow core tool of 60 mm coil distance and 2.34 mm with varying Current	49
Figure 3.28	Result analysis of force v/s current at 2.34 mm gap and 60 mm coil distance	50
Figure 3.29	FE simulation of the BEMRF hollow core tool of 65 mm coil distance	51

	and 0.66 mm with varying Current	
Figure 3.30	Result analysis of force v/s current at 0.66 mm gap and 65 mm coil distance	52
Figure 3.31	FE simulation of the BEMRF hollow core tool of 65 mm coil distance and 1.5 mm with varying Current	53
Figure 3.32	Result analysis of force v/s current at 1.5 mm gap and 65 mm coil distance	54
Figure 3.33	FE simulation of the BEMRF hollow core tool of 65 mm coil distance and 2.34 mm with varying Current	55
Figure 3.34	Result analysis of force v/s current at 2.34 mm gap and 65 mm coil distance	56
Figure 3.35	Electromagnet model of BEMRF solid core tool	57
Figure 3.36	CIP chain arrangement in working gap with solid core tool	58
Figure 3.37	FE simulation of the BEMRF solid core tool of 45 mm coil distance and 0.66 mm with varying Current	59
Figure 3.38	Result analysis of force v/s current at 0.66 mm gap and 45 mm coil distance in solid core	60
Figure 3.39	FE simulation of the BEMRF solid core tool of 45 mm coil distance and 1.5 mm with varying Current	61
Figure 3.40	Result analysis of force v/s current at 1.5 mm gap and 45 mm coil distance in solid core	62
Figure 3.41	FE simulation of the BEMRF solid core tool of 45 mm coil distance and 2.34 mm with varying Current	63
Figure 3.42	Result analysis of force v/s current at 2.34 mm gap and 45 mm coil distance in solid core	64
Figure 3.43	FE simulation of the BEMRF solid core tool of 50 mm coil distance and 0.66 mm with varying Current	65
Figure 3.44	Result analysis of force v/s current at 0.66 mm gap and 50 mm coil distance in solid core	66
Figure 3.45	FE simulation of the BEMRF solid core tool of 50 mm coil distance and 1.5 mm with varying Current	67
Figure 3.46	Result analysis of force v/s current at 1.5 mm gap and 50 mm coil distance in solid core	68

Figure 3.47	FE simulation of the BEMRF solid core tool of 50 mm coil distance and 2.34 mm with varying Current	69
Figure 3.48	Result analysis of force v/s current at 2.34 mm gap and 50 mm coil distance in solid core	70
Figure 3.49	Result analysis of force by variation in working gap at constant current and coil position	71
Figure 3.50	Result analysis of force by variation in current at constant working gap and coil position	72
Figure 3.51	Result analysis of force by variation in coil position at 0.66 mm working gap	73
Figure 3.52	Result analysis of force by variation in coil position at 1.5 mm working gap	74
Figure 3.53	Result analysis of force by variation in coil position at 2.34 mm working gap	75
Figure 3.54	Result analysis of force by use of solid core tool at 0.66 mm working gap	76

# List of Tables

Table 3.1	Result analysis of forces at different magnetizing current with 0.66 mm gap and 45mm coil distance	28
Table 3.2	Result analysis of forces at different magnetizing current with 1.5 mm gap and 45mm coil distance	30
Table 3.3	Result analysis of forces at different magnetizing current with 2.34 mm gap and 45mm coil distance	32
Table 3.4	Result analysis of forces at different magnetizing current with 0.66 mm gap and 50 mm coil distance	34
Table 3.5	Result analysis of forces at different magnetizing current with 1.5 mm gap and 50 mm coil distance	36
Table 3.6	Result analysis of forces at different magnetizing current with 2.34 mm gap and 50 mm coil distance	38
Table 3.7	Result analysis of forces at different magnetizing current with 0.66 mm gap and 55 mm coil distance	40
Table 3.8	Result analysis of forces at different magnetizing current with 1.5 mm gap and 55 mm coil distance	42
Table 3.9	Result analysis of forces at different magnetizing current with 2.34 mm gap and 55 mm coil distance	44
Table 3.10	Result analysis of forces at different magnetizing current with 0.66 mm gap and 60 mm coil distance	46
Table 3.11	Result analysis of forces at different magnetizing current with 1.5 mm gap and 60 mm coil distance	48
Table 3.12	Result analysis of forces at different magnetizing current with 2.34 mm gap and 60 mm coil distance	50
Table 3.13	Result analysis of forces at different magnetizing current with 0.66 mm gap and 65 mm coil distance	52
Table 3.14	Result analysis of forces at different magnetizing current with 1.5 mm gap and 65 mm coil distance	54
Table 3.15	Result analysis of forces at different magnetizing current with 2.34 mm gap and 65 mm coil distance	56
Table 3.16	Result analysis of forces at different magnetizing current with 0.66 mm gap and 70 mm coil distance	60

	mm gap and 45 mm coil distance in solid core	
Table 3.17	Result analysis of forces at different magnetizing current with 1.5 mm gap and 45 mm coil distance in solid core	62
Table 3.18	Result analysis of forces at different magnetizing current with 2.34 mm gap and 45 mm coil distance in solid core	64
Table 3.19	Result analysis of forces at different magnetizing current with 0.66 mm gap and 50 mm coil distance in solid core	66
Table 3.20	Result analysis of forces at different magnetizing current with 1.5 mm gap and 50 mm coil distance in solid core	68
Table 3.21	Result analysis of forces at different magnetizing current with 2.34 mm gap and 50 mm coil distance in solid core	70
Table 3.22	Comparison of electromagnetic forces by variation of working gap at constant magnetizing current and coil position	71
Table 3.23	Comparison of electromagnetic forces by variation of magnetizing current at constant working gap and coil position	72
Table 3.24	Effect on electromagnetic forces by variation of coil distance at 0.66 mm working gap	73
Table 3.25	Effect on electromagnetic forces by variation of coil distance at 1.5 mm working gap	74
Table 3.26	Effect on electromagnetic forces by variation of coil distance at 2.34 mm working gap	75
Table 3.27	Effect on electromagnetic forces by using solid core tool of coil distance at 0.66 mm working gap	76
Table 3.28	Validation of induced magnetic normal forces on the workpiece surface with recorded calculated magnetic normal forces	77
Table 3.29	Validation of induced magnetic normal forces on the workpiece surface with recorded experimental magnetic normal forces	77

# Nomenclature

A	Area of flux path in m <sup>2</sup>
D	Length of variable working gap in mm
d	Diameter of MRP fluid in working in mm
V	Volume of flux in working gap mm <sup>3</sup>
N <sub>iron</sub>	Number of CIP in volume V
N <sub>iron(chain)</sub>	Number of CIP in one chain
N <sub>AAB</sub>	Number of active abrasive particles

# Abbreviations

MRF	Magnetorheological finishing
CIP	Carbonyl iron particle
MR	Magnetorheological
MRP	Magnetorheological polishing
DC	Direct current
MRAFF	Magnetorheological abrasive flow finishing
AFM	Abrasive flow machining
3D	Three dimensional
BEMRF	Ball end magnetorheological finishing

# CHAPTER -1

## INTRODUCTION

---

### 1.1 Introduction

Surface finishing is a wide range of manufacturing processes that modify the surface of a manufactured item to attain a certain property. The main aim of finishing processes are to reduce surface friction, better sealing capability, better compatibility with other surfaces, to attain press fit requirements, to achieve consistent thickness and remove burs.

### 1.2 Traditional finishing processes

These processes have been utilized from the initial times because of their ability to produce smooth surface at close tolerances. These processes utilize multipoint cutting edges in the form of abrasives, to do cutting action.

#### 1.2.1 Grinding

In grinding the relative action of grinding wheel removed the material from the work piece surface. There are abrasive particles surrounded on the outside edge of grinding wheel which take part in material removal. The abrasive particles are bonded together to form absorbent rotating body, which perform the material removal (Shaw, 1996). The significant parameter is abrasive grin size. For better finish small gain size abrasive required.

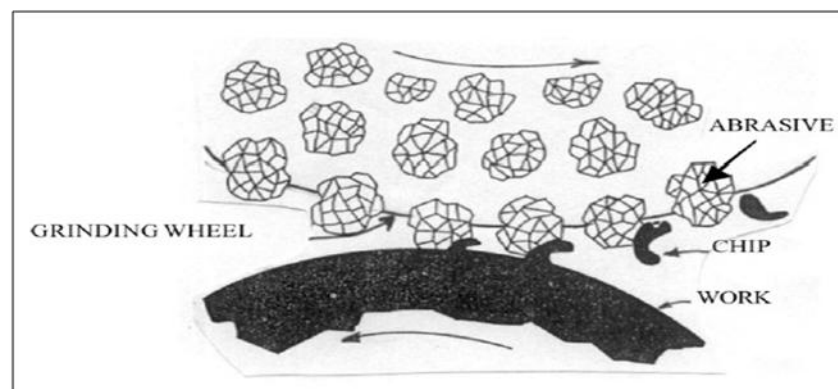


Figure 1.1: Grinding process (Jain, 2009)

## 1.2.2 Lapping

In this process finish is done by loss abrasive particles. The abrasive slurry is introduced between work piece and lap surface and the work piece is apprehended against lap. After that the work piece moved in arbitrary paths with pressure. This process is used for more accuracy and material removal rate is insignificant.

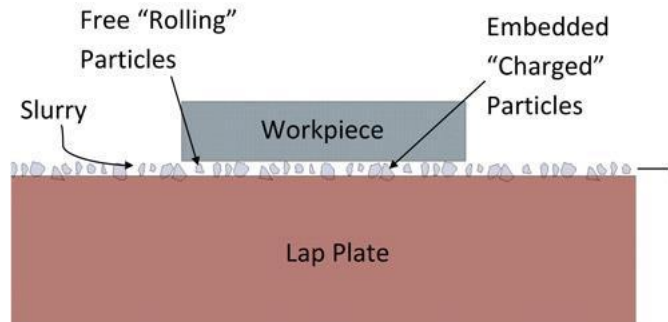


Figure 1.2: Lapping process

([http://d2n4wb9orp1vta.cloudfront.net/resources/images/cdn/cms/DiamondLapping\\_a.jpg](http://d2n4wb9orp1vta.cloudfront.net/resources/images/cdn/cms/DiamondLapping_a.jpg))

## 1.2.3 Honing

For finishing of internal cylindrical surface this process is used. In honing process workpiece is stationary but tool has rotary and reciprocating motion. The abrasive sticks which are fitted on the outside edge of honing tool (Schey, 1987). The pressure of abrasive sticks against the work piece is controlled by use of springs. Unit pressure, honing speed and time are affecting the material removal rate and quality of finishing.



Figure 1.3: Honing Process

([http://www.ohiotoolworks.com/upload/images/products/Horizontal\\_Machines/OTW-3000\\_Bore\\_\\_Tool\\_Grey.jpg](http://www.ohiotoolworks.com/upload/images/products/Horizontal_Machines/OTW-3000_Bore__Tool_Grey.jpg))

## 1.2.4 Polishing and Buffing

- Polishing: To remove the burrs from machined surface, Polishing is used. This process is used to build up a very smooth surface. The outer edge of polishing wheel is glued with abrasive grains (Schey, 1987). The uneven shapes and deep recesses are complicated to polish.
- Buffing: In this process revolving wheel consist of cloth buffing. Very fine abrasive has been charged on the wheel and work is brought in contact with it. The application of this process is in automotive industry, sport items, furniture and utensils. The luster by this finishing process is very high.

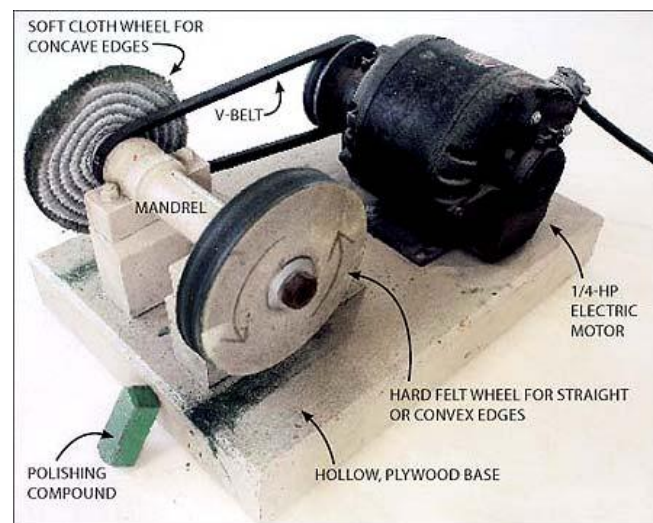


Figure 1.4: Buffing machine

(<http://canadianhomeworkshop.com/files/2011/10/buffingwheeldiagram.jpg>)

## 1.2.5 Super finishing

In super finishing a single stick of abrasive is used to complete finishing operation. The tool reciprocates higher frequency and smaller amplitudes. For cooling and cleaning function cutting fluid is used. Aluminium oxide abrasives are generally used for steel and silicon carbide for non-ferrous metals (Lepadatescu, 1998). Super finishing leaves a strongly controlled cross-hatch model. In this process stone oscillate with pressure on rotary workpiece.

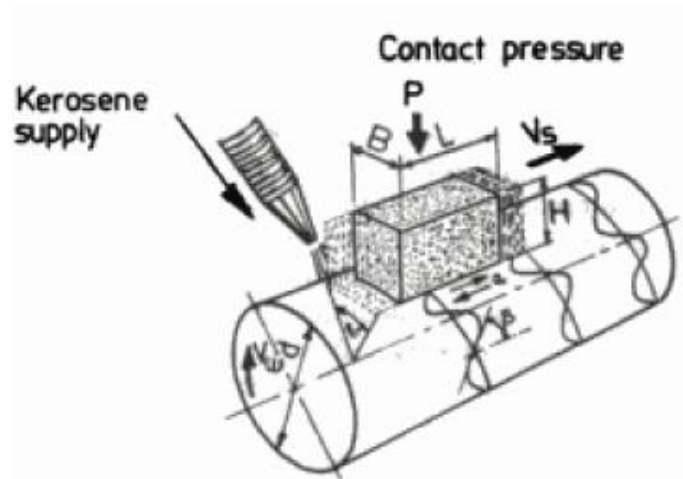


Figure 1.5: Schematics of the super finishing process  
 (<http://www.wseas.us/e-library/conferences/2009/cambridge/SEPADS/SEPADS09.pdf>)

### 1.3 Advanced finishing processes

The traditional finishing processes are not capable to produce ultra-fine surface roughness value due to lesser control over the abrading forces. A large amount of heat is generated during the traditional processes which results in the failure of the material. The different types of advanced finishing process have been developed in order to produces a ultra-fine surface roughness values with the better control over the forces. Some of the advanced finishing processes have been discussed as follows:

#### 1.3.1 Abrasive Flow Machining (AFM)

Abrasive flow machining process was developed in 1960s by means of an abrasive viscoplastic polymer. In this process the main considerable factor is viscosity of polymeric intermediate. Material removal rate depends upon variation in the rheological characteristics of medium (Jain, 2008). In this setup there are two vertically opposed cylinders, which extrude an abrasive intermediate reverse and forward through passage created by the workpiece and tooling. Material removal occurs when the intermediate passes through the restrictive way. The application of this process is to finish the complicated surfaces.

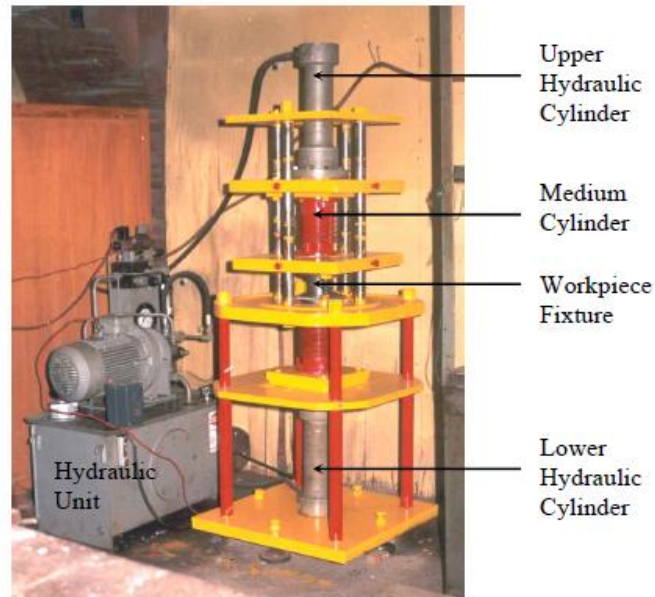


Figure 1.6: Experimental setup of abrasive flow machining (Rhodes, 1988)

### 1.3.2 Magnetorheological Finishing (MRF)

This process is used for finishing of a flat, convex or concave workpiece surface. In this process MR fluid is used to finishing of surfaces. MR fluid contains micro sized carbonyl iron particles, abrasives and nonmagnetic oil. By application of magnetic field, MR fluid gets stiffened due to magnetizing properties of CIP chains and finishing spot is formed between the working gap (Jain, 2008). Surface finishing takes place during the shear stress produced as the magnetorheological polishing ribbon is dragged into the working gap among the workpiece and carrier surface. Position of workpiece is above a rotating wheel that supports and carries a layer of magnetorheological fluid. There is a DC electromagnet below the rotating wheel surface which is used to produce magnetic field. Due to magnetic field the fluid get stiffened before it comes in contact with workpiece.

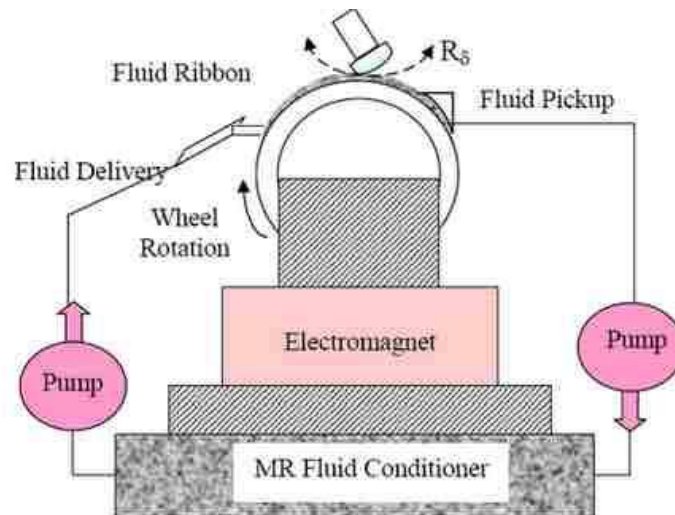


Figure 1.7: A Vertical MRF Machine (<http://www.opticam.rochester.edu>)

### 1.3.3 Magnetorheological Abrasive Flow Finishing (MRAFF)

In this process forces depend on rheological characteristics of fluid and difficult to control by external means. This process has properties of both MRF process as well as AFM process. In MRAFF process magnetically stiffened slugs of fluid is extruded forward and reverse throughout the way formed by workpiece and fixture (Jha and Jain, 2004). Material removal occurs at that points where magnetic field is applied. Magnetic field strength depends on the viscosity of fluid. More magnetic field strength results better surface finish. CIP chains maintain on holding abrasives more positively with good magnetic strength. This method has ability of finishing complex internal geometries up to nanometer level.

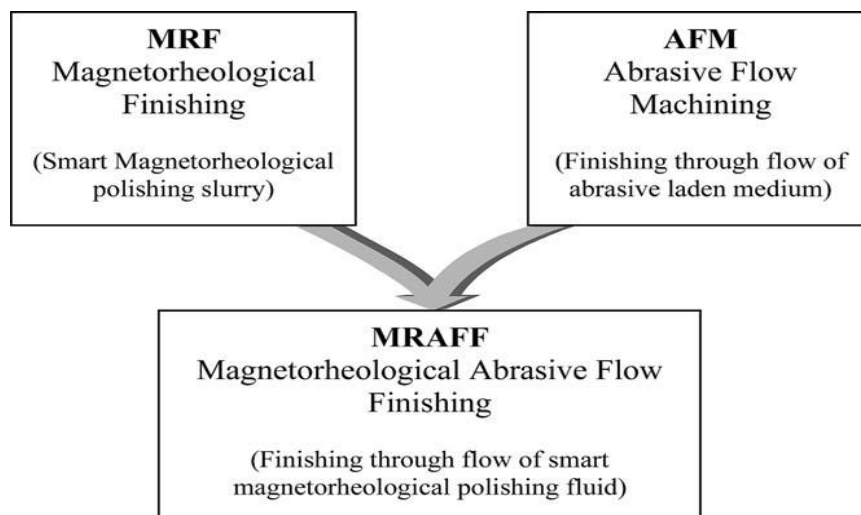


Figure 1.8: Magnetorheological Abrasive Flow Finishing Process (Jha and Jain, 2004)

### 1.3.4 Ball end magnetorheological finishing

Ball end magnetorheological finishing process is used to finish 3D complex surfaces. A tool is used to flow the MR fluid through the central hole of the rotating core. MR fluid takes form of a ball end shape when it becomes stiffened. This ball end of controlled size and shape is used as a finishing medium. Computer controlled 3-axes motion guiding it to follow the surface to be finished. Electromagnetic forces make MR fluid stiff at tip surface of the tool whose physical shape was found like a ball end (Singh et. al 2013). CIP chains are used to closely surround the nonmagnetic abrasive particles. The active abrasives are responsible for the material removal during the finishing process. MR fluid becomes stiffer when magnetic flux density increase at the tool tip and produces high magnetic forces on abrasive particles which result in more wear out from surface.

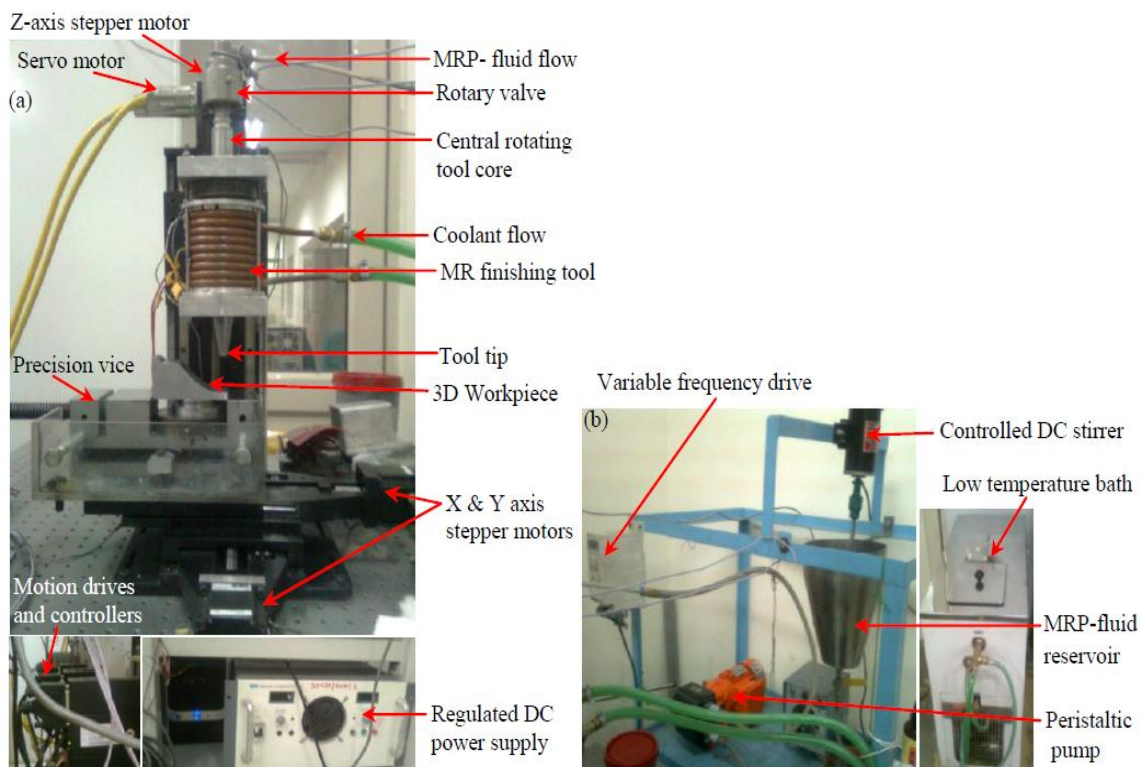


Figure 1.9: Photograph of (a) an experimental set-up and (b) MR polishing (MRP) fluid delivery system (Singh et. al 2013)

## 1.4 Application of magnetorheological finishing

- Medical industries
- Optical industries
- Aerospace and automobile industries

# CHAPTER -2

## Literature Review

---

### 2.1 Literature Review

Finishing processes are developed as per the necessity of surface finishing at various level and applications. Finishing processes have been developed from traditional to advance finishing processes. To overcome the disabilities of traditional finishing processes, the advanced finishing processes have been developed in order to produces a ultra fine surface roughness values with the better control over the forces.

**Jha and Jain (2004)** developed magnetorheological abrasive flow finishing to finish complicated internal geometries. This process gives a better control over rheological characteristics of abrasive in magnetorheological fluid. A Hydraulically powered experimental setup was designed to study the process characteristics and performance. Experiments were conducted on stainless steel workpiece at different magnetic field strength to observe its effect on final surface finish. No measureable change in surface roughness was observed after finishing at zero magnetic fields.

**Jha and Jain (2006)** discussed that material removal rate depends upon the forces acting on abrasive particles due to magnetizing of carbonyl iron particles (CIP) due to external magnetic field. Experiments were performed on steel workpiece with special combinations of CIP and Sic particles in magnetorheological fluid. The value of acting forces on abrasive particles was calculated.

**Sadiq and Shunmugam (2009)** design and improvement of magnetorheological abrasive honing arrangement were done. Experiments were performed with aluminum workpiece to know the result of magnetic field. Better finish was achieved for rougher surface and higher revolving speed of workpiece.

**Sadiq and Shunmugam (2010)** performed FE analysis of magnetic field developed by using Ansys software. Results have been cross checked with actual measurements. Prediction about final roughness value was main aim for simulation. Simulation results by variation of

important variables like different work materials, magnetic flux density, rotation of work piece and procedure timings that were better conformity with experimental results.

**Sidpara and Jain (2011)** record forces acting on workpiece by use of dynamometer and virtual instrumentation. Planning of experiments done by ANOVA and compare the forces and process parameters. The most significant parameter was working gap, second important factor was CIP concentration while the least role was noted by the wheel speed.

**Hong et al. (2012)** performed their experiment on MR polishing for finishing of alumina reinforced zircon ceramics (3YTZP/Al<sub>2</sub>O<sub>3</sub>-20%). The finishing was carried out with MR fluid (50% CIPs, abrasive diamond particles and DI water). The main process parameters (speed- 200 and 300 RPM, magnetic field- 3.8, 4.7, 5.5 and 6.1KA/m, Time- 10, 20, 40 and 60 min). The results concluded that with 300 RPM, magnetic field- 3.8 KA/m and electric current- 0.5 Amp the surface roughness decreases from 0.272  $\mu\text{m}$  to 1.960 nm.

**Singh et al. (2012)** evaluated surface finishing of complex 3D surfaces by using BEMRF process. To study the consequence of number of finishing passes on final results, experiments were done on at dissimilar angles of projection like flat, 30 deg and 45 deg. To study the magnetic flux density the finite element analysis (FE) was also done. The results were found as 16.6 nm, 30.4 nm, 71 nm in order on flat, 30 deg, 45 deg for 60 passes of finishing.

**Judal et al. (2013)** developed a new vibration dependent magnetic abrasive finishing process for finishing of aluminum workpiece. The finishing was carried out with the help of steel grit and Al<sub>2</sub>O<sub>3</sub> abrasive. The effect of different process parameters such as rotational speed, frequency, magnetic flux density and size of abrasive particles on material removal rate was investigated. The result concluded that with the increase in rotation speed and magnetic flux density and frequency of vibration, the value of material removal rate increases. The surface roughness value Ra reduces to 0.18  $\mu\text{m}$ .

**Singh et al. (2013)** developed the mathematical modeling of magnetic normal force for ball end type magnetorheological finishing and compared the results of mathematical modeling with experimental results. The effect of difference in magnetic normal force was also compared with change in roughness during experiments.

**Sidpara and Jain (2013)** performed an experiment to measure the forces on the freeform surface in real time. The angles of curvature of the workpiece, rotational speed of the tool and feed rate on normal, tangential and axial forces which are the parameters of the process were given by the researchers. It was found that the normal force was more dominant as compared to other forces. Model of normal force and tangential force acting on the workpiece was also proposed to improve the understanding of the workpiece abrasive particles interaction in the MR polishing fluid which was based on finishing process. Theoretical and experimental results were carried out and compared to validate the proposed models.

**Gheisari et al. (2014)** developed a magnetorheological finishing method for ultra precision finishing of Aluminium work material (cylindrical type). The MR fluid consists of water based suspension of micron sized diamond particles. The process parameters were (current- 9A and working gap- 5 mm). The initial surface roughness of the work material was 170 nm.. The results concluded that with the increase in rotational speed (1000 rpm), the surface roughness value improves by 40 nm. With the increase in finishing time (90 min), the surface roughness value decreases to 42 nm whereas, when the fast RAM (with 0.5 m/sec) was applied, the surface roughness value improves by 78 nm.

## **2.2 Research Gap**

In available literature, researchers had done work to study the ball end magnetorheological finishing process. The mathematically modeling of magnetically induced average normal force had been also done to study their effect in change of surface roughness during finishing operation. But, it has been found that some analysis related to magnetic normal force acting on abrasives particles during finishing operation in ball end magnetorheological finishing process with hollow core tool and solid core tool still have not been reported. Therefore, this has been taken as motivation for the present work.

## **2.3 Objectives of the present work**

To develop the electromagnetic model of ball end magnetorheological tool with hollow core and solid core using the Maxwell Ansoft V13 software (student version).

- To study the number of carbonyl iron particles (CIPs) chains formation per active abrasives on the workpiece surface.

- To develop the electromagnetic model of carbonyl iron particles with active abrasives on the ferromagnetic workpiece surface under the effect of magnetic flux density at the tool tip surface.
- To study the effect of magnetostatic finite element simulation results of magnetically induced normal force on the active abrasives during the finishing of workpiece surfaces using ball end type magnetorheological finishing tool with hollow core and solid core by varying the magnetizing currents, working gaps and distance of coil from tool tip surfaces.
- To compare the effect of magnetically induced normal force on the active abrasive particles in the case of ball end type magnetorheological finishing tool with hollow core and solid core.

## **2.4 Methodology**

- To model and finite element analysis of ball end type magnetorheological finishing tool with hollow core and solid core, Maxwell Ansoft V13 (student version) would be used.
- With the help of different magnetic field concepts and MR fluid, formation of number of CIP chain on the workpiece surface would be studied.
- For study the effect of number of CIP chain on the work piece surface, magneto static simulation of developed model will be carried out.
- For study the effect of number of CIP chain on the work piece surface, the position of coil, amount of current and gap will be varied.
- Compare the results of magnetostatic simulation of magnetically induced normal force for both hollow core tool and solid core tool.
- From finite element analysis, the simulated results of the effect of magnetic normal force on the workpiece surface would be validate with already reported results.

# CHAPTER-3

## Finite Element Analysis of Magnetic Normal Force on the active abrasives acting on workpiece surfaces in Ball End Type Magnetorheological Finishing Process

---

Ball end type magnetorheological finishing process is used to finish 3D and flat surfaces with the help of MR fluid. In this process fluid is allow to flow through the central hole of rotating core. MR fluid takes form of a ball end shape when it becomes stiffened. This ball end of controlled size and shape is used as a finishing medium. Computer controlled 3-axes motion guiding it to follow the surface to be finished. Electromagnetic forces make MR fluid stiff at tip surface of the tool whose physical shape was found like a ball end. CIP chains are used to closely surround the nonmagnetic abrasive particles. The active abrasives are responsible for the material removal during the finishing process. MR fluid becomes stiffer when magnetic flux density increase at the tool tip and produces high magnetic forces on abrasive particles which result in more wear out from surface (Singh *et. al* 2013).

In this chapter, Maxwell ANSOFT V13 software is used for analysis of effect of number of CIP chain on the work piece surface in ball end magnetorheological finishing process by variation in coil position, current density and gap in both hollow core and solid core tool.

### 3.1 Ansoft Maxwell V13 Software (student version)

Maxwell is an interactive software package that uses finite element analysis (FEA) to simulate electromagnetic field problems. Maxwell integrates with other Ansoft software packages to perform complex tasks while remaining simple to use. Modelling and Simulation of the tool is done in MAXWELL ANSOFT V13 software. Variations in position of coil, current density and gap are made to analysis the effect of CIP chain on work piece surface.

#### 3.1.1 Maxwell - Solution Type:

- **Magnetostatic:** Static magnetic fields, forces, torques and inductances caused by DC currents, static external magnetic fields and permanent magnets. Linear or nonlinear materials.

- **Eddy Current:** Sinusoidally-varying magnetic fields, forces, torques and impedances caused by AC currents and oscillating external magnetic fields.
- **Transient Magnetic :** Transient magnetic fields caused by permanent magnets, conductors and windings supplied by voltage and/or current sources with arbitrary variation as functions of time, rotation or translation effects can be included in the simulation.
- **Electrostatic:** Electrostatic fields caused by user specified distribution of voltages and charges.
- **Electric Field:** Electric field in conductors characterized by a spatial distribution of voltage, electric current density.

### 3.1.2 Setting up Design:

In Ansoft Maxwell software the following order is recommended:

- **Setting Up Design :**
  - **Open and save a new Project :**

A project is a collection of one or more designs that is saved in a single \*.mxwl file. Open Maxwell, add a new design and save the default project with a new name.

    - (a) Double-click the Maxwell icon on your desktop to open the software.
    - (b) Click Project>Insert Maxwell Design.
    - (c) Click File>Save As.
    - (d) Type File name and click Save.
  - **Specify a Solution Type :**

There are multiple types of Maxwell solutions are possible to choose from depending on the specific application.

    - (a) Click Maxwell>Solution Type from the menu. The Solution Type dialog box appears.
    - (b) Select the solution as per your application.
    - (c) Click OK.
  - **Set the Drawing Units :**
    - (a) Click Modeler>Units.
    - (b) Select mm from the Select Units pull down menu.

(c) Click OK.

- **Creating the geometry model :**

Before creating the geometry, make sure that the XY drawing plane is selected and that 3D is selected as the movement mode.

- (a) Create Rotating Central Core.
- (b) Create the passage for MRP fluid.
- (c) Create the coil.
- (d) Create the coil terminal.
- (e) Create the work piece.

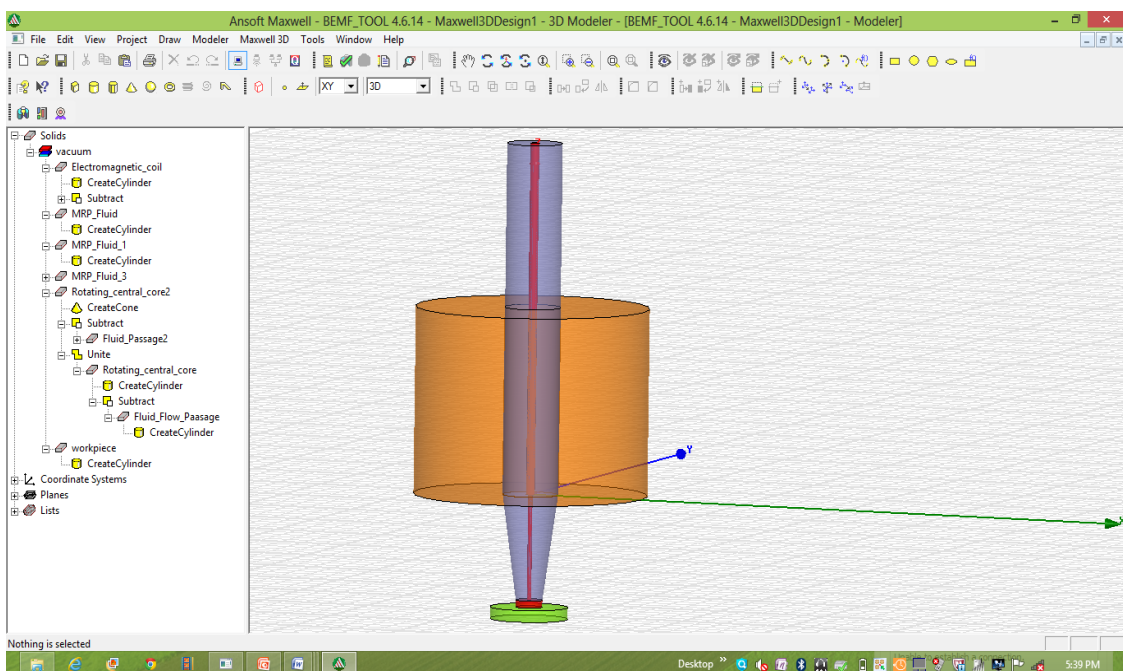


Figure 3.1: Modeling of a ball end type magnetorheological tool

- **Defining Material Properties :**

In the properties window with the Attribute tab selected, material properties are already present and some default property (Vacuum) is already assigned to objects. We can change the material property of any object as soon as the object is defined.

- (a) Using the Modeler Materials toolbar, choose Select.
- (b) Type Material in the Search by Name field.
- (c) Click OK button.

- **Assign Excitations :**

Currents need to be defined and assigned as excitations for the coil terminals.

- (a) Select each terminal by click in it in the history tree window.
- (b) Select the menu item Maxwell>Boolean>Separate Bodies.
- (c) Current Excitation: General.
  - Name: Current1.
  - Value: 1 amp to 5 amp

- **Set Up Parameter Calculation :**

- (a) Select the Rotating Core object by clicking its name in history tree window.
- (b) Select the Maxwell3D>Parameter>Assign>Force.
- (c) Click OK.

- **Setting Up and Running the Analysis :**

To set up the analysis:

- (a) Select the Maxwell3D>Analysis Setup>Add Solution Setup.
- (b) Accept the defaults (Maximum number of passes = 10 and Percentage Error = 1).  
 These settings instruct the solver to solve upto 10 passes as the automatic adaptive mesh refinement refines the mesh and improves the accuracy of the solution at run time.
- (c) Select the previously set up torque calculation from the Display Force/Torque in Convergence pull-down list.

To run the analysis:

- (a) To validate the model, Select the menu item Maxwell 3D>Validation Check.
- (b) To start solution process, Select the menu item Maxwell 3D>Analyze All.

## **3.2 Formation of Carbonyl Iron Particle Chain**

The following assumptions have been made to simplify the study of formation of carbonyl iron particle chain (Singh *et. al*, 2013)

- a) Shape of all carbonyl iron particles and all abrasive particles is assumed to be spherical.
- b) Diameter of Carbonyl iron particle is 23 $\mu\text{m}$
- c) Diameter of Abrasive Particle is 19  $\mu\text{m}$ .

- d) Magnetic losses and leakages are not considered.
- e) Cross sectional area of flux path is assumed to the area where magnetic lines of flux cross perpendicular from MR fluid layer in working gap. It is almost equal to projected area (A) of MR fluid layer on workpiece.

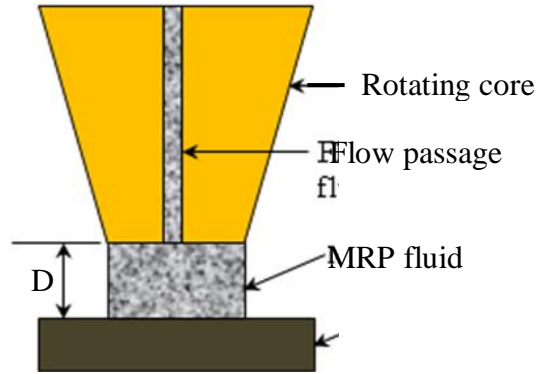


Figure 3.2: MRP fluid layer in working gap (Singh *et. al*, 2013)

### 3.2.1 Number of CIP Chains in the working gap

The calculation for the number of CIP chains particle has been taken from the previous research work (Singh *et. al*, 2013).

D = Length of variable working gap in mm.

d = Diameter of MRP fluid in working gap = 12mm.

Area of Flux Path,  $A = \pi r^2 = 113.29 \text{ mm}^2$

Volume of Flux in working gap,  $V = AD = (113.29) D \text{ mm}^3$

Number of carbonyl iron particle in volume V of MRP fluid:

$$N_{iron} = \frac{\% \text{ volume fraction of CIP in MR Fluid} \times \text{Volume of flux in working gap}}{\text{Volume of single CIP}}$$

$$\text{Volume of single CIP} = \frac{4}{3} \pi (d_{iron})^3 = 6370.63 \times 10^{-9} \text{ mm}^3$$

% volume fraction of CIP in MR fluid is 20%.

$$\text{Therefore, } N_{iron} = (2465690) * D$$

$$\text{Number of CIP in one Chain} = \frac{D}{d_{iron}} = (44) * D$$

$$N_{(iron)chains} = \frac{N_{iron}}{\text{Number of CIP in one chain}} = 56038$$

### 3.2.2 Numbers of CIP chains per active abrasive:

Numbers of active abrasive particles are responsible for removals of material during finishing operation are:

$$N_{AAB} = \frac{\% \text{ volume fraction of SiC in MR fluid} \times A \times \text{Diameter of SiC}}{\text{Volume of single SiC particle}}$$

% Volume fraction of SiC in MR Fluid = 20 % = 0.2

Diameter of SiC particle = 19  $\mu\text{m}$

Therefore,  $N_{AAB} = 83103$

Number of CIP chains per active abrasive =  $\frac{N(\text{iron}) \text{ Chains}}{N_{AAB}} = 0.67$

The number of CIP chains for three active abrasive =  $0.67 \times 3 = 2$

### 3.3 Electromagnetic modeling of ball end type magnetorheological finishing (BEMRF) tool with hollow core

The electromagnetic modeling of BEMRF hollow core tool was done using Maxwell Ansoft V13 software (student version) as shown in figure 3.3. The iron with a relative permeability of 600 has been assigned for central rotating core of diameter 25 mm and length of 245 mm (Singh *et. al*, 2013). Material has been assigned for coil is copper with relative permeability 1 and the number of turns of coil are 2000. The flow passage for MRP fluid of 2 mm diameter is also provided in center of rotating core. Ferromagnetic material with relative permeability 600 has been assigned for the workpiece of diameter 40 mm and height 5mm. There is a working gap between tool tip surface and ferromagnetic workpiece surface. MR polishing fluid get stiffened under the influence of electromagnetic forces and form the shape of ball end between this gap. The actual size of active abrasive particle and carbonyl iron particles was 19  $\mu\text{m}$  and 23  $\mu\text{m}$  respectively, but for visibility during finite element it has been taken ten times of actual size. Active abrasives of 0.19 mm are closely surrounded by chains of 0.23 mm CIPs between the working gap. In the present work three abrasives have been plotted on the surface of the workpiece and the results of finite element magnetostatic simulation for magnetic normal force acting on the three active abrasives has been considered as average of three magnetic normal forces. Force parameter is also assigned to abrasive and CIP. The electromagnet model of ball end type magnetorheological finishing hollow core tool is shown in figure 3.3 and carbonyl iron particle arrangement with hollow core tool is shown in figure 3.4.

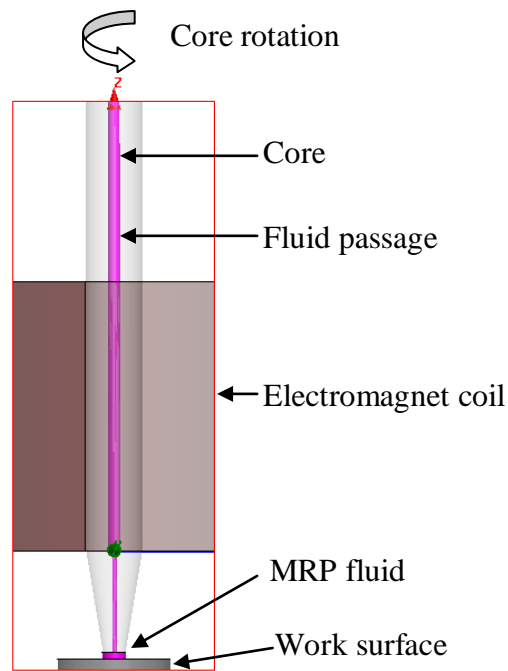


Figure 3.3: Electromagnet model of ball end type magnetorheological finishing hollow core tool

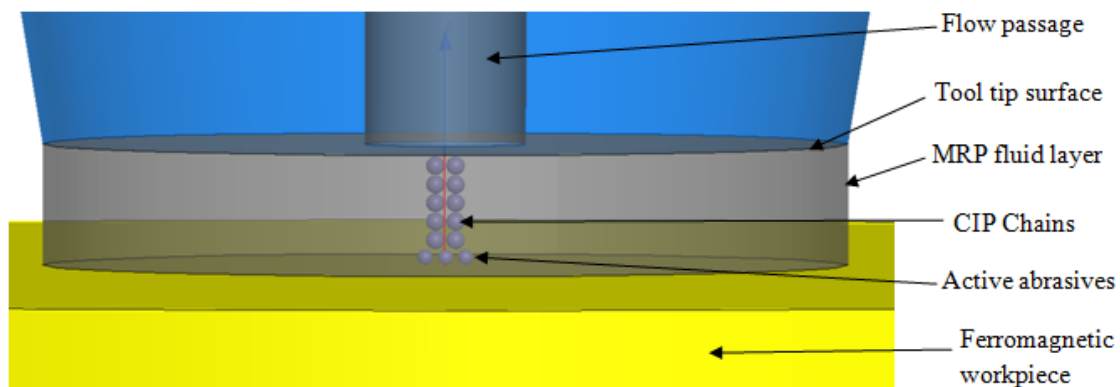


Figure 3.4: CIP chains arrangement in the working gap with hollow core tool

### 3.4 Finite Element (FE) Analysis of BEMRF process for hollow core tool

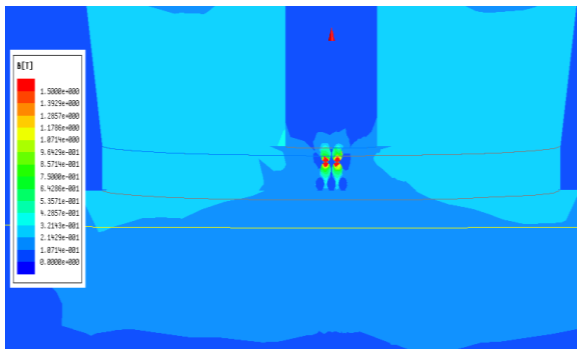
In hollow core tool there is a passage of 2mm diameter in center of rotating core for flow the MRP fluid. Performing the simulation to analysis the effect of CIP chain on active abrasive particles after modeling of BEMRF tool along with MRP fluid and work piece. The main objective of this analysis to find out the magnitude of forces on active abrasives by variation in current density, coil position and gap between tool tip and work piece surface. By variation in gap between tool tip and work piece there is variation in number of CIP per chain, which

plays important role in finishing. The following different cases have been considered for FE analysis:

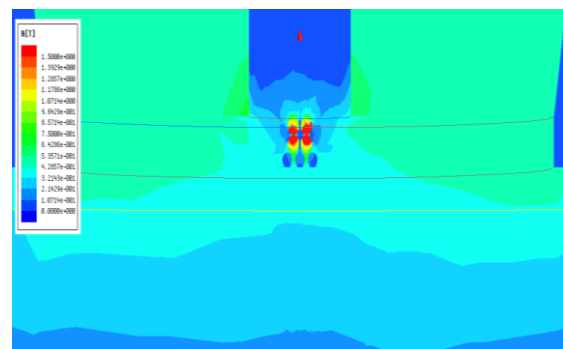
- Electromagnet coil distance 45 mm and gap 0.66 mm while varying the magnetizing current from 1 amp to 5 amp
- Electromagnet coil distance 45 mm and gap 1.5 mm while varying the magnetizing current from 1 amp to 5 amp
- Electromagnet coil distance 45 mm and gap 2.34 mm while varying the magnetizing current from 1 amp to 5 amp
- Electromagnet coil distance 50 mm and gap 0.66 mm while varying the magnetizing current from 1 amp to 5 amp
- Electromagnet coil distance 50 mm and gap 1.5 mm while varying the magnetizing current from 1 amp to 5 amp
- Electromagnet coil distance 50 mm and gap 2.34 mm while varying the magnetizing current from 1 amp to 5 amp
- Electromagnet coil distance 55 mm and gap 0.66 mm while varying the magnetizing current from 1 amp to 5 amp
- Electromagnet coil distance 55 mm and gap 1.5 mm while varying the magnetizing current from 1 amp to 5 amp
- Electromagnet coil distance 55 mm and gap 2.34 mm while varying the magnetizing current from 1 amp to 5 amp
- Electromagnet coil distance 60 mm and gap 0.66 mm while varying the magnetizing current from 1 amp to 5 amp
- Electromagnet coil distance 60 mm and gap 1.5 mm while varying the magnetizing current from 1 amp to 5 amp
- Electromagnet coil distance 60 mm and gap 2.34 mm while varying the magnetizing current from 1 amp to 5 amp
- Electromagnet coil distance 65 mm and gap 0.66 mm while varying the magnetizing current from 1 amp to 5 amp
- Electromagnet coil distance 65 mm and gap 1.5 mm while varying the magnetizing current from 1 amp to 5 amp
- Electromagnet coil distance 65 mm and gap 2.34 mm while varying the magnetizing current from 1 amp to 5 amp

### 3.4.1 Electromagnet coil distance 45 mm and gap 0.66 mm while varying the magnetizing current from 1 amp to 5 amp

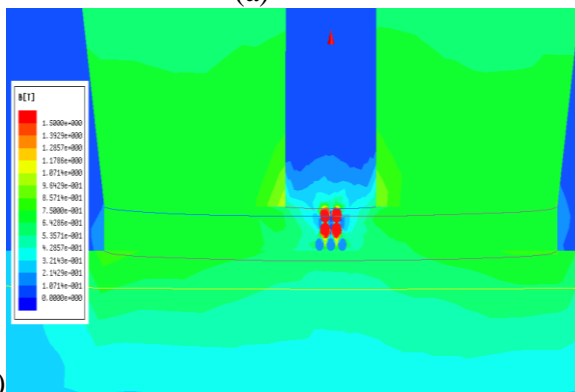
Tool modeled and simulated by taking coil distance from tool tip surface = 45 mm, diameter of rotating core = 25 mm, length of core = 245 mm, type of core = hollow, diameter of passage of MRP fluid = 2 mm, gap = 0.66 mm, number of turns of coil = 2000 turns, diameter of abrasive = 0.19 mm, diameter of CIP = 0.23 mm and number of abrasives for two CIP chain = 3. Current is varied from 1 amp per turn to 5 amp per turn to analysis the variation in effect of force due to variation in current.



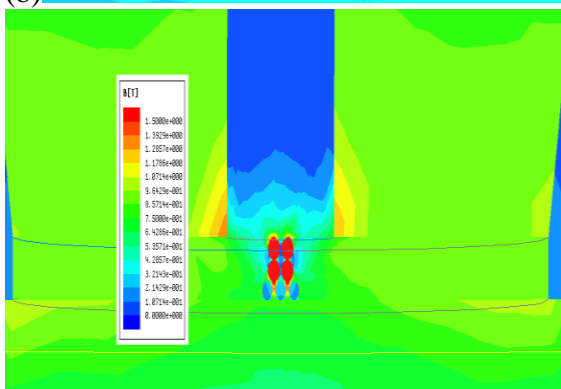
(a)



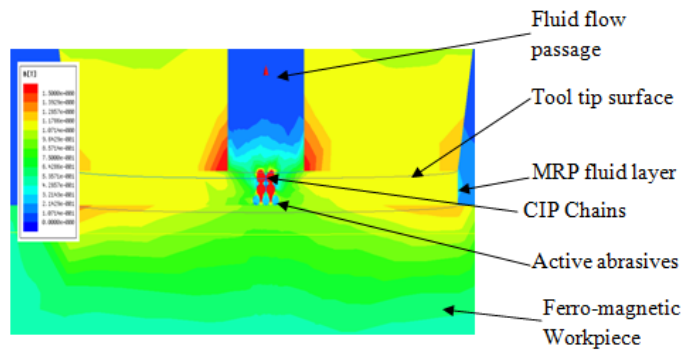
(d)



(b)



(c)



(e)

Figure 3.5: FE simulation of the BEMRF with hollow core tool of 45 mm coil distance and 0.66 mm with Current (a) 1 amp (b) 2 amp (c) 3 amp (d) 4 amp (e) 5 amp

Table 3.1 Result analysis of forces at different magnetizing current with 0.66 mm gap and 45mm coil distance from the tool tip surface

Force	1 amp	2 amp	3 amp	4 amp	5 amp
Average Force (N)	1.22941E-0	0.0000491	0.00011064	0.00019670	0.00030735

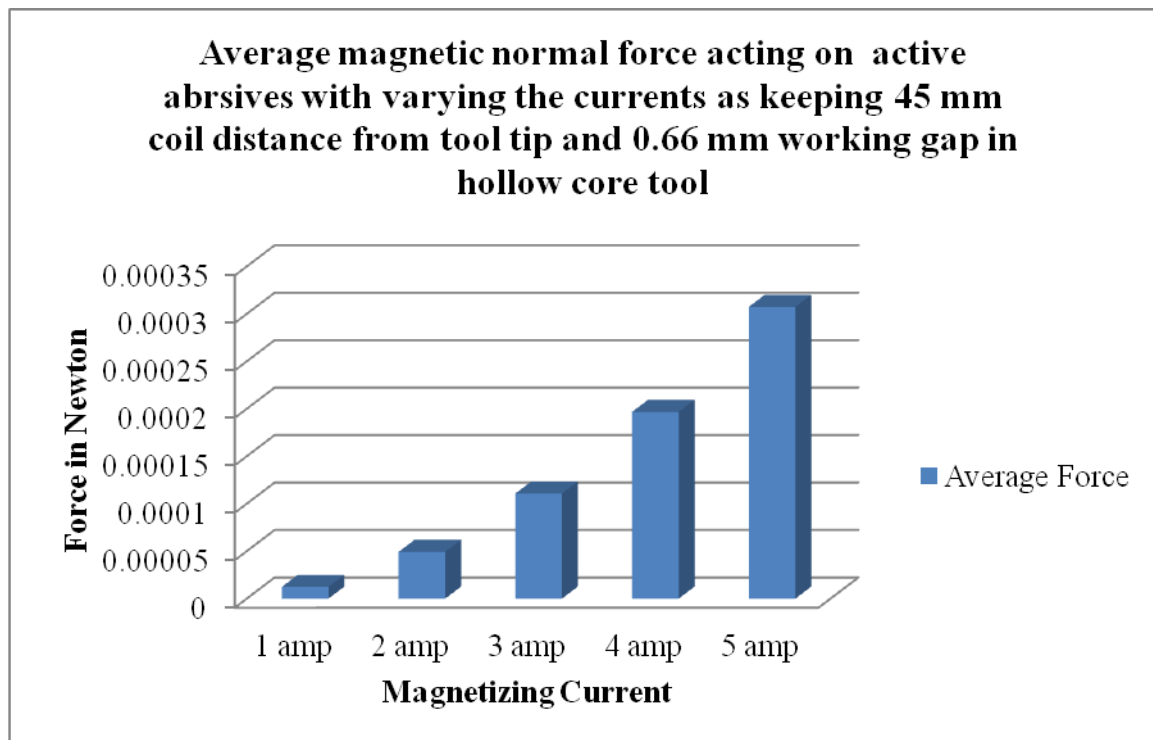
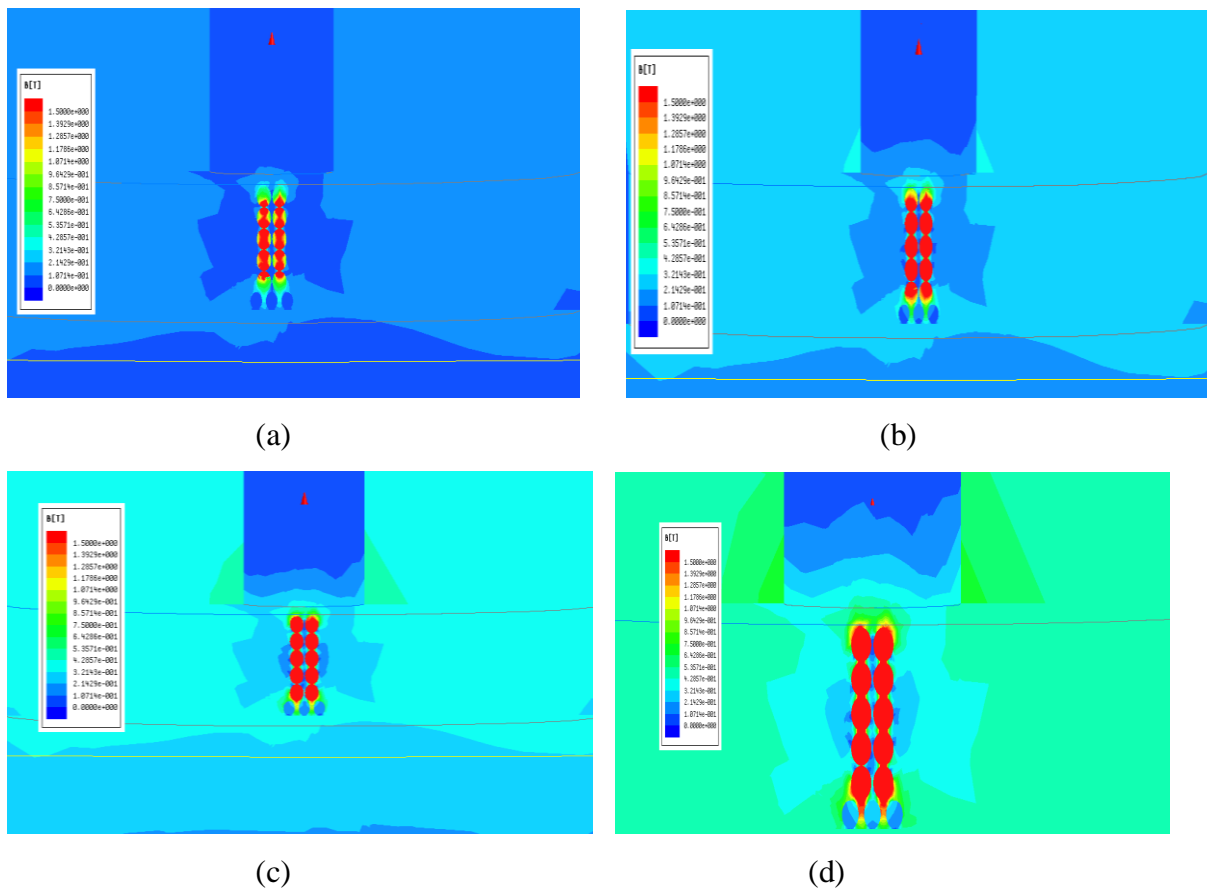


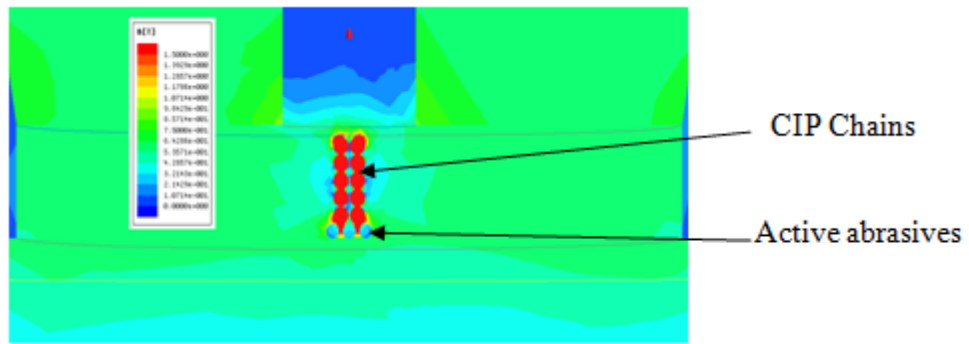
Figure 3.6: Result analysis of force v/s current at 0.66 mm gap and 45mm coil distance from tool tip surface

Figure 3.6 shows the variation of magnetically induced normal force on the active abrasive particles with magnetizing current (1A to 5A) while working gap was kept as 0.66 mm and electromagnetic coil distance from the tool tip surface as 45 mm. The same result has been reported in table 3.1.

### 3.4.2 Electromagnet coil distance 45 mm and gap 1.5 mm while varying the magnetizing current from 1 amp to 5 amp

Tool modeled and simulated by taking coil distance from tool tip surface = 45 mm, diameter of rotating core = 25 mm, length of core = 245 mm, type of core = hollow, diameter of passage of MRP fluid = 2 mm, gap = 1.5 mm, number of turns of coil = 2000 turns, diameter of abrasive = 0.19 mm, diameter of CIP = 0.23 mm and number of abrasives for two CIP chain = 3. Current is varied from 1 amp per turn to 5 amp per turn to analysis the variation in effect of force due to variation in current.





(e)

Figure 3.7: FE simulation of the BEMRF with hollow core tool of 45 mm coil distance and 1.5 mm with Current (a) 1 amp (b) 2 amp (c) 3 amp (d) 4 amp (e) 5 amp

Table 3.2 Result analysis of forces at different magnetizing current with 1.5 mm gap and 45mm coil distance from the tool tip surface

Force	1 amp	2 amp	3 amp	4 amp	5 amp
Average Force (N)	1.13745E-05	0.0000454	0.0001023	0.00018199	0.000284363

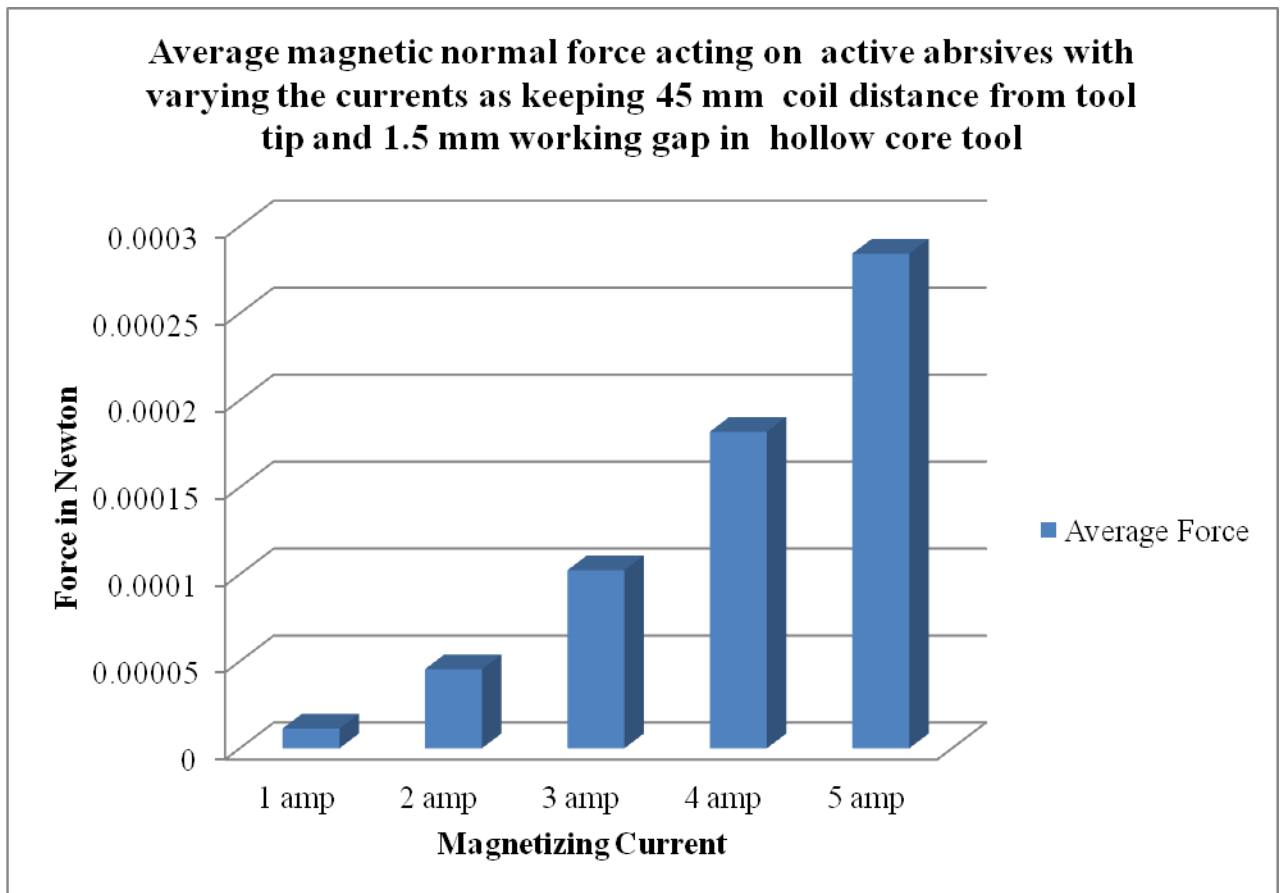


Figure 3.8: Result analysis of force v/s current at 1.5 mm gap and 45mm coil distance

Figure 3.8 shows the variation of magnetically induced normal force on the active abrasive particles with magnetizing current (1A to 5A) while working gap was kept as 1.5 mm and electromagnetic coil distance from the tool tip surface as 45 mm. The same result has been reported in table 3.2.

### 3.4.3 Electromagnet coil distance 45 mm and gap 2.34 mm while varying the magnetizing current from 1 amp to 5 amp

Tool modeled and simulated by taking coil distance from tool tip surface = 45 mm, diameter of rotating core = 25 mm, length of core = 245 mm, type of core = hollow, diameter of passage of MRP fluid = 2 mm, gap = 2.34 mm, number of turns of coil = 2000 turns, diameter of abrasive = 0.19 mm, diameter of CIP = 0.23 mm and number of abrasives for two CIP chain = 3. Current is varied from 1 amp per turn to 5 amp per turn to analysis the variation in effect of force due to variation in current.

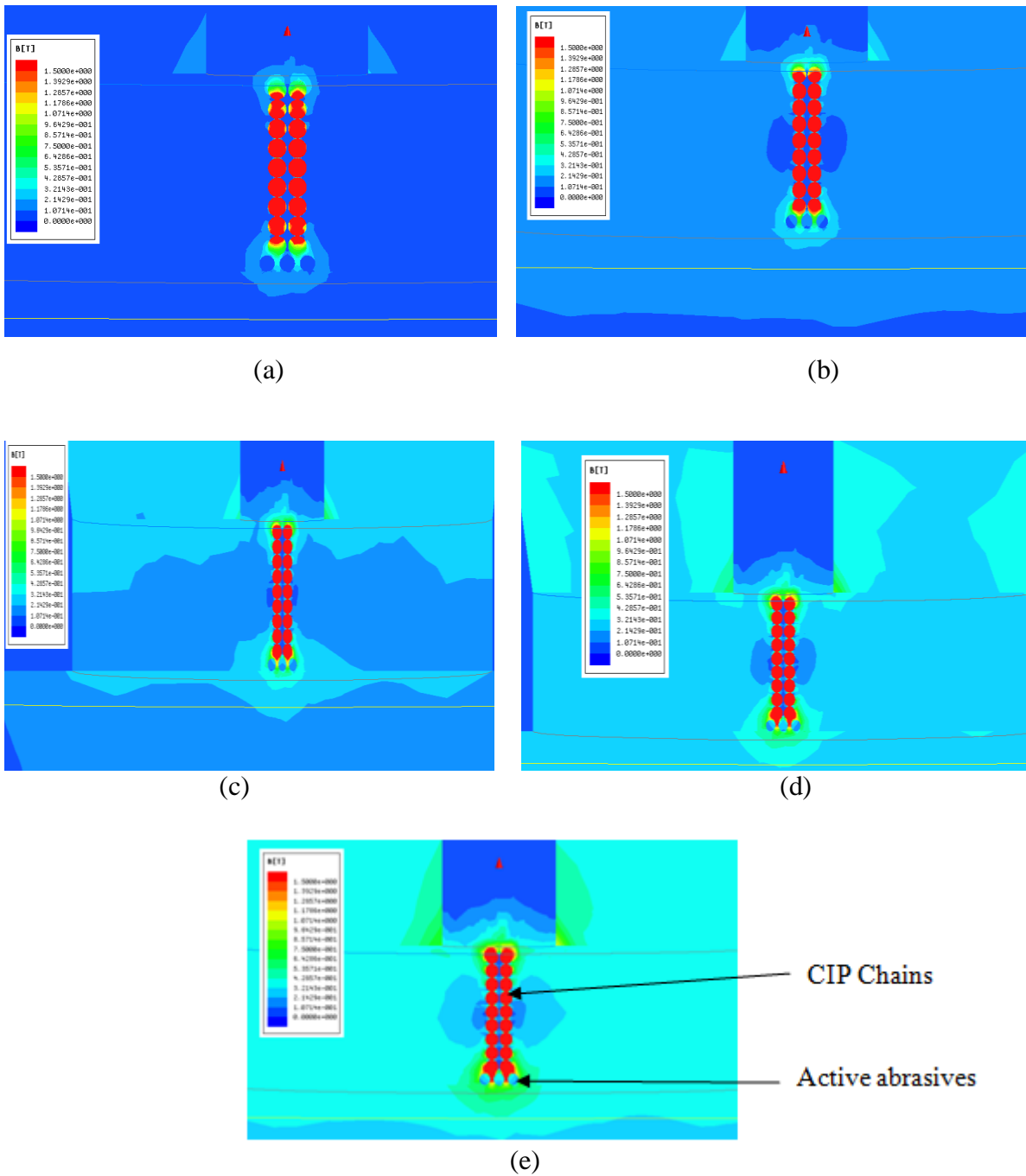


Figure 3.9: FE simulation of the BEMRF with hollow core tool of 45 mm coil distance and 2.34 mm with Current (a) 1 amp (b) 2 amp (c) 3 amp (d) 4 amp (e) 5 amp

Table 3.3 Result analysis of forces at different magnetizing current with 2.34 mm gap and 45mm coil distance from the tool tip surface

Force	1 amp	2 amp	3 amp	4 amp	5 amp
Average Force (N)	1.08675E-05	4.34703E-05	9.78067E-05	0.00017388	0.00027169

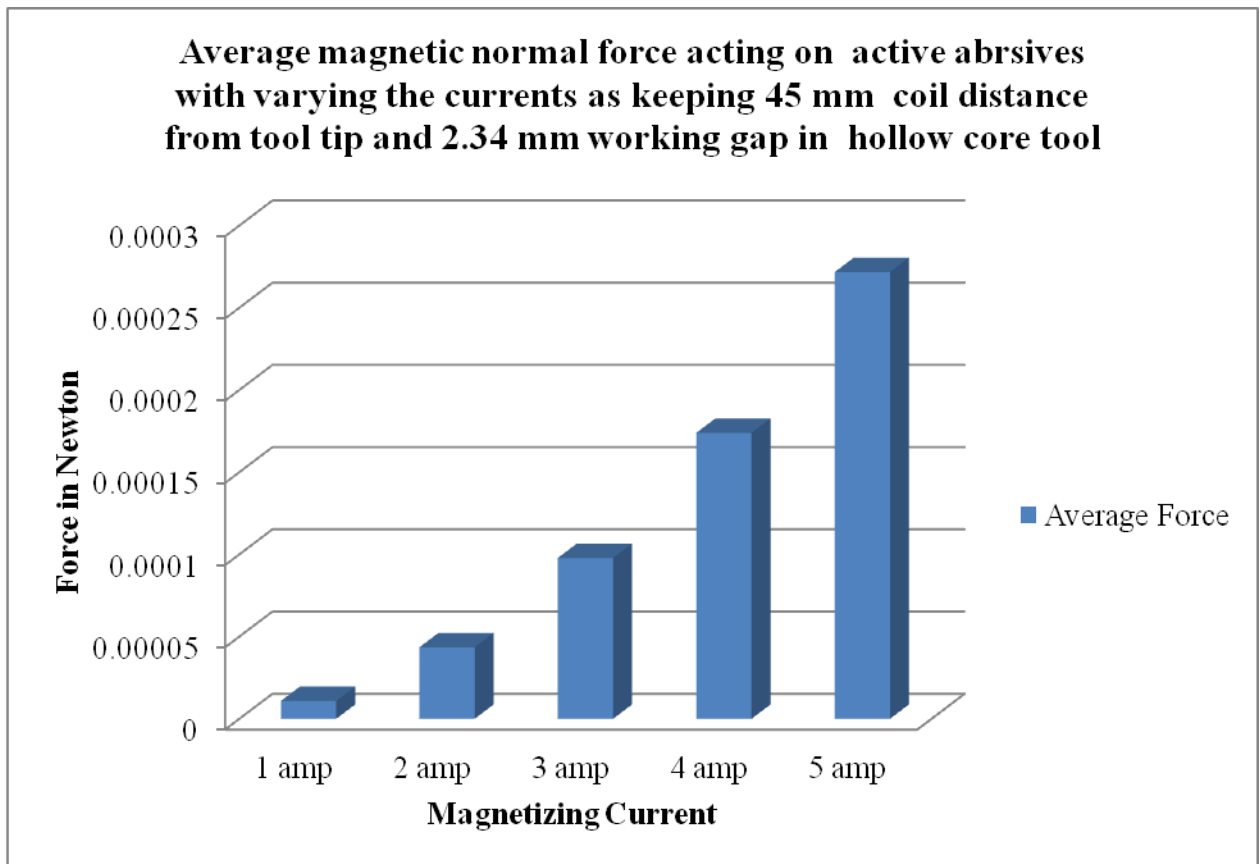


Figure 3.10: Result analysis of force v/s current at 2.34 mm gap and 45mm coil distance

Figure 3.10 shows the variation of magnetically induced normal force on the active abrasive particles with magnetizing current (1A to 5A) while working gap was kept as 2.34 mm and electromagnetic coil distance from the tool tip surface as 45 mm. The same result has been reported in table 3.3.

### **3.4.4 Electromagnet coil distance 50 mm and gap 0.66 mm while varying the magnetizing current from 1 amp to 5 amp**

Tool modeled and simulated by taking coil distance from tool tip surface = 50 mm, diameter of core = 25 mm, length of core = 245 mm, type of core = hollow, diameter of passage of MRP fluid = 2 mm, gap = 0.66 mm, number of turns of coil = 2000 turns, diameter of abrasive = 0.19 mm, diameter of CIP = 0.23 mm and number of abrasives for two CIP chain = 3. Current is varied from 1 amp per turn to 5 amp per turn to analysis the variation in effect of force due to variation in current.

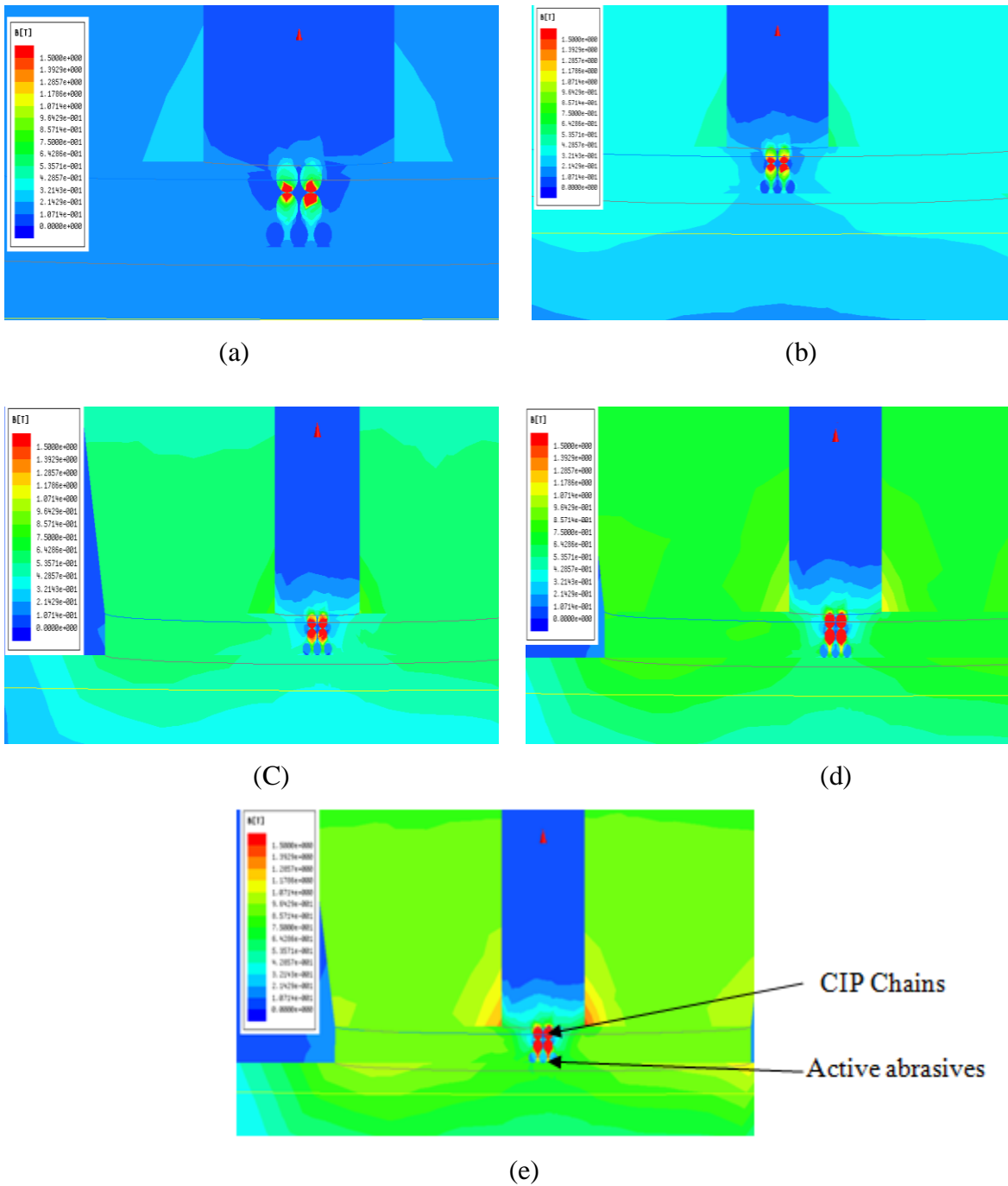


Figure 3.11: FE simulation of the BEMRF with hollow core tool of 50 mm coil distance and 0.66 mm with Current (a) 1 amp (b) 2 amp (c) 3 amp (d) 4 amp (e) 5 amp

Table 3.4 Result analysis of forces at different magnetizing current with 0.66 mm gap and 50 mm coil distance from the tool tip surface

Force	1 amp	2 amp	3 amp	4 amp	5 amp
Average Force (N)	9.30663E-06	0.000037227	0.000083762	0.00014891	0.000232667

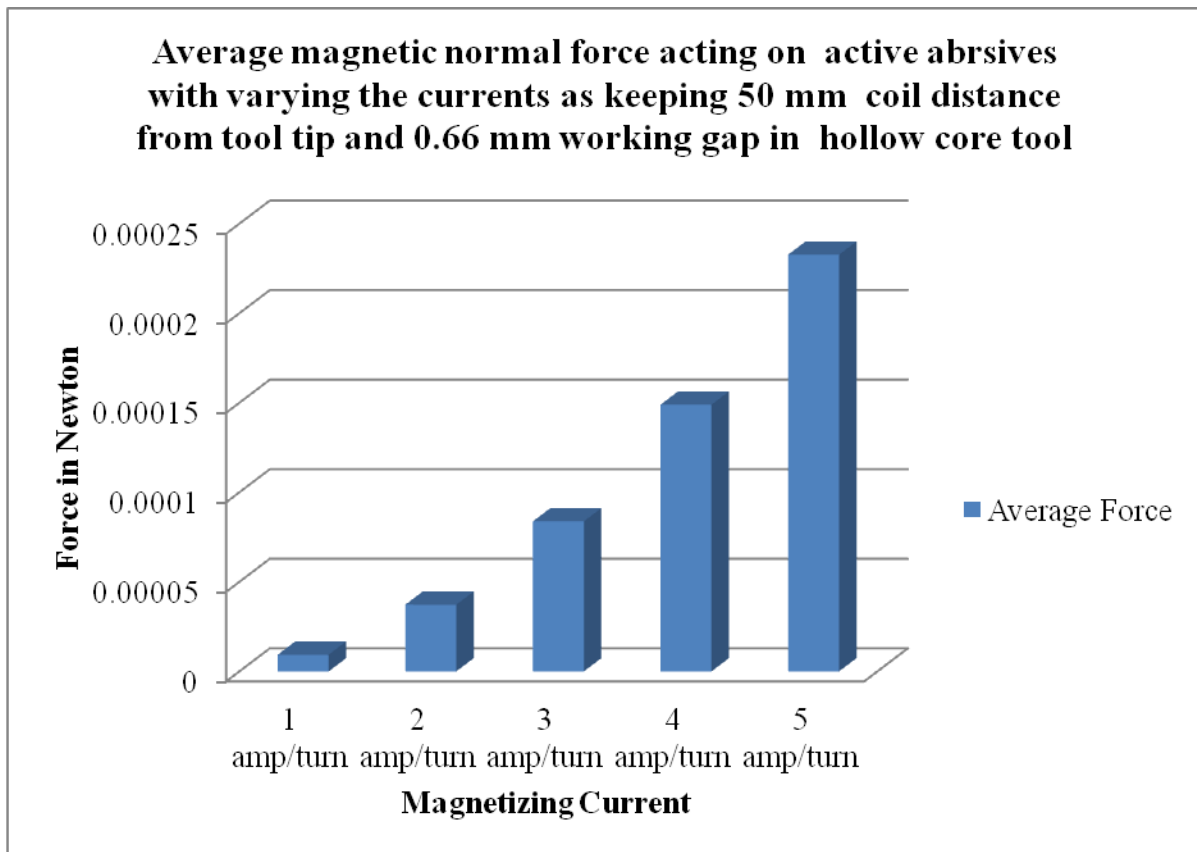


Figure 3.12: Result analysis of force v/s current at 0.66 mm gap and 50 mm coil distance

Figure 3.12 shows the variation of magnetically induced normal force on the active abrasive particles with magnetizing current (1A to 5A) while working gap was kept as 0.66 mm and electromagnetic coil distance from the tool tip surface as 50 mm. The same result has been reported in table 3.4.

### **3.4.5 Electromagnet coil distance 50 mm and gap 1.5 mm while varying the magnetizing current from 1 amp to 5 amp**

Tool modeled and simulated by taking coil distance from tool tip surface = 50 mm, diameter of rotating core = 25 mm, length of core = 245 mm, type of core = hollow, diameter of passage of MRP fluid = 2 mm, gap = 1.5 mm, number of turns of coil = 2000 turns, diameter of abrasive = 0.19 mm, diameter of CIP = 0.23 mm and number of abrasives for two CIP chain = 3. Current is varied from 1 amp per turn to 5 amp per turn to analysis the variation in effect of force due to variation in current.

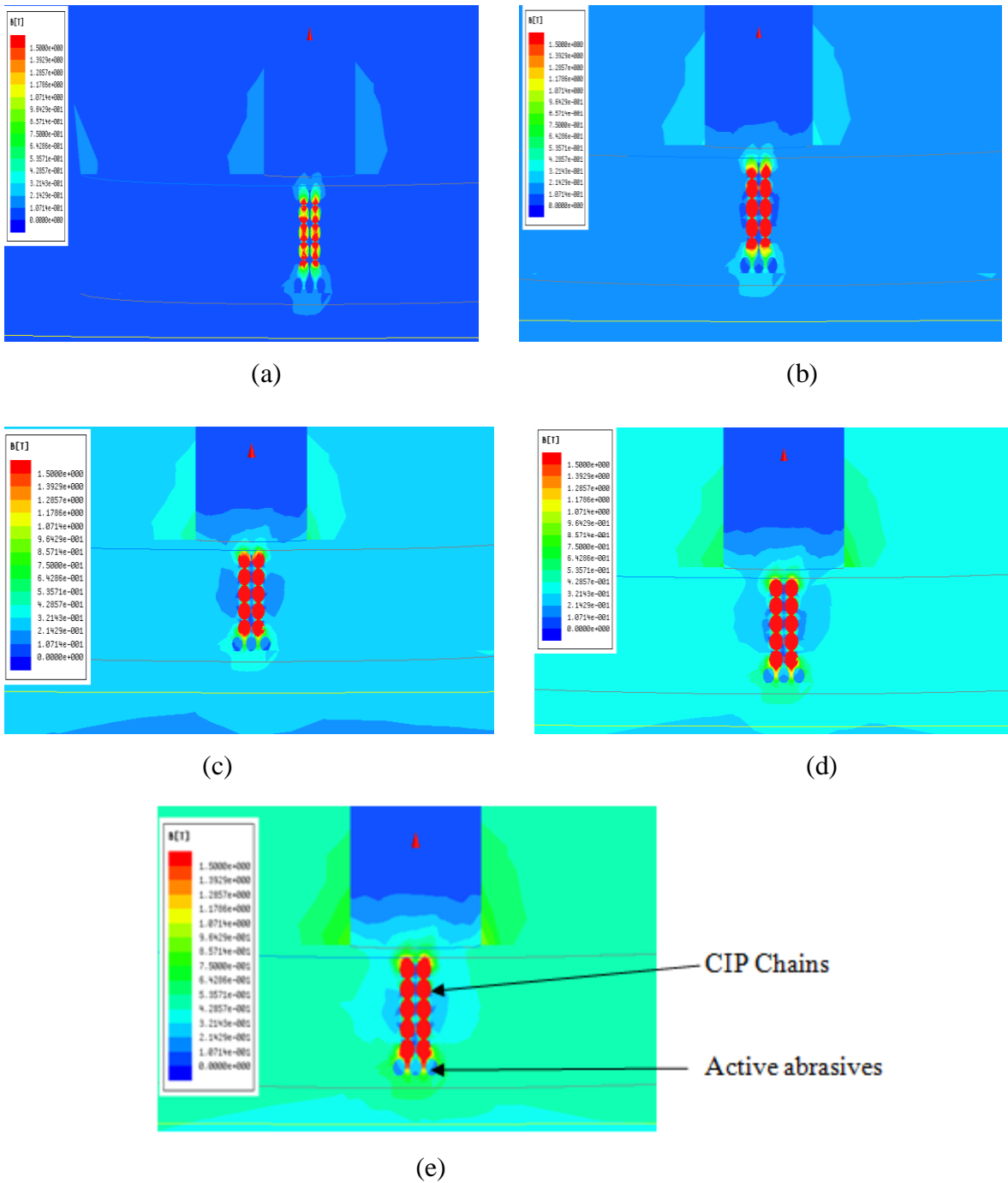


Figure 3.13: FE simulation of the BEMRF with hollow core tool of 50 mm coil distance and 1.5 mm with Current (a) 1 amp (b) 2 amp (c) 3 amp (d) 4 amp (e) 5 amp

Table 3.5 Result analysis of forces at different magnetizing current with 1.5 mm gap and 50 mm coil distance from the tool tip surface

Force	1 amp	2 amp	3 amp	4 amp	5 amp
Average Force (N)	5.74943E-06	2.29973E-05	5.17453E-05	9.19927E-05	0.000143739

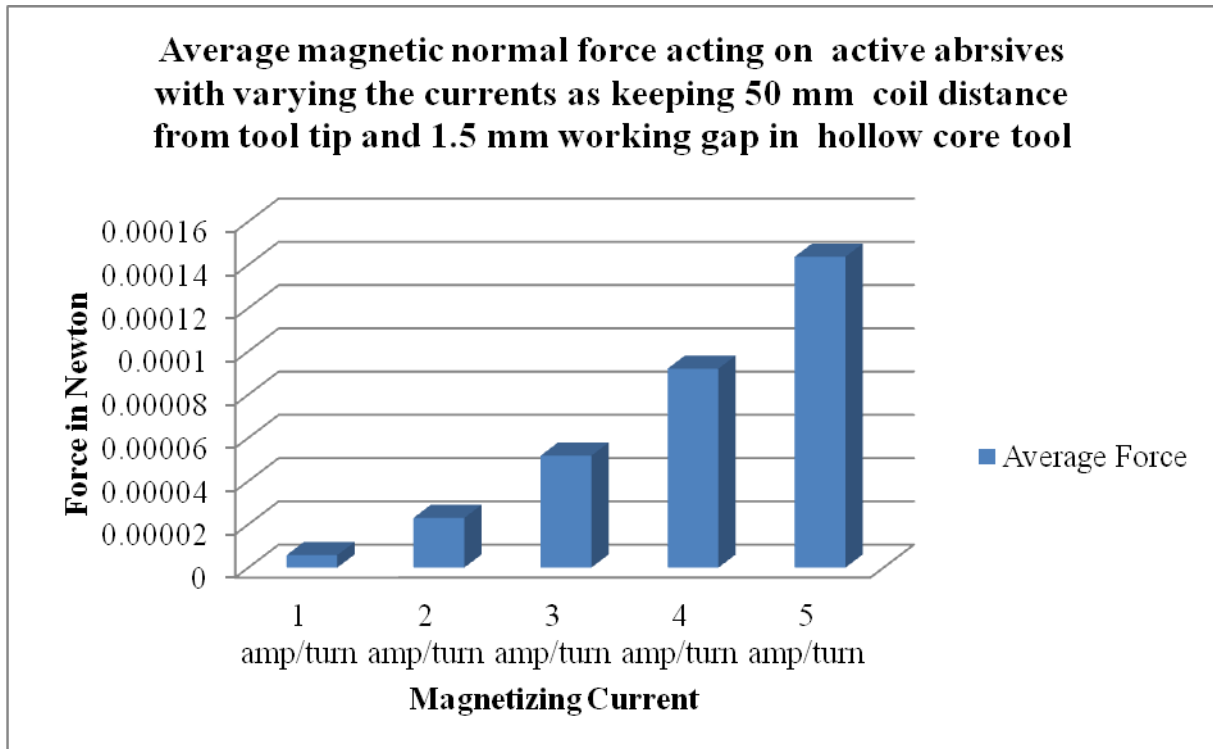


Figure 3.14: Result analysis of force v/s current at 1.5 mm gap and 50 mm coil distance

Figure 3.14 shows the variation of magnetically induced normal force on the active abrasive particles with magnetizing current (1A to 5A) while working gap was kept as 1.5 mm and electromagnetic coil distance from the tool tip surface as 50 mm. The same result has been reported in table 3.5.

### **3.4.6 Electromagnet coil distance 50 mm and gap 2.34 mm while varying the magnetizing current from 1 amp to 5 amp**

Tool modeled and simulated by taking coil distance from tool tip surface = 50 mm, diameter of rotating core = 25 mm, length of core = 245 mm, type of core = hollow, diameter of passage of MRP fluid = 2 mm, gap = 2.34 mm, number of turns of coil = 2000 turns, diameter of abrasive = 0.19 mm, diameter of CIP = 0.23 mm and number of abrasives for two CIP chain = 3. Current is varied from 1 amp per turn to 5 amp per turn to analysis the variation in effect of force due to variation in current.

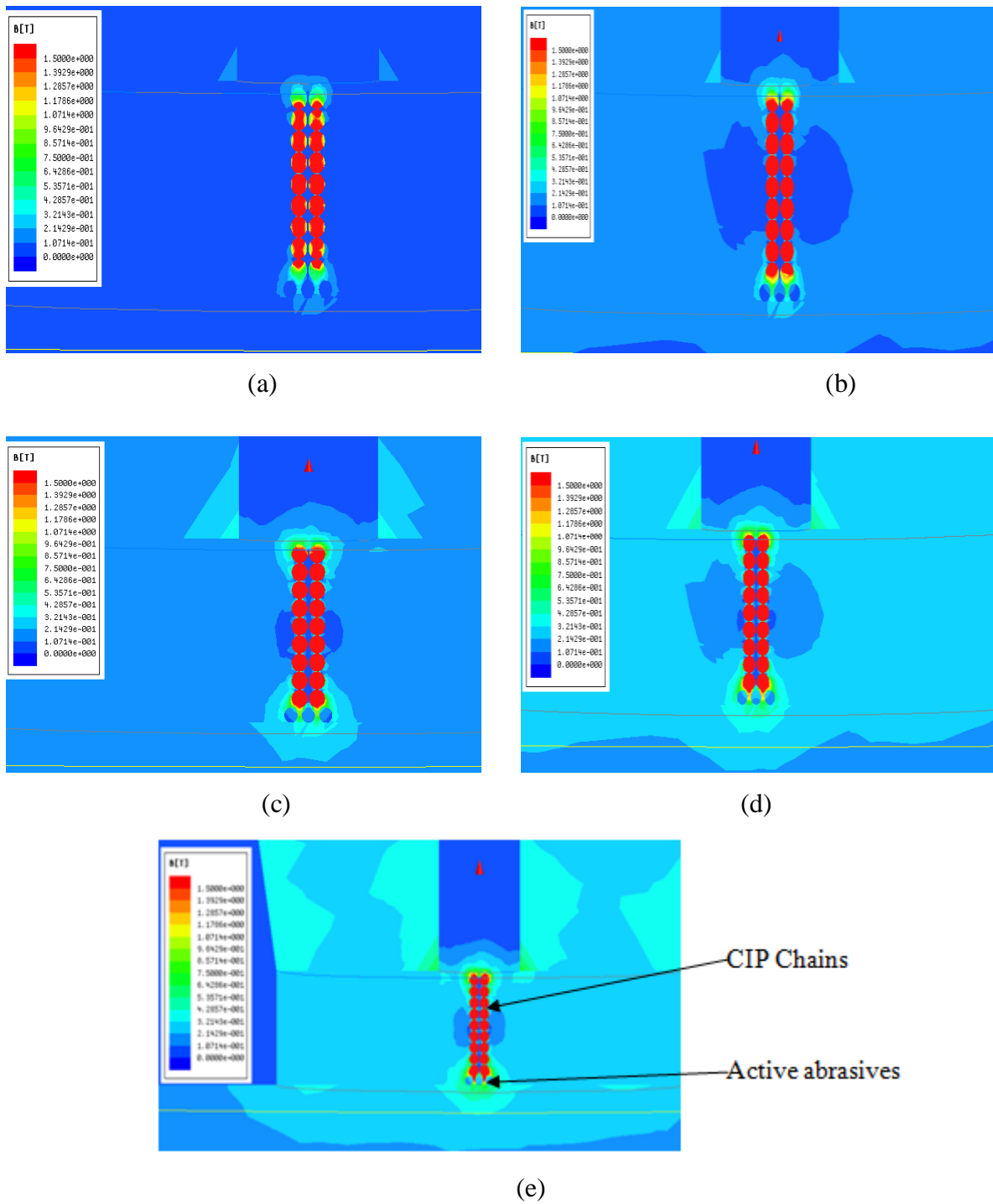


Figure 3.15: FE simulation of the BEMRF with hollow core tool of 50 mm coil distance and 2.34 mm with Current (a) 1 amp (b) 2 amp (c) 3 amp (d) 4 amp (e) 5 amp

Table 3.6 Result analysis of forces at different magnetizing current with 2.34 mm gap and 50 mm coil distance from the tool tip surface

Force	1 amp	2 amp	3 amp	4 amp	5 amp
Average Force (N)	1.05228E-05	4.00917E-05	0.000090705	0.000150367	0.000243073

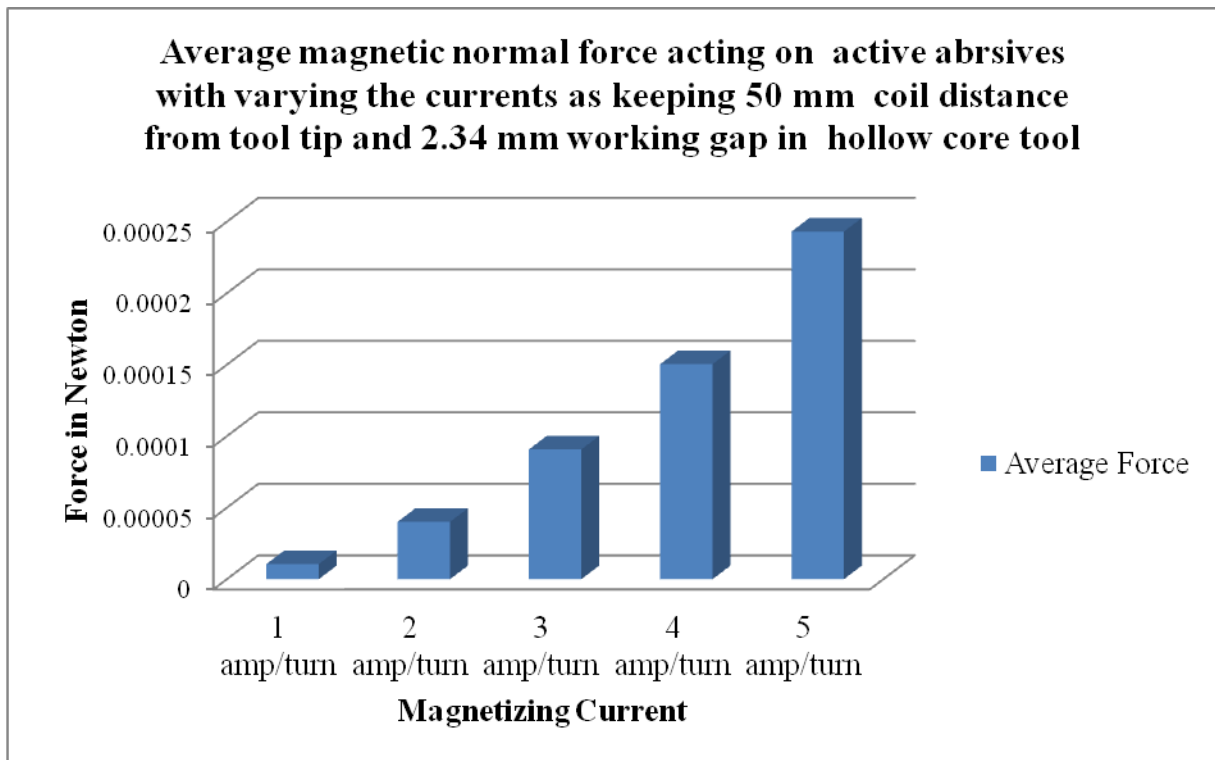


Figure 3.16: Result analysis of force v/s current at 2.34 mm gap and 50 mm coil distance

Figure 3.16 shows the variation of magnetically induced normal force on the active abrasive particles with magnetizing current (1A to 5A) while working gap was kept as 2.34 mm and electromagnetic coil distance from the tool tip surface as 50 mm. The same result has been reported in table 3.6.

### 3.4.7 Electromagnet coil distance 55 mm and gap 0.66 mm while varying the magnetizing current from 1 amp to 5 amp

Tool modeled and simulated by taking coil distance from tool tip surface = 55 mm, diameter of rotating core = 25 mm, length of core = 245 mm, type of core = hollow, diameter of passage of MRP fluid = 2 mm, gap = 0.66 mm, number of turns of coil = 2000 turns, diameter of abrasive = 0.19 mm, diameter of CIP = 0.23 mm and number of abrasives for two CIP chain = 3. Current is varied from 1 amp per turn to 5 amp per turn to analysis the variation in effect of force due to variation in current.

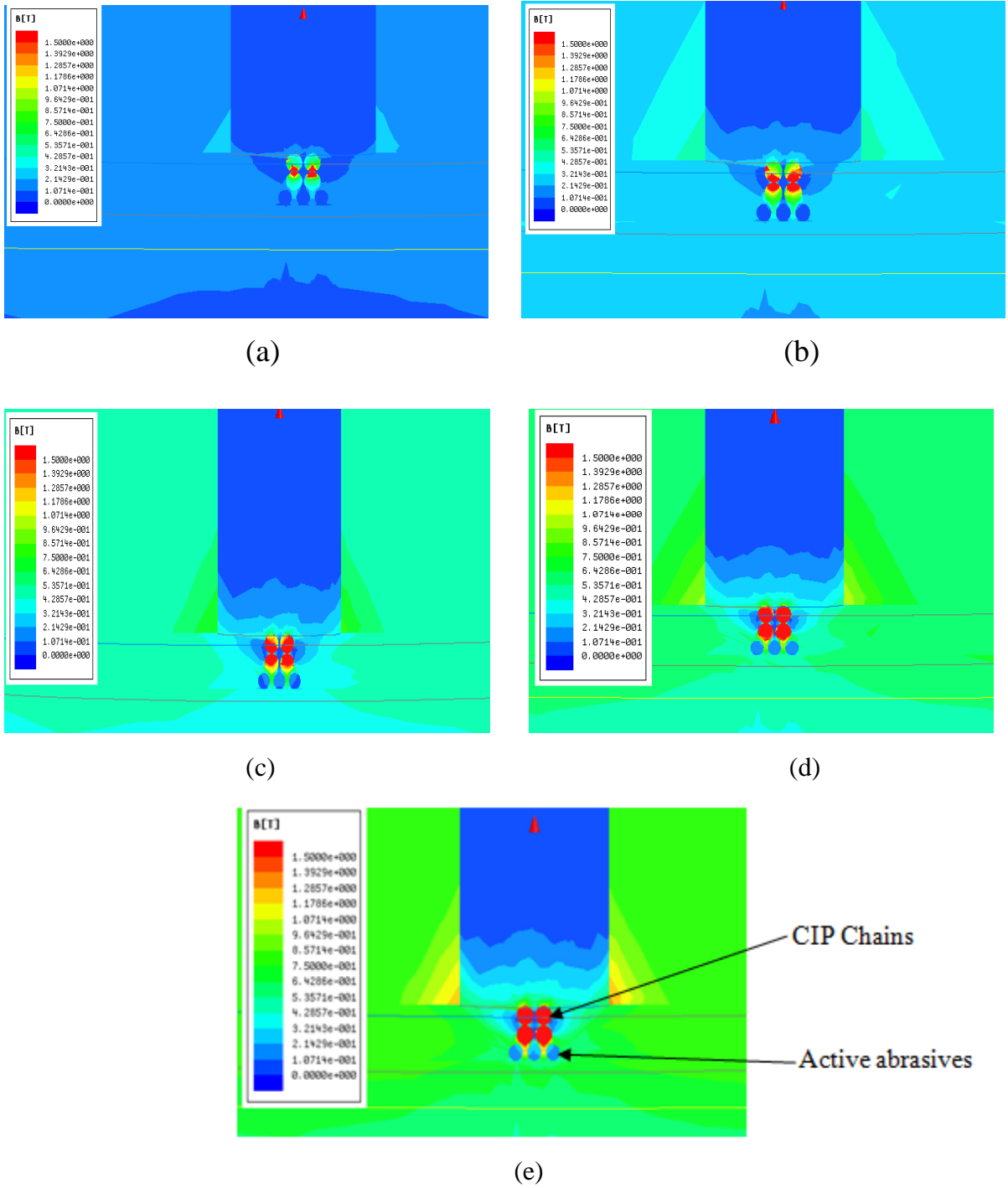


Figure 3.17: FE simulation of the BEMRF with hollow core tool of 55 mm coil distance and 0.66 mm with Current (a) 1 amp (b) 2 amp (c) 3 amp (d) 4 amp (e) 5 amp

Table 3.7 Result analysis of forces at different magnetizing current with 0.66 mm gap and 55 mm coil distance from the tool tip surface

Force	1 amp	2 amp	3 amp	4 amp	5 amp
-------	-------	-------	-------	-------	-------

Average Force (N)	4.0579E-06	1.92317E-05	0.000052521	8.89263E-05	0.000126448
-------------------	------------	-------------	-------------	-------------	-------------

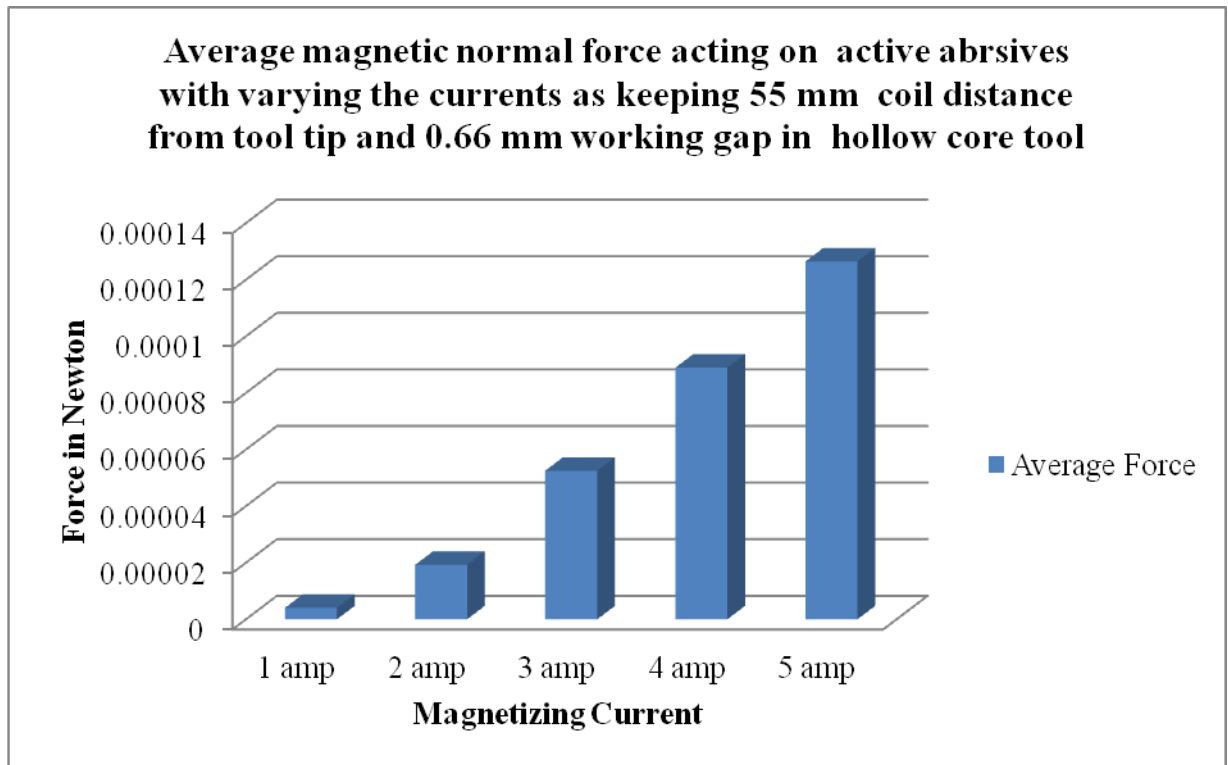


Figure 3.18: Result analysis of force v/s current at 0.66 mm gap and 55 mm coil distance

Figure 3.18 shows the variation of magnetically induced normal force on the active abrasive particles with magnetizing current (1A to 5A) while working gap was kept as 0.66 mm and electromagnetic coil distance from the tool tip surface as 55 mm. The same result has been reported in table 3.7.

### 3.4.8 Electromagnet coil distance 55 mm and gap 1.5 mm while varying the magnetizing current from 1 amp to 5 amp

Tool modeled and simulated by taking coil distance from tool tip surface = 55 mm, diameter of rotating core = 25 mm, length of core = 245 mm, type of core = hollow, diameter of passage of MRP fluid = 2 mm, gap = 1.5 mm, number of turns of coil = 2000 turns, diameter of abrasive = 0.19 mm, diameter of CIP = 0.23 mm and number of abrasives for two CIP chain = 3. Current is varied from 1 amp per turn to 5 amp per turn to analysis the variation in effect of force due to variation in current.

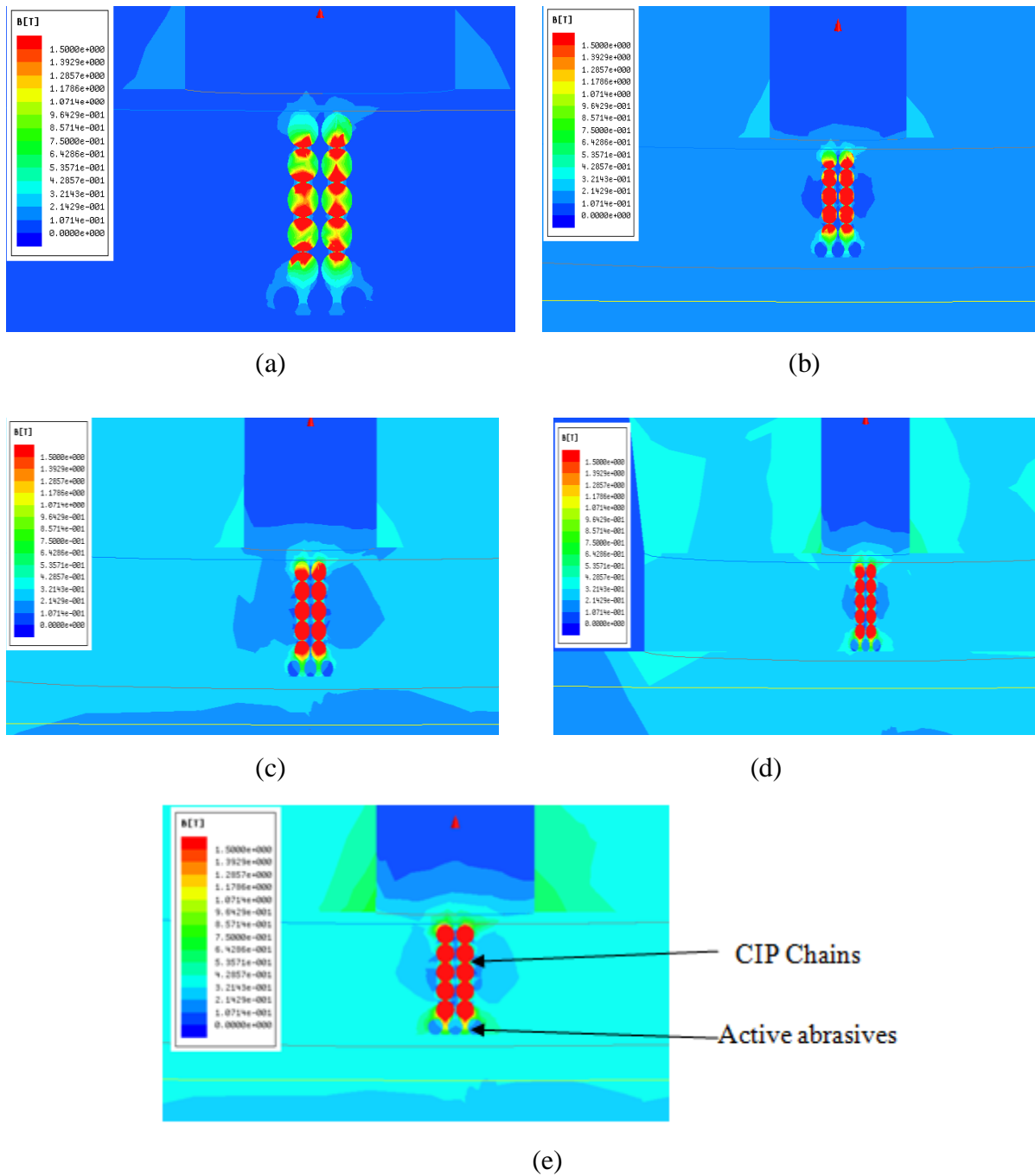


Figure 3.19 : FE simulation of the BEMRF with hollow core tool of 55 mm coil distance and 1.5 mm with Current (a) 1 amp (b) 2 amp (c) 3 amp (d) 4 amp (e) 5 amp

Table 3.8 Result analysis of forces at different magnetizing current with 1.5 mm gap and 55 mm coil distance from the tool tip surface

Force	1 amp	2 amp	3 amp	4 amp	5 amp
Average Force	5.28607E-06	2.05443E-05	4.89747E-05	8.41773E-05	0.000127152

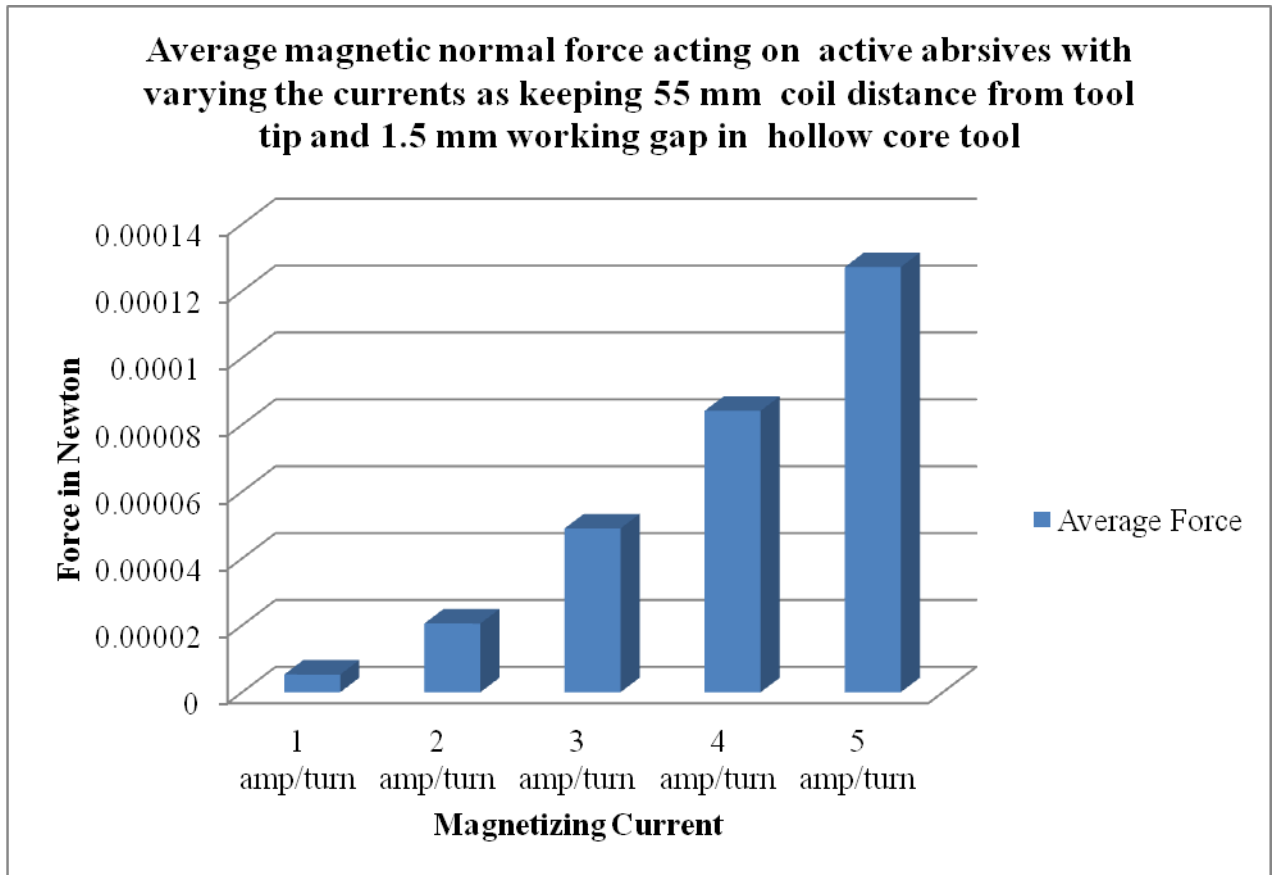


Figure 3.20 : Result analysis of force v/s current at 1.5 mm gap and 55 mm coil distance

Figure 3.20 shows the variation of magnetically induced normal force on the active abrasive particles with magnetizing current (1A to 5A) while working gap was kept as 1.5 mm and electromagnetic coil distance from the tool tip surface as 55 mm. The same result has been reported in table 3.8.

### **3.4.9 Electromagnet coil distance 55 mm and gap 2.34 mm while varying the magnetizing current from 1 amp to 5 amp**

Tool modeled and simulated by taking coil distance from tool tip surface = 55 mm, diameter of rotating core = 25 mm, length of core = 245 mm, type of core = hollow, diameter of passage of MRP fluid = 2 mm, gap = 2.34 mm, number of turns of coil = 2000 turns, diameter of abrasive = 0.19 mm, diameter of CIP = 0.23 mm and number of abrasives for two CIP chain = 3. Current is varied from 1 amp per turn to 5 amp per turn to analysis the variation in effect of force due to variation in current.

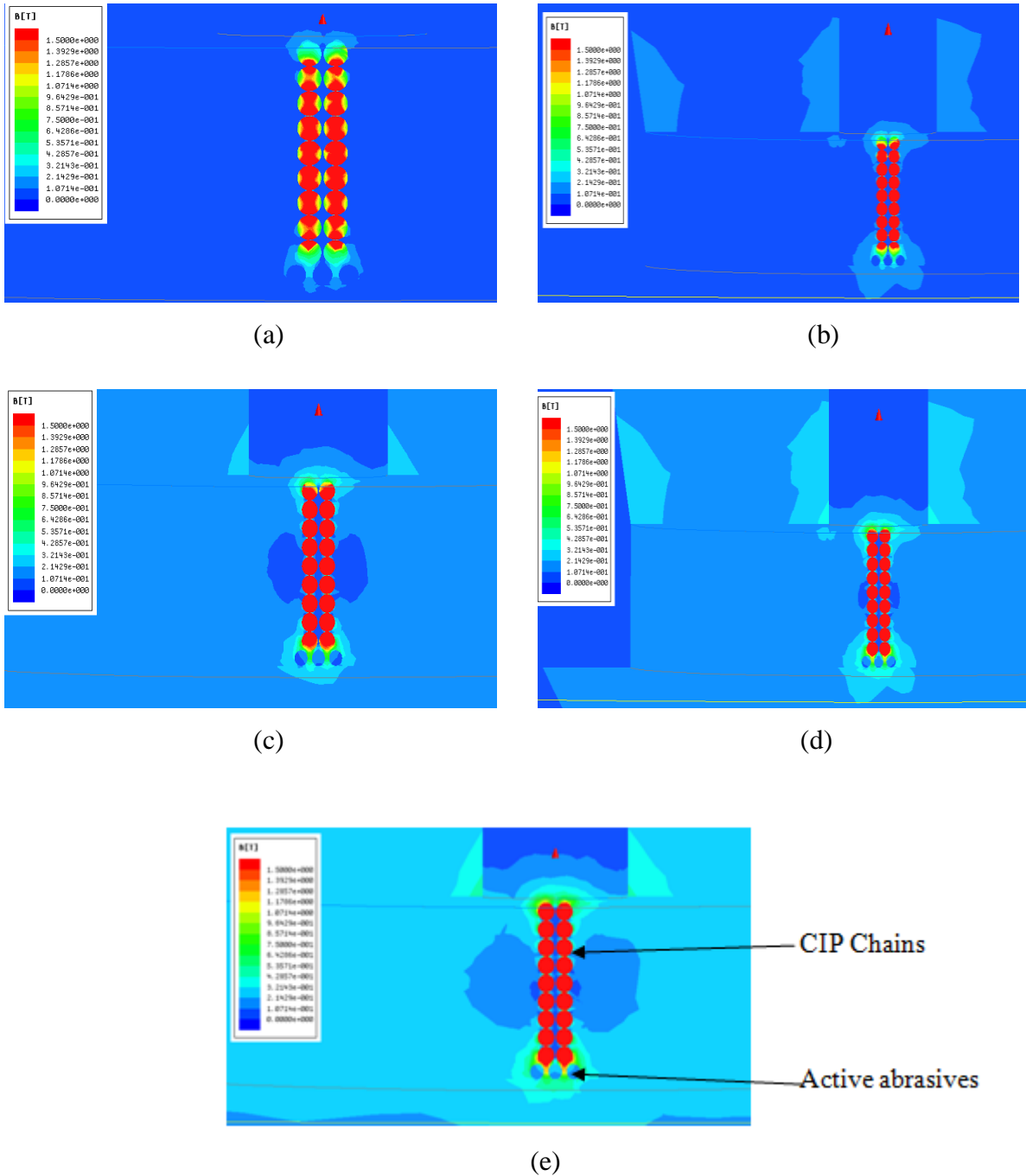


Figure 3.21 : FE simulation of the BEMRF with hollow core tool of 55 mm coil distance and 2.34 mm with Current (a) 1 amp (b) 2 amp (c) 3 amp (d) 4 amp (e) 5 amp

Table 3.9 Result analysis of forces at different magnetizing current with 2.34 mm gap and 55 mm coil distance from the tool tip surface

Force	1 amp	2 amp	3 amp	4 amp	5 amp
Average Force (N)	4.85433E-06	1.94173E-05	4.36893E-05	7.76687E-05	0.000121358

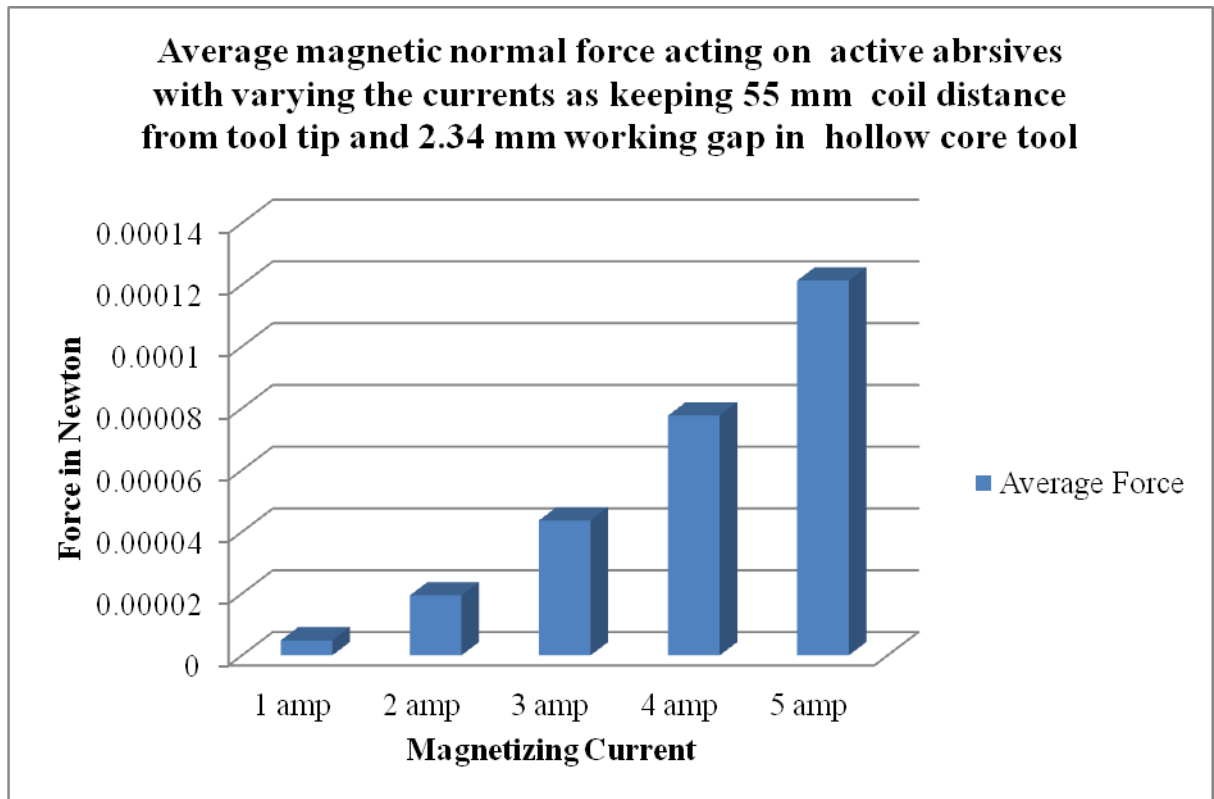


Figure 3.22 : Result analysis of force v/s current at 2.34 mm gap and 55 mm coil distance

Figure 3.22 shows the variation of magnetically induced normal force on the active abrasive particles with magnetizing current (1A to 5A) while working gap was kept as 2.34 mm and electromagnetic coil distance from the tool tip surface as 55 mm. The same result has been reported in table 3.9.

### 3.4.10 Electromagnet coil distance 60 mm and gap 0.66 mm while varying the magnetizing current from 1 amp to 5 amp

Tool modeled and simulated by taking coil distance from tool tip surface = 60 mm, diameter of rotating core = 25 mm, length of core = 245 mm, type of core = hollow, diameter of passage of MRP fluid = 2 mm, gap = 0.66 mm, number of turns of coil = 2000 turns, diameter of abrasive = 0.19 mm, diameter of CIP = 0.23 mm and number of abrasives for two CIP chain = 3. Current is varied from 1 amp per turn to 5 amp per turn to analysis the variation in effect of force due to variation in current.

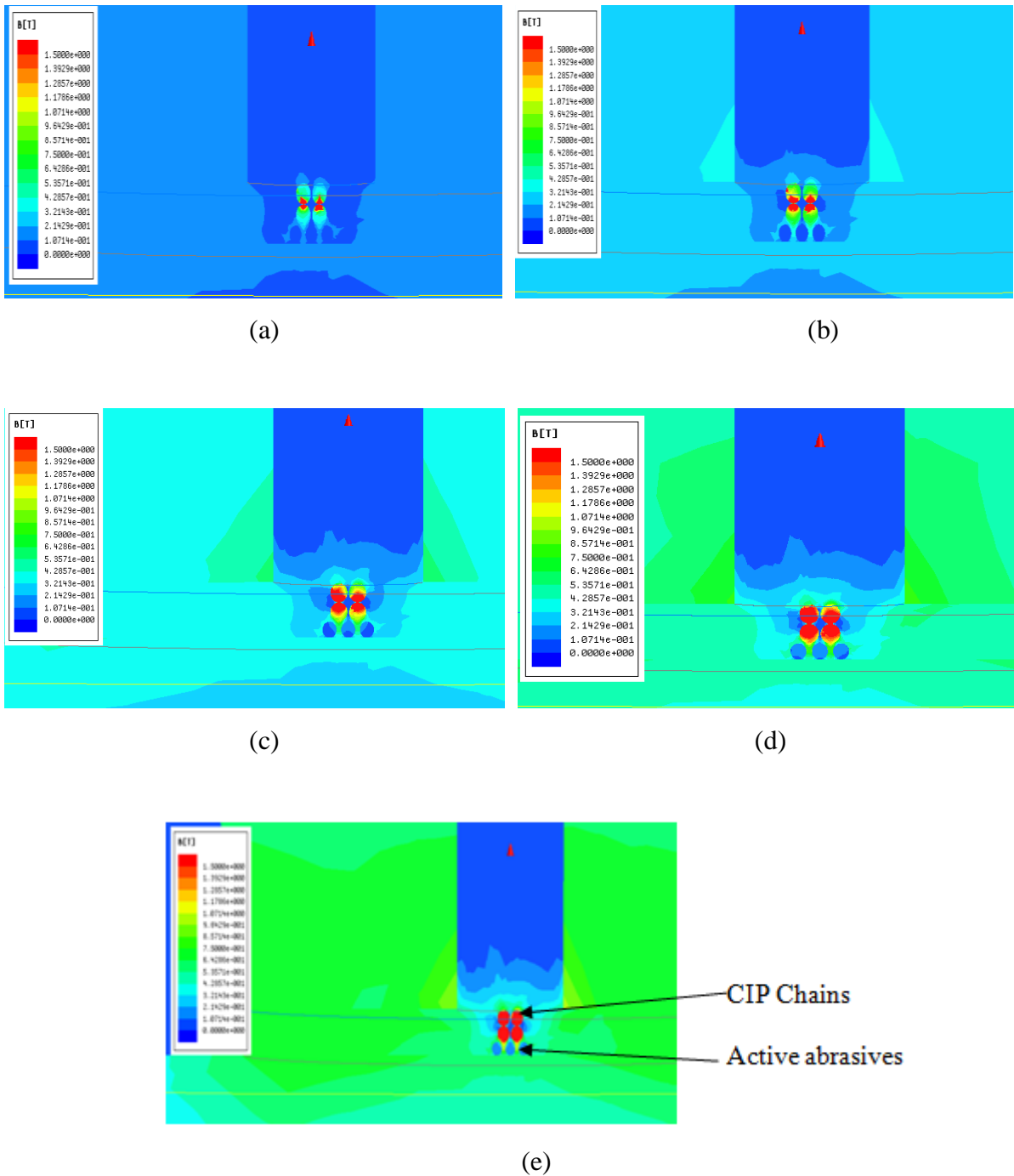


Figure 3.23 : FE simulation of the BEMRF with hollow core tool of 60 mm coil distance and 0.66 mm with current (a) 1 amp (b) 2 amp (c) 3 amp (d) 4 amp (e) 5 amp

Table 3.10 Result analysis of forces at different magnetizing current with 0.66 mm gap and 60 mm coil distance from the tool tip surface

Force	1 amp	2 amp	3 amp	4 amp	5 amp
Average Force	3.57893E-06	1.43157E-05	3.22103E-05	0.000057263	8.94733E-05

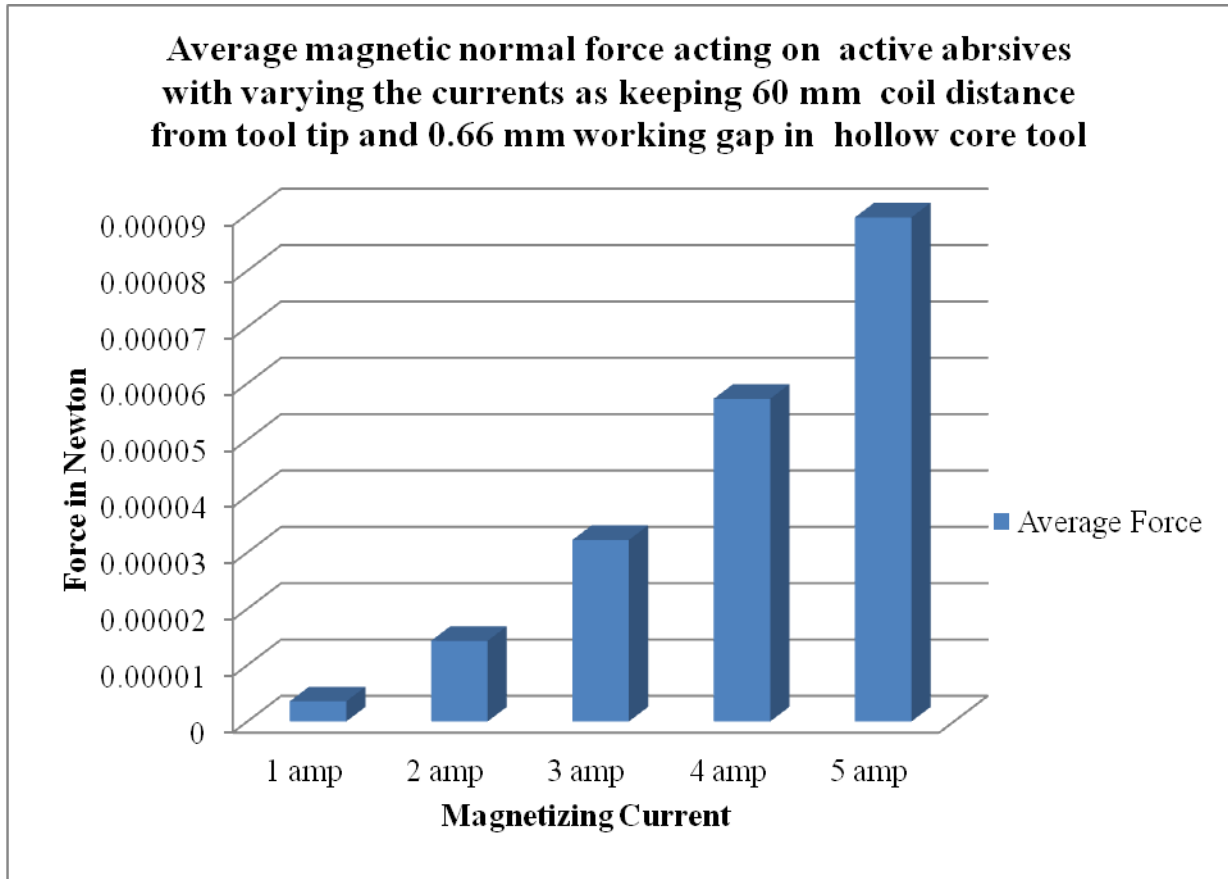


Figure 3.24 : Result analysis of force v/s current at 0.66 mm gap and 60 mm coil distance

Figure 3.24 shows the variation of magnetically induced normal force on the active abrasive particles with magnetizing current (1A to 5A) while working gap was kept as 0.66 mm and electromagnetic coil distance from the tool tip surface as 60 mm. The same result has been reported in table 3.10.

### **3.4.11 Electromagnet coil distance 60 mm and gap 1.5 mm while varying the magnetizing current from 1 amp to 5 amp**

Tool modeled and simulated by taking coil distance from tool tip surface = 60 mm, diameter of rotating core = 25 mm, length of core = 245 mm, type of core = hollow, diameter of passage of MRP fluid = 2 mm, gap = 1.5 mm, number of turns of coil = 2000 turns, diameter of abrasive = 0.19 mm, diameter of CIP = 0.23 mm and number of abrasives for two CIP chain = 3. Current is varied from 1 amp per turn to 5 amp per turn to analysis the variation in effect of force due to variation in current.

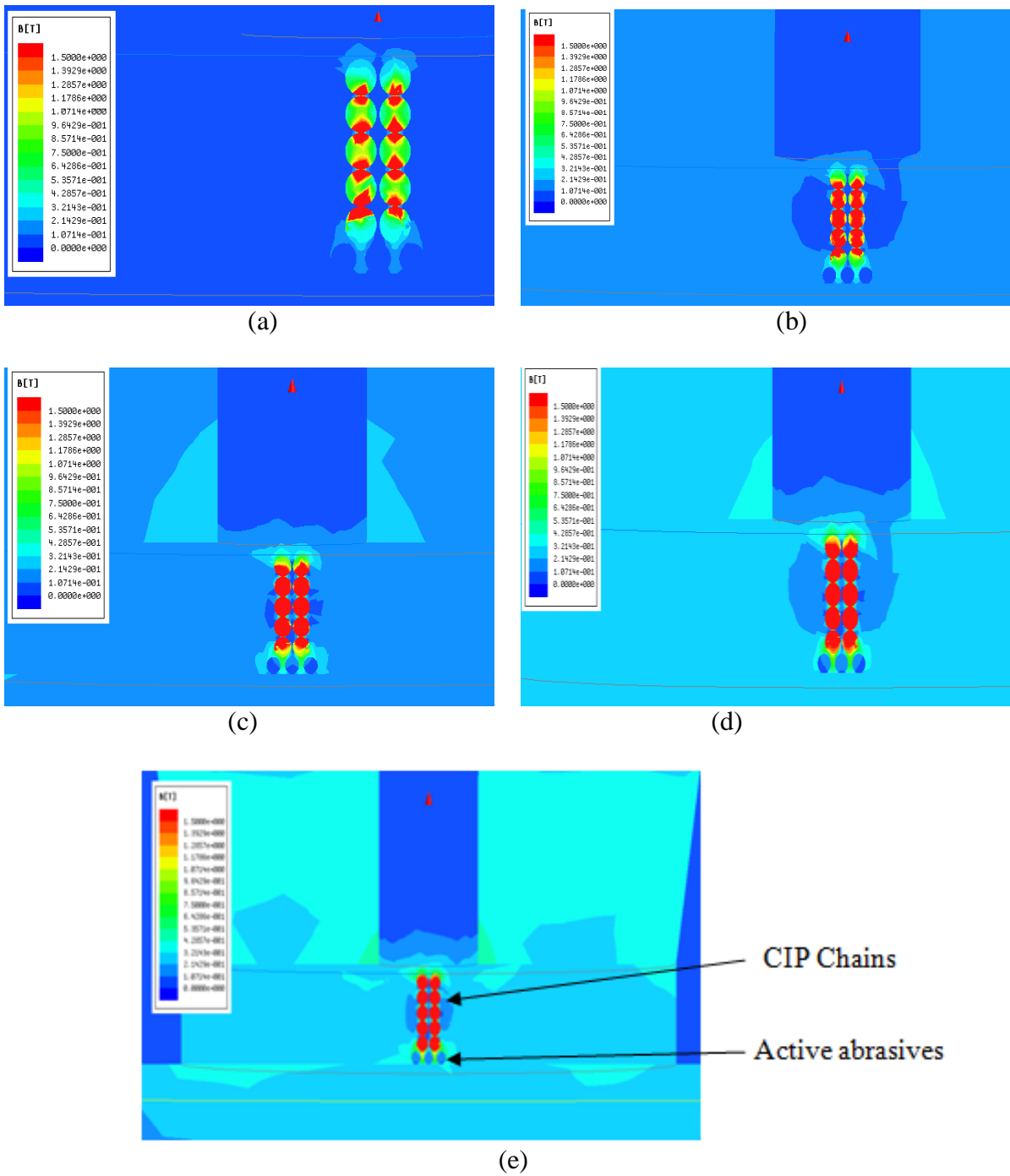


Figure 3.25 : FE simulation of the BEMRF with hollow core tool of 60 mm coil distance and 1.5 mm with Current (a) 1 amp (b) 2 amp (c) 3 amp (d) 4 amp (e) 5 amp

Table 3.11 Result analysis of forces at different magnetizing current with 1.5 mm gap and 60 mm coil distance

Force	1 amp	2 amp	3 amp	4 amp	5 amp
Average Force	0.000004742	1.89681E-05	0.000042678	7.58723E-05	0.000118551

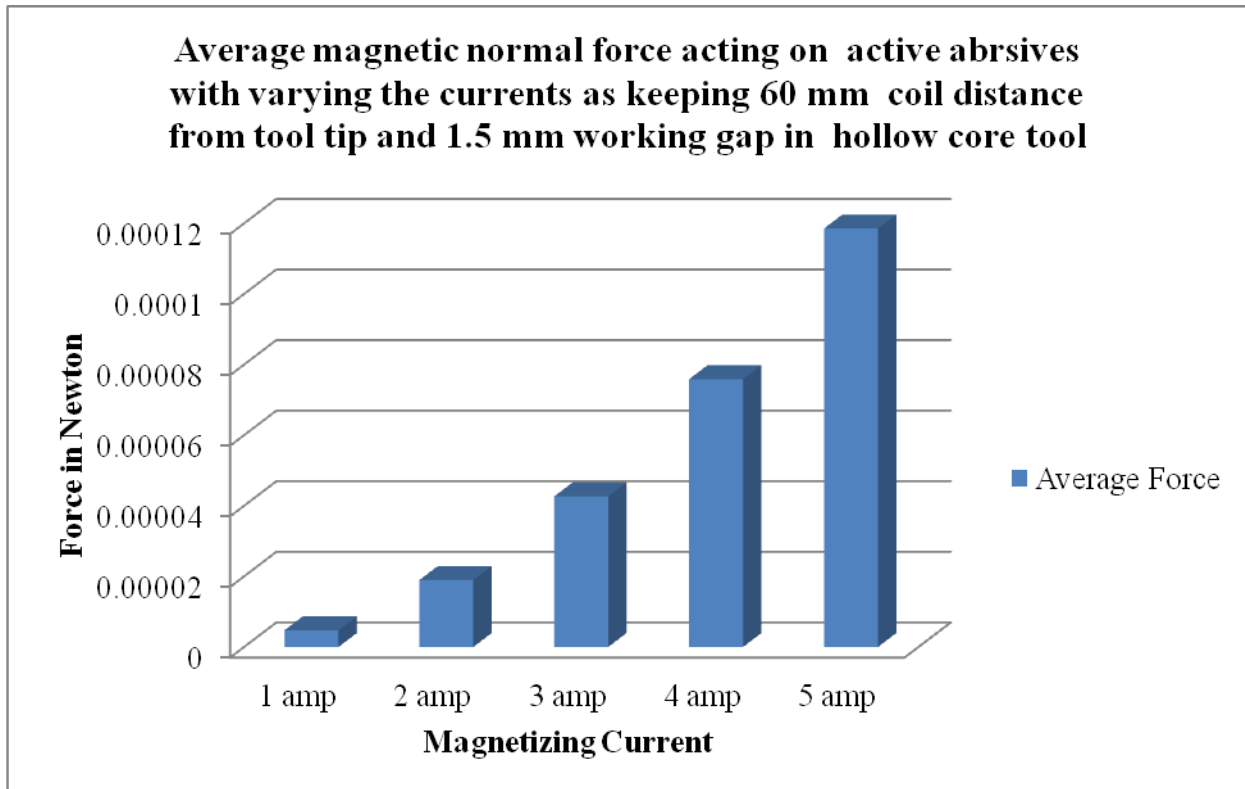


Figure 3.26 : Result analysis of force v/s current at 1.5 mm gap and 60 mm coil distance

Figure 3.26 shows the variation of magnetically induced normal force on the active abrasive particles with magnetizing current (1A to 5A) while working gap was kept as 0.66 mm and electromagnetic coil distance from the tool tip surface as 60 mm. The same result has been reported in table 3.11.

### **3.4.12 Electromagnet coil distance 60 mm and gap 2.34 mm while varying the magnetizing current from 1 amp to 5 amp**

Tool modeled and simulated by taking coil distance from tool tip surface = 60 mm, diameter of rotating core = 25 mm, length of core = 245 mm, type of core = hollow, diameter of passage of MRP fluid = 2 mm, gap = 2.34 mm, number of turns of coil = 2000 turns, diameter of abrasive = 0.19 mm, diameter of CIP = 0.23 mm and number of abrasives for two CIP chain = 3. Current is varied from 1 amp per turn to 5 amp per turn to analysis the variation in effect of force due to variation in current.

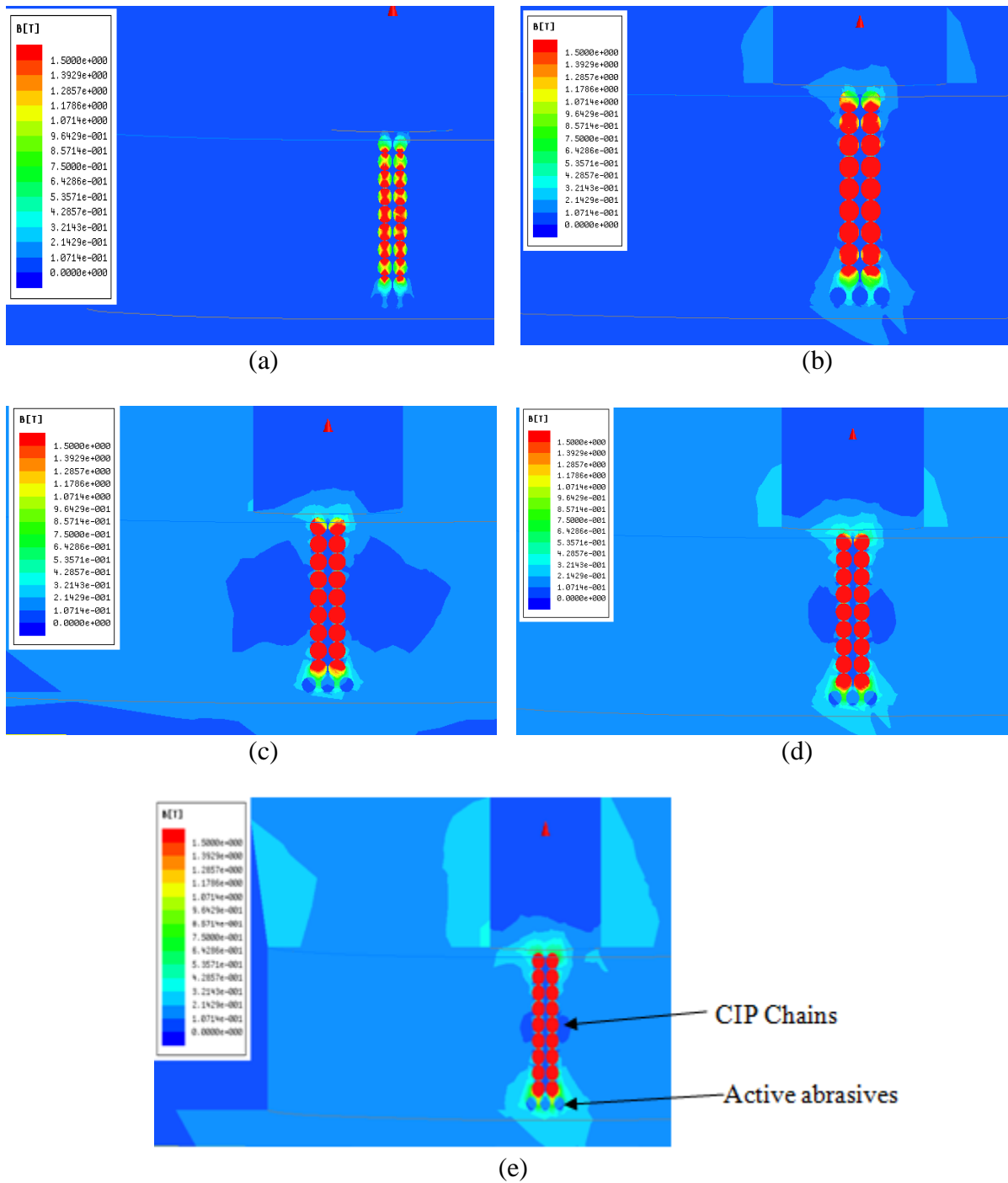


Figure 3.27 : FE simulation of the BEMRF with hollow core tool of 60 mm coil distance and 2.34 mm with Current (a) 1 amp (b) 2 amp (c) 3 amp (d) 4 amp (e) 5 amp

Table 3.12 Result analysis of forces at different magnetizing current with 2.34 mm gap and 60 mm coil distance from the tool tip surface

Force	1 amp	2 amp	3 amp	4 amp	5 amp
Average Force	3.52157E-06	1.40862E-05	3.16937E-05	0.000056345	8.80397E-05

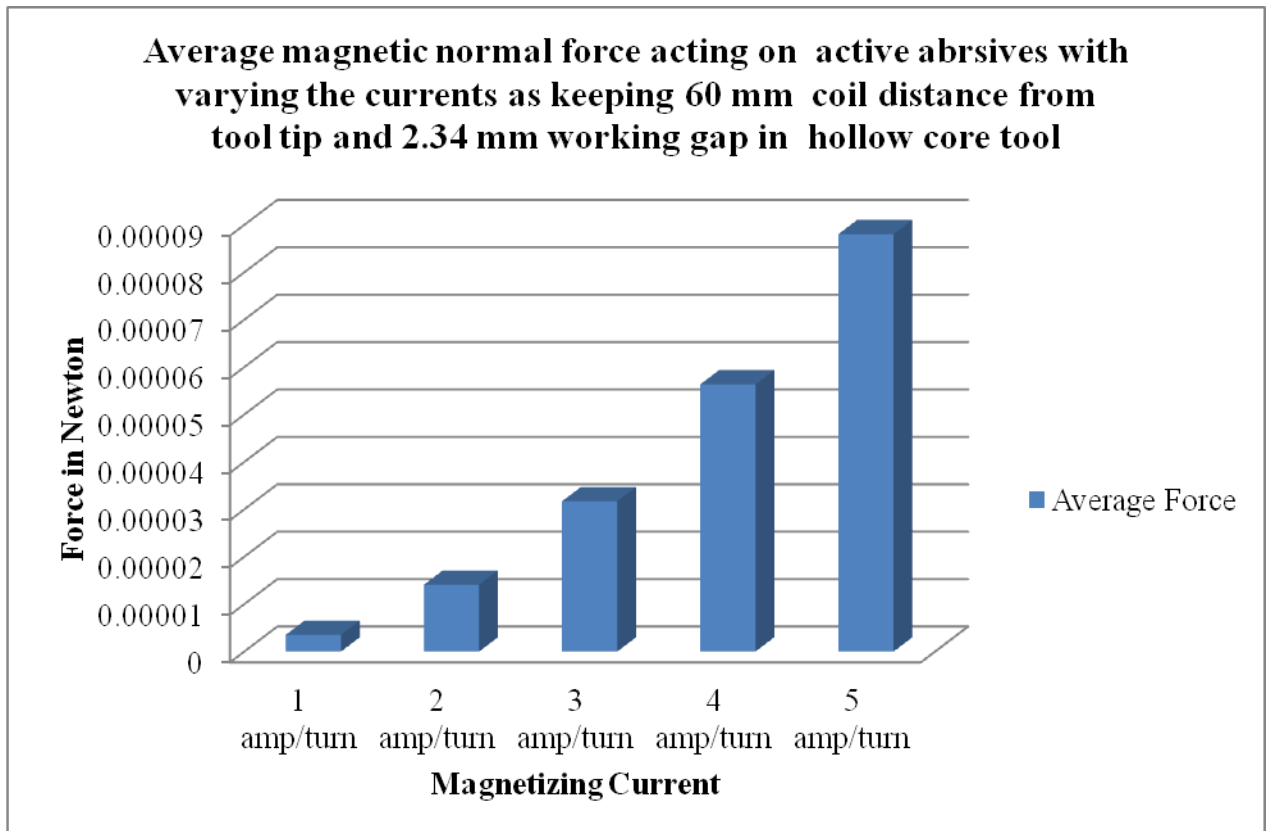


Figure 3.28 : Result analysis of force v/s current at 2.34 mm gap and 60 mm coil distance

Figure 3.28 shows the variation of magnetically induced normal force on the active abrasive particles with magnetizing current (1A to 5A) while working gap was kept as 2.34 mm and electromagnetic coil distance from the tool tip surface as 60 mm. The same result has been reported in table 3.12.

### **3.4.13 Electromagnet coil distance 65 mm and gap 0.66 mm while varying the magnetizing current from 1 amp to 5 amp**

Tool modeled and simulated by taking coil distance from tool tip surface = 65 mm, diameter of rotating core = 25 mm, length of core = 245 mm, type of core = hollow, diameter of passage of MRP fluid = 2 mm, gap = 0.66 mm, number of turns of coil = 2000 turns, diameter of abrasive = 0.19 mm, diameter of CIP = 0.23 mm and number of abrasives for two CIP chain = 3. Current is varied from 1 amp per turn to 5 amp per turn to analysis the variation in effect of force due to variation in current.

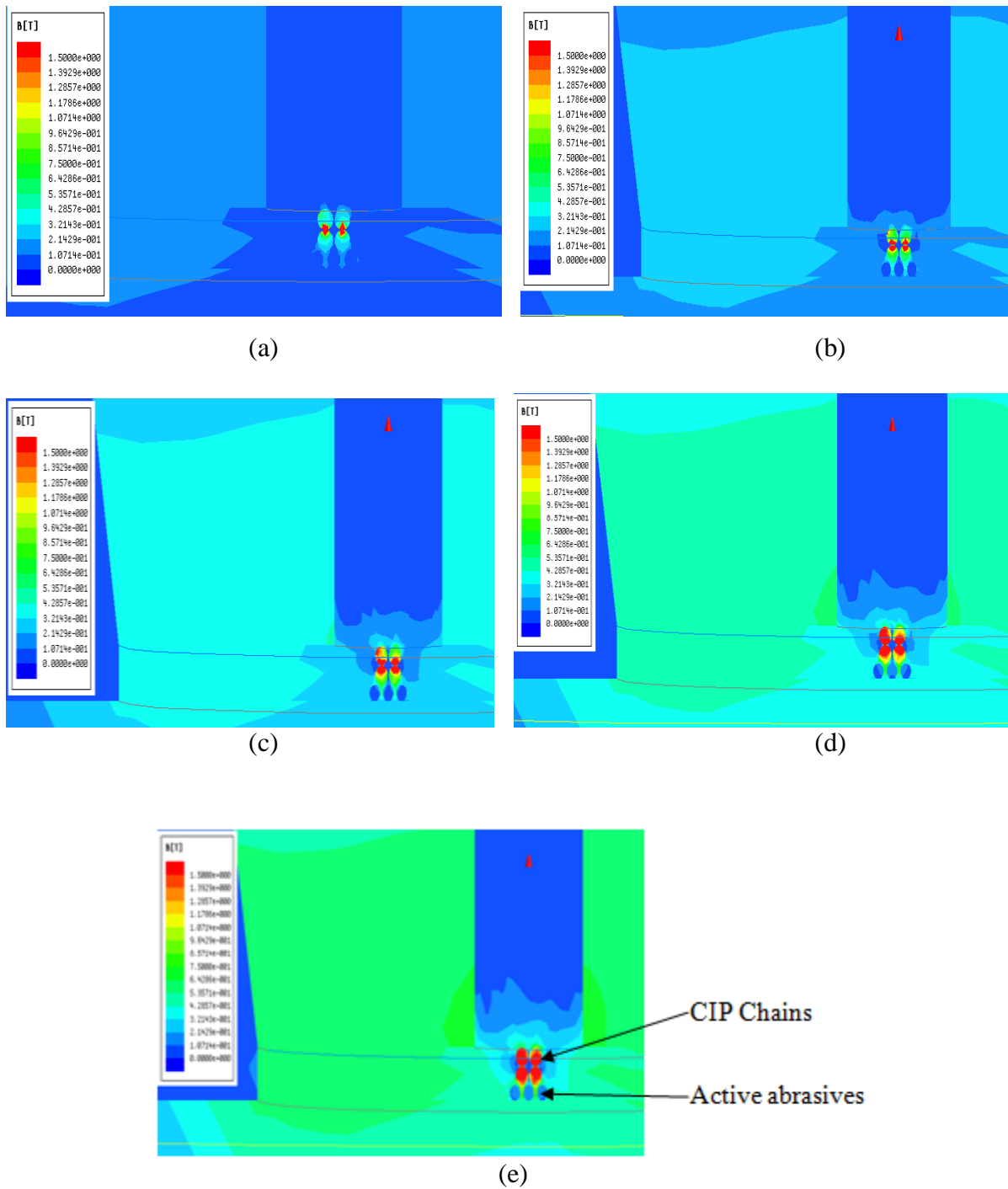


Figure 3.29 : FE simulation of the BEMRF with hollow core tool of 65 mm coil distance and 0.66 mm with Current (a) 1 amp (b) 2 amp (c) 3 amp (d) 4 amp (e) 5 amp

Table 3.13 Result analysis of forces at different magnetizing current with 0.66 mm gap and 65 mm coil distance from the tool tip surface

Force	1 amp	2 amp	3 amp	4 amp	5 amp
Average Force (N)	2.45217E-06	9.8088E-06	2.20697E-05	3.92347E-05	6.13047E-05

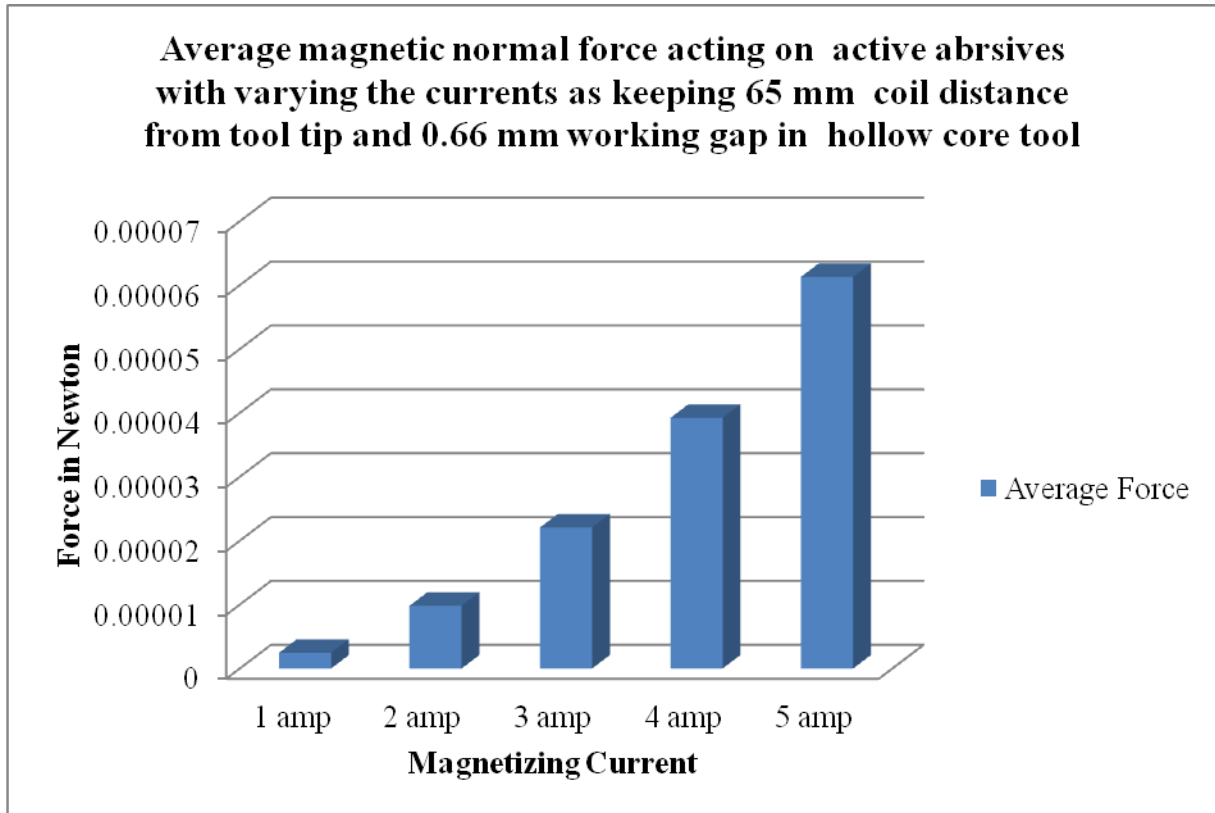


Figure 3.30 : Result analysis of force v/s current at 0.66 mm gap and 65 mm coil distance

Figure 3.30 shows the variation of magnetically induced normal force on the active abrasive particles with magnetizing current (1A to 5A) while working gap was kept as 0.66 mm and electromagnetic coil distance from the tool tip surface as 65 mm. The same result has been reported in table 3.13.

### **3.4.14 Electromagnet coil distance 65 mm and gap 1.5 mm while varying the magnetizing current from 1 amp to 5 amp**

Tool modeled and simulated by taking coil distance from tool tip surface = 65 mm, diameter of rotating core = 25 mm, length of core = 245 mm, type of core = hollow, diameter of passage of MRP fluid = 2 mm, gap = 1.5 mm, number of turns of coil = 2000 turns, diameter of abrasive = 0.19 mm, diameter of CIP = 0.23 mm and number of abrasives for two CIP chain = 3. Current is varied from 1 amp per turn to 5 amp per turn to analysis the variation in effect of force due to variation in current.

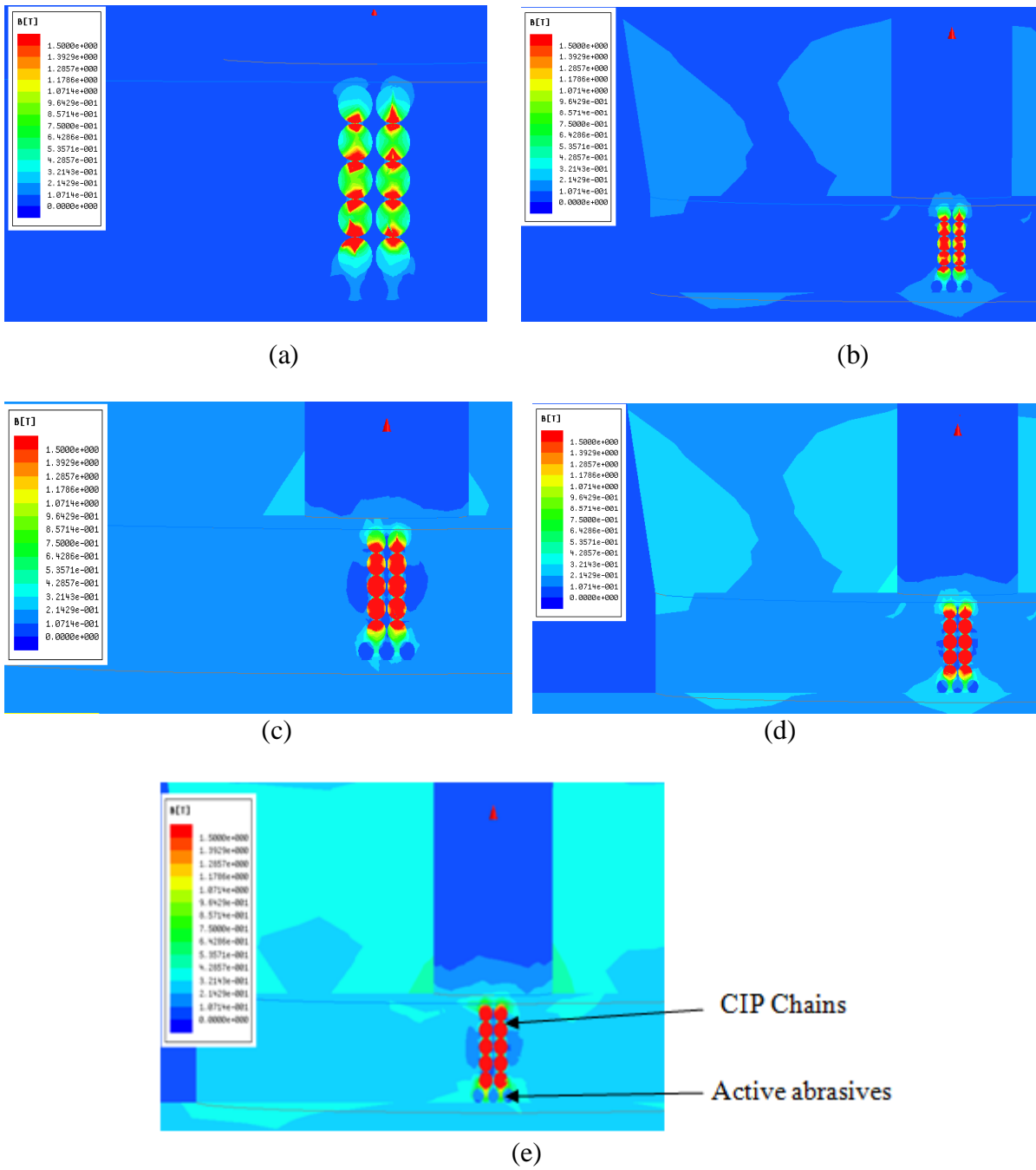


Figure 3.31 : FE simulation of the BEMRF with hollow core tool of 65 mm coil distance and 1.5 mm with Current (a) 1 amp (b) 2 amp (c) 3 amp (d) 4 amp (e) 5 amp

Table 3.14 Result analysis of forces at different magnetizing current with 1.5 mm gap and 65 mm coil distance from the tool tip surface

Force	1 amp	2 amp	3 amp	4 amp	5 amp
Average Force (N)	2.9273E-06	1.17093E-05	2.63457E-05	0.000046837	0.000073184

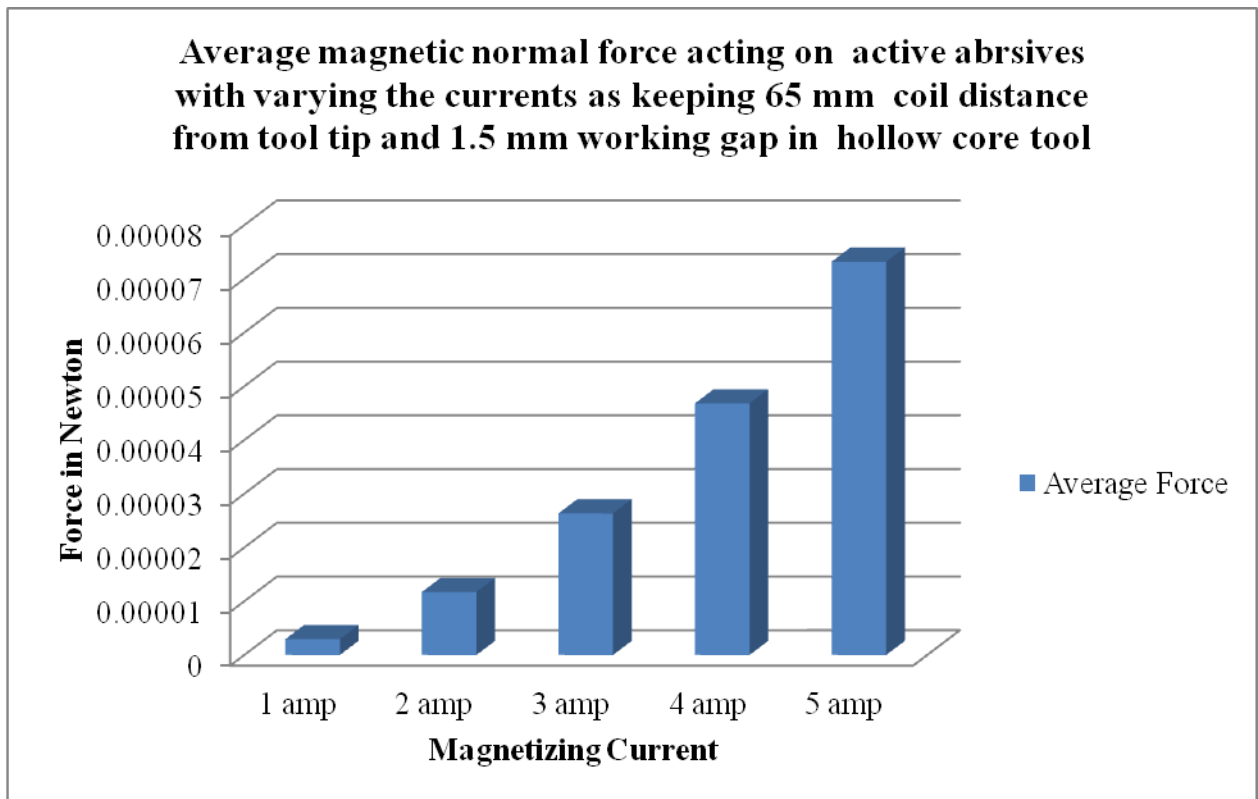


Figure 3.32 : Result analysis of force v/s current at 1.5 mm gap and 65 mm coil distance

Figure 3.32 shows the variation of magnetically induced normal force on the active abrasive particles with magnetizing current (1A to 5A) while working gap was kept as 1.5 mm and electromagnetic coil distance from the tool tip surface as 65 mm. The same result has been reported in table 3.14.

### 3.4.15 Electromagnet coil distance 65 mm and gap 2.34 mm while varying the magnetizing current from 1 amp to 5 amp

Tool modeled and simulated by taking coil distance from tool tip surface = 65 mm, diameter of rotating core = 25 mm, length of core = 245 mm, type of core = hollow, diameter of passage of MRP fluid = 2 mm, gap = 2.34 mm, number of turns of coil = 2000 turns, diameter of abrasive = 0.19 mm, diameter of CIP = 0.23 mm and number of abrasives for two CIP chain = 3. Current is varied from 1 amp per turn to 5 amp per turn to analysis the variation in effect of force due to variation in current.

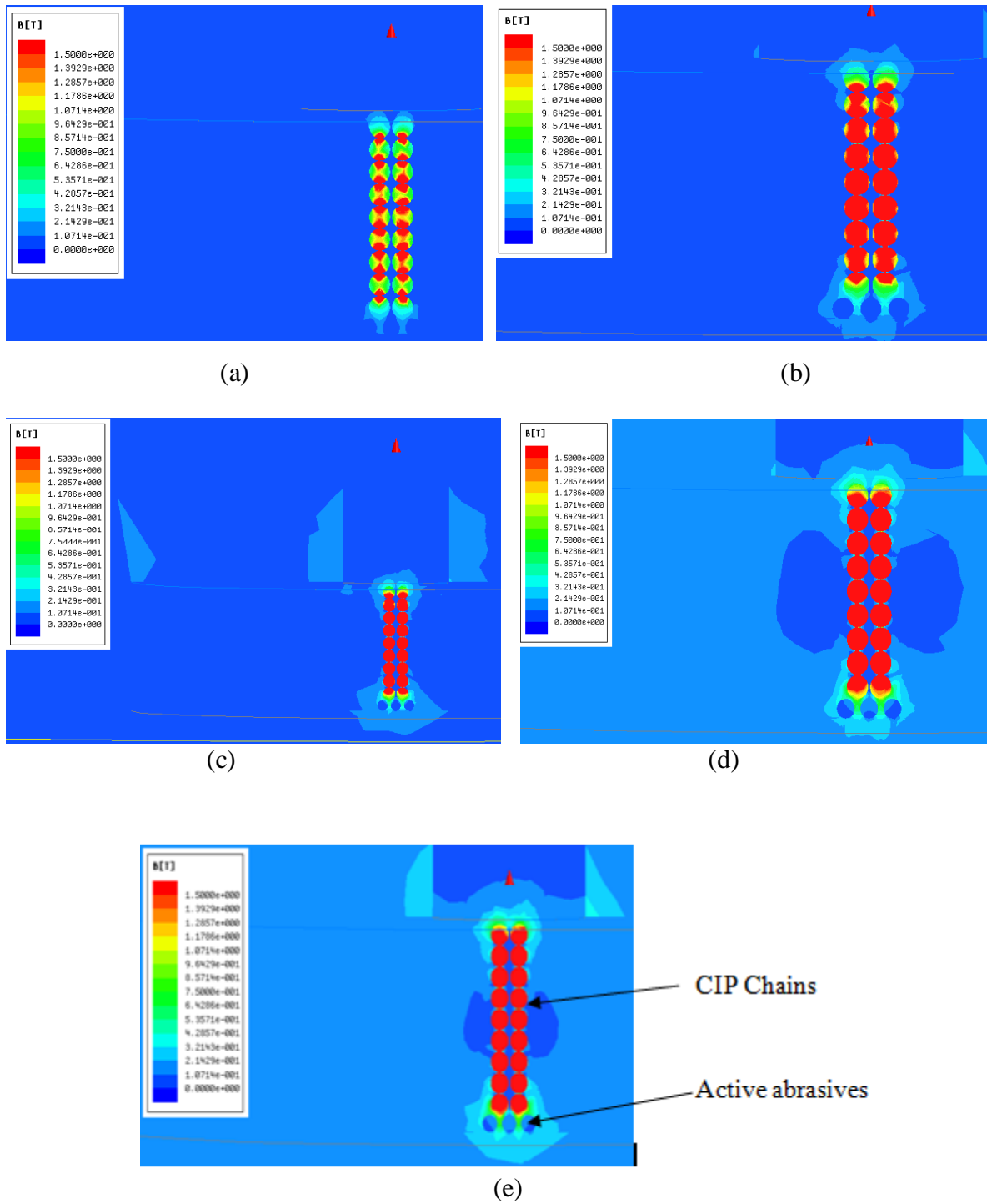


Figure 3.33: FE simulation of the BEMRF with hollow core tool of 65 mm coil distance and 2.34 mm with Current (a) 1 amp (b) 2 amp (c) 3 amp (d) 4 amp (e) 5 amp

Table 3.15 Result analysis of forces at different magnetizing current with 2.34 mm gap and 65 mm coil distance from the tool tip surface

Force	1 amp	2 amp	3 amp	4 amp	5 amp
Average Force	2.51724E-06	1.00691E-05	2.26552E-05	0.000040276	6.29297E-05

(N)

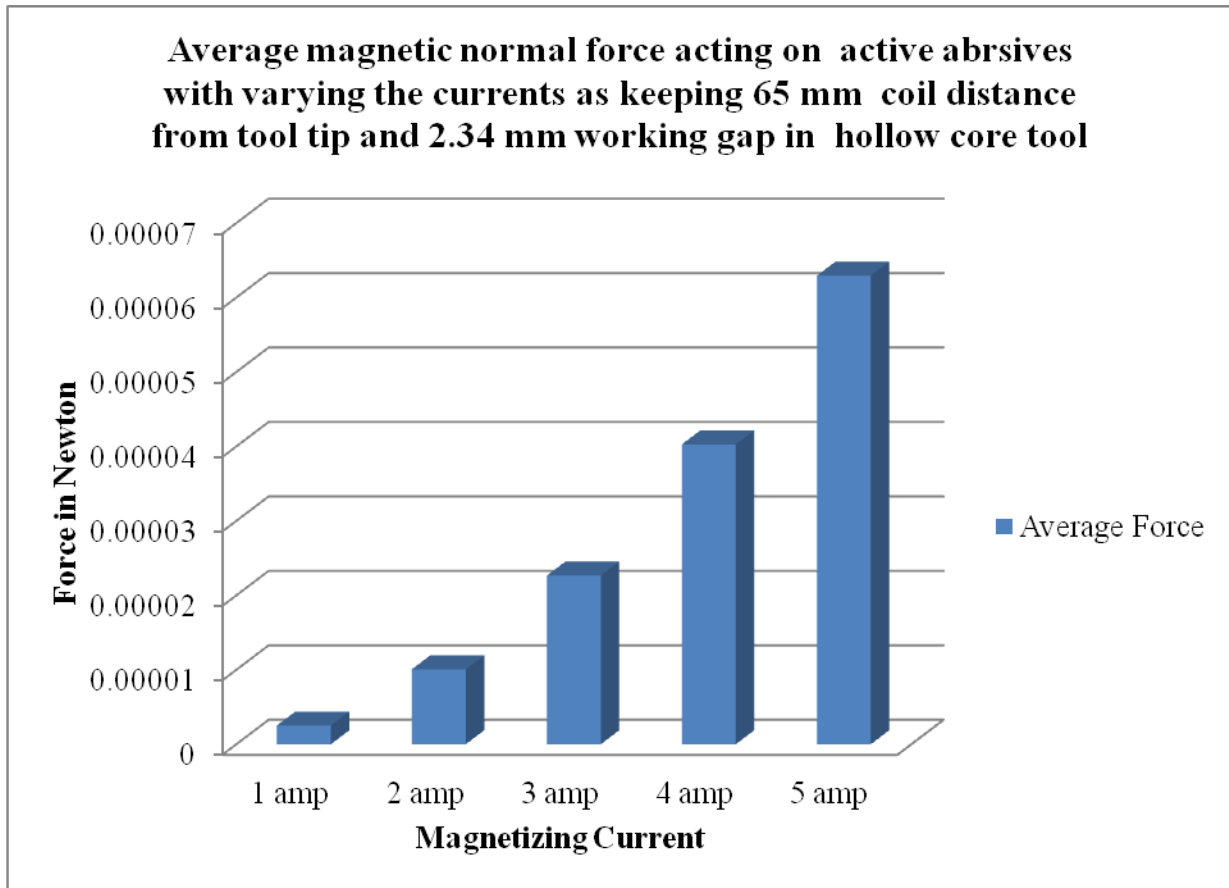


Figure 3.34 : Result analysis of force v/s current at 2.34 mm gap and 65 mm coil distance

Figure 3.34 shows the variation of magnetically induced normal force on the active abrasive particles with magnetizing current (1A to 5A) while working gap was kept as 2.34 mm and electromagnetic coil distance from the tool tip surface as 65 mm. The same result has been reported in table 3.15.

### 3.5 Electromagnetic modeling of ball end type magnetorheological finishing (BEMRF) tool with solid core

The electromagnetic modeling of BEMRF solid core tool was done using Maxwell Ansoft V13 software (student version) as shown in figure 3.3. The iron with a relative permeability of 600 has been assigned for central rotating core of diameter 25 mm and length of 245 mm

(Singh *et. al*, 2013). Material has been assigned for coil is copper with relative permeability 1 and the number of turns of coil are 2000. Ferromagnetic material with relative permeability 600 has been assigned for the workpiece of diameter 40 mm and height 5mm. There is a working gap between tool tip surface and ferromagnetic workpiece surface. The actual size of active abrasive particle and carbonyl iron particles was 19  $\mu\text{m}$  and 23  $\mu\text{m}$  respectively, but for visibility during finite element it has been taken ten times of actual size. Active abrasives of 0.19 mm are closely surrounded by chains of 0.23 mm CIPs between the working gap. Force parameter is also assigned to abrasive and CIP. The three abrasives have been plotted on the surface of the workpiece and the results of finite element magnetostatic simulation for magnetic normal force acting on the three active abrasives has been considered as average of three magnetic normal forces. The electromagnet model of ball end type magnetorheological finishing hollow core tool is shown in figure 3.35 and carbonyl iron particle arrangement with hollow core tool is shown in figure 3.36.

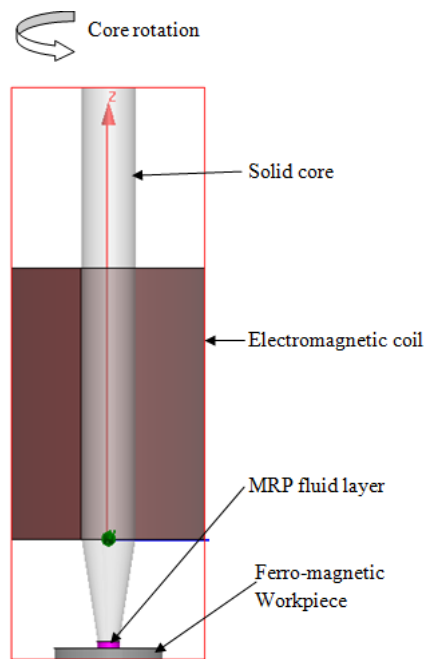


Figure 3.35: Electromagnet model of ball end type magnetorheological finishing solid core tool

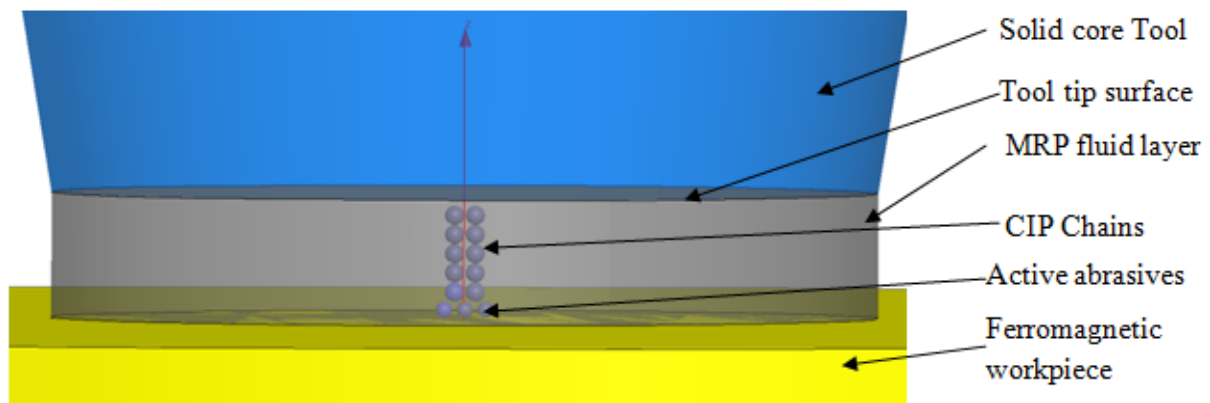


Figure 3.36 CIP chain arrangements in working gap with solid core tool

### 3.6 Finite Element (FE) Analysis of BEMRF process for solid core tool

In solid core tool there is a solid rotating core and MRP fluid is directly applied to tool tip surface. The layers of MRP fluid on tool tip get stiffened by magnetic field and take the shape of a ball end. Performing the simulation to analysis the effect of CIP chain on active abrasive particles after modeling of BEMRF tool along with MRP fluid and work piece. The main objective of this analysis to find out the magnitude of forces on active abrasives by variation in current density, coil position and gap between tool tip and work piece surface and compare the results with hollow core tool results. Different cases considered for analysi :-

- Electromagnet coil distance 45 mm and gap 0.66 mm while varying the magnetizing current from 1 amp to 5 amp
- Electromagnet coil distance 45 mm and gap 1.5 mm while varying the magnetizing current from 1 amp to 5 amp
- Electromagnet coil distance 45 mm and gap 2.34 mm while varying the magnetizing current from 1 amp to 5 amp
- Electromagnet coil distance 50 mm and gap 0.66 mm while varying the magnetizing current from 1 amp to 5 amp
- Electromagnet coil distance 50 mm and gap 1.5 mm while varying the magnetizing current from 1 amp to 5 amp
- Electromagnet coil distance 50 mm and gap 2.34 mm while varying the magnetizing current from 1 amp to 5 amp

### 3.6.1 Electromagnet coil distance 45 mm and gap 0.66 mm while varying the magnetizing current from 1 amp to 5 amp

Tool modeled and simulated by taking coil distance from tool tip surface = 45 mm, diameter of rotating core = 25 mm, length of core = 245 mm, type of core = solid, gap = 0.66 mm, number of turns of coil = 2000 turns, diameter of abrasive = 0.19 mm, diameter of CIP = 0.23 mm and number of abrasives for two CIP chain = 3. Current is varied from 1 amp per turn to 5 amp per turn to analysis the variation in effect of force due to variation in current.

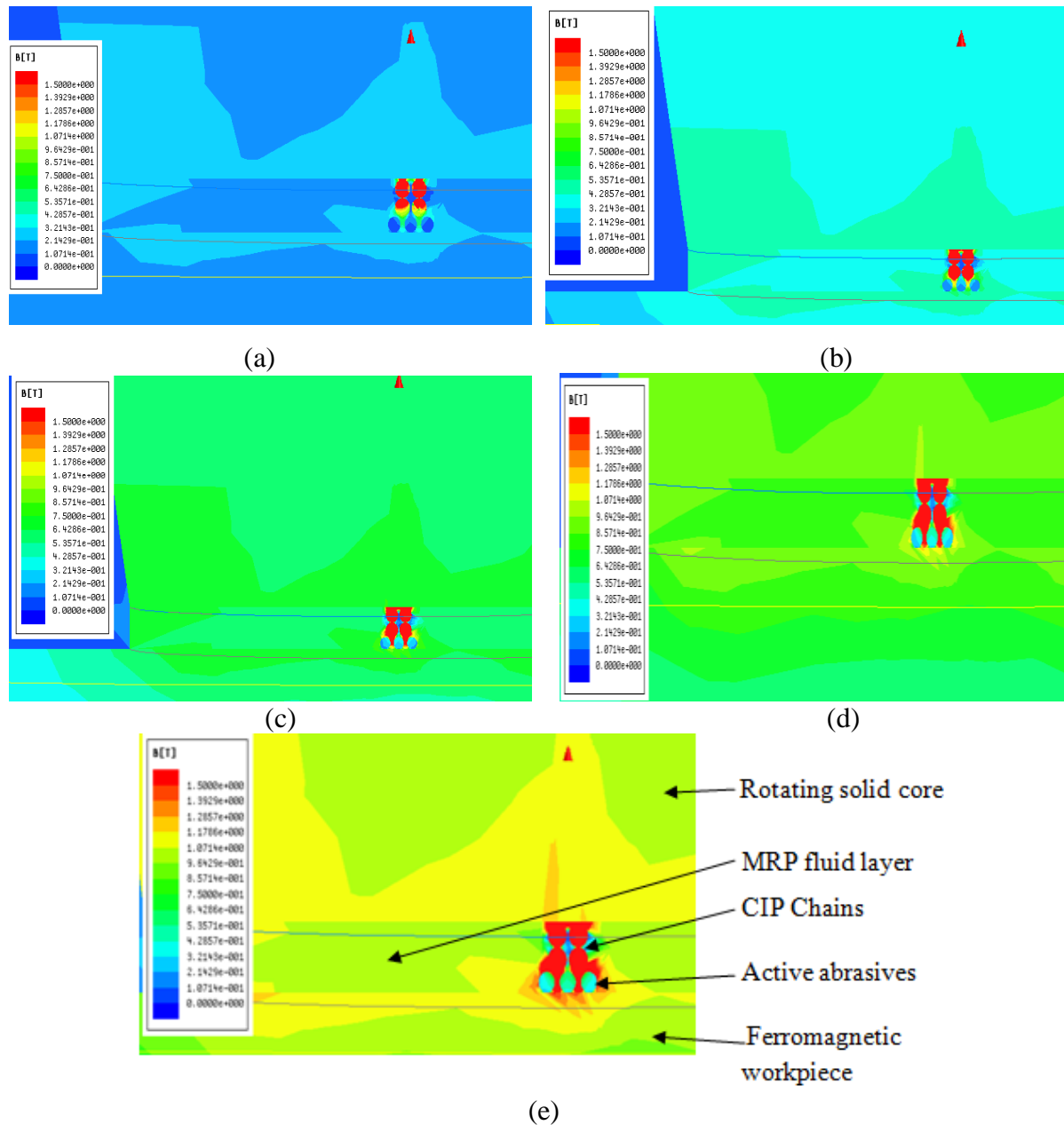


Figure 3.37 : FE simulation of the BEMRF with solid core tool of 45 mm coil distance and 0.66 mm with Current (a) 1 amp (b) 2 amp (c) 3 amp (d) 4 amp (e) 5 amp

Table 3.16 Result analysis of forces at different magnetizing current with 0.66 mm gap and 45 mm coil distance from the tool tip surface in solid core

S.No	Abrasive	1 amp	2 amp	3 amp	4 amp	5 amp
1	Average force (N)	2.656E-05	0.0001062	0.00023904	0.00042496	0.00066401

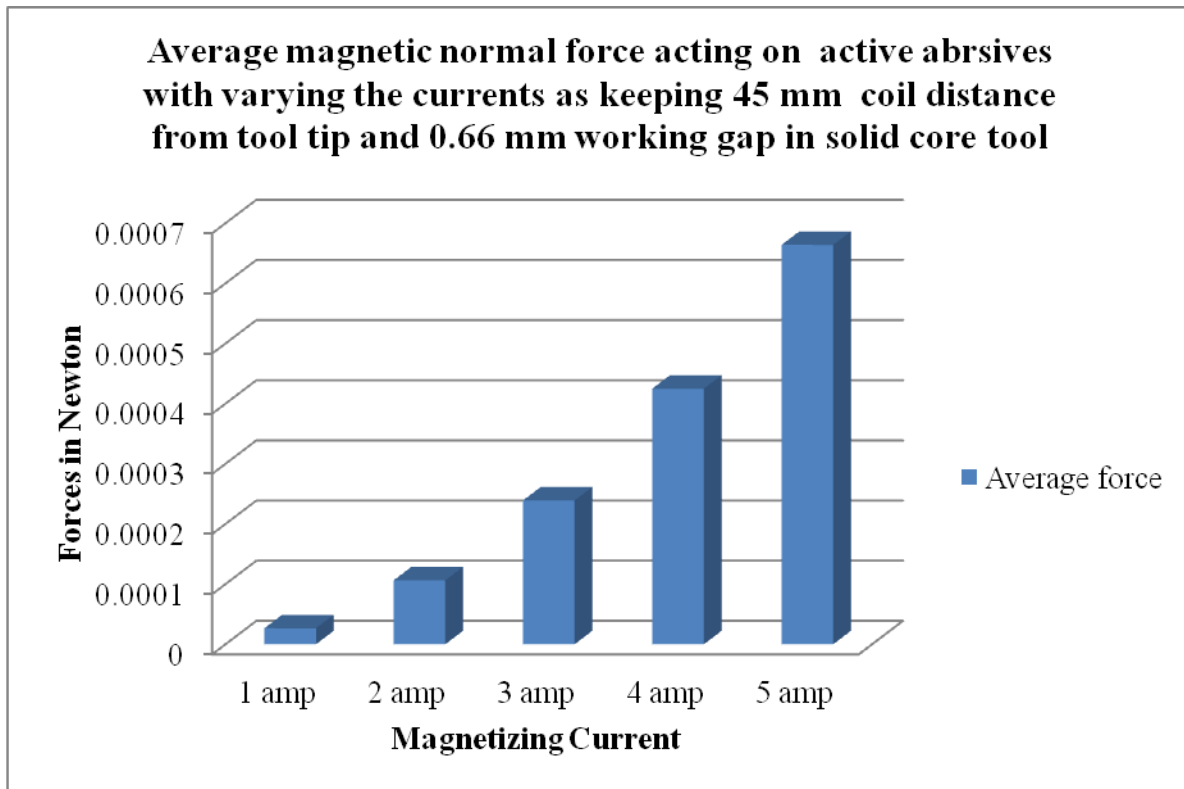


Figure 3.38 : Result analysis of force v/s current at 0.66 mm gap and 45 mm coil distance in solid core

Figure 3.38 shows the variation of magnetically induced normal force on the active abrasive particles with magnetizing current (1A to 5A) while working gap was kept as 0.66 mm and electromagnetic coil distance from the tool tip surface as 45 mm with solid core tool. The same result has been reported in table 3.16.

### 3.6.2 Electromagnet coil distance 45 mm and gap 1.5 mm while varying the magnetizing current from 1 amp to 5 amp

Tool modeled and simulated by taking coil distance from tool tip surface = 45 mm, diameter of rotating core = 25 mm, length of core = 245 mm, type of core = solid, gap = 1.5 mm,

number of turns of coil = 2000 turns, diameter of abrasive = 0.19 mm, diameter of CIP = 0.23 mm and number of abrasives for two CIP chain = 3. Current density is varied from 1 amp per turn to 5 amp per turn to analysis the variation in effect of force due to variation in current

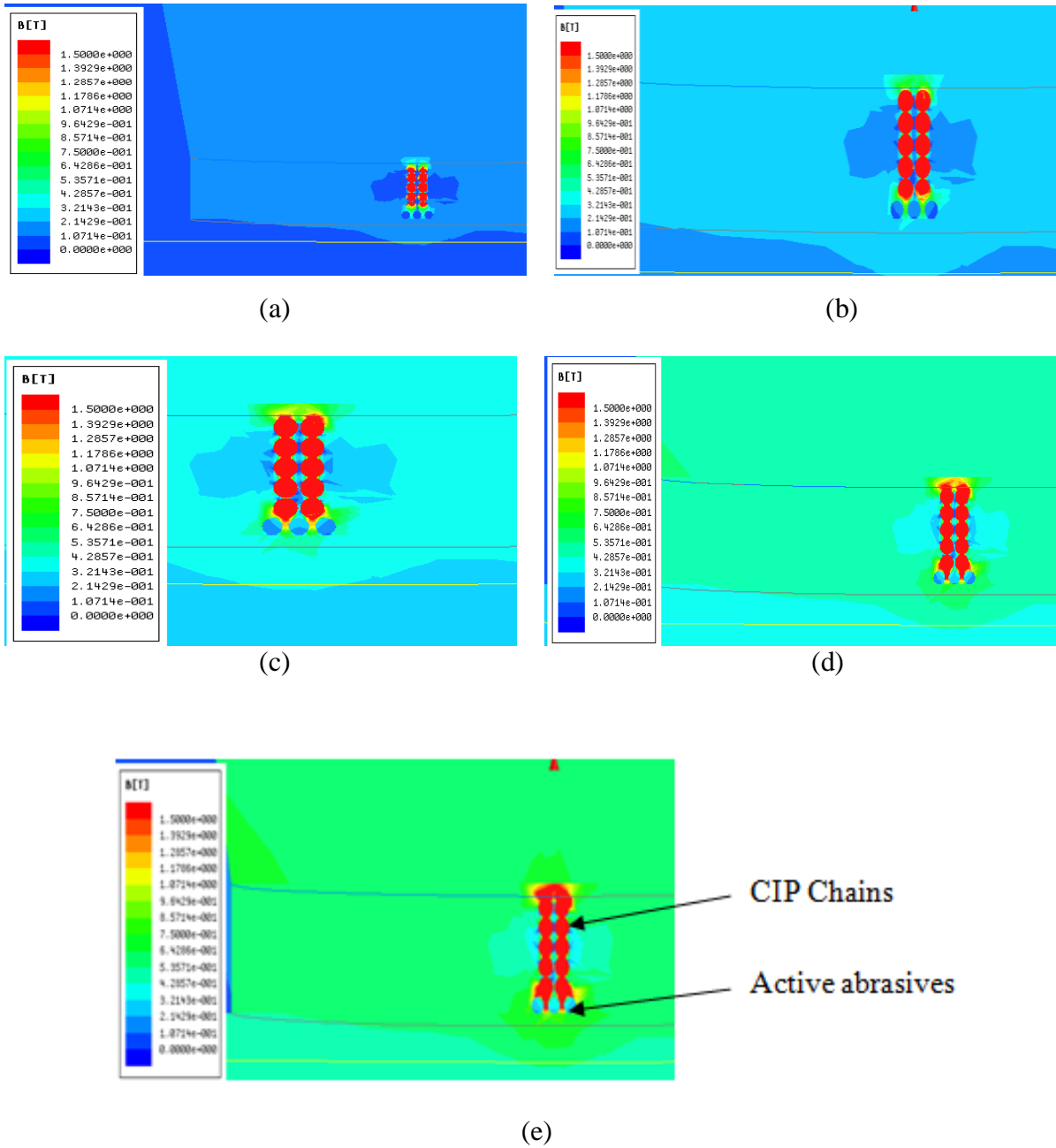


Figure 3.39 : FE simulation of the BEMRF with solid core tool of 45 mm coil distance and 1.5 mm with Current (a) 1 amp (b) 2 amp (c) 3 amp (d) 4 amp (e) 5 amp

Table 3.17 Result analysis of forces at different magnetizing current with 1.5 mm gap and 45 mm coil distance from the tool tip surface in solid core

S.No	Abrasive	1 amp	2 amp	3 amp	4 amp	5 amp
1	Average force (N)	1.93267E-05	7.731E-05	0.000173937	0.000309223	0.000483163

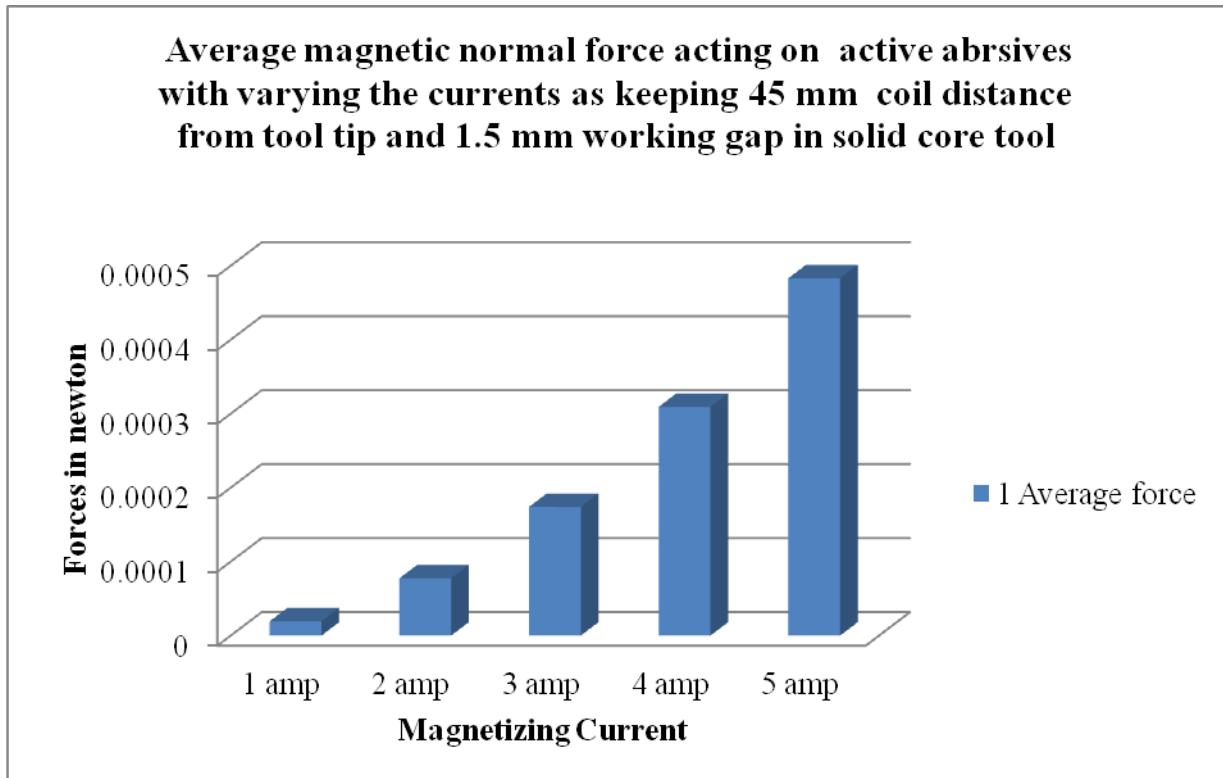


Figure 3.40 : Result analysis of force v/s current at 1.5 mm gap and 45 mm coil distance in solid core

Figure 3.40 shows the variation of magnetically induced normal force on the active abrasive particles with magnetizing current (1A to 5A) while working gap was kept as 1.5 mm and electromagnetic coil distance from the tool tip surface as 45 mm with solid core tool. The same result has been reported in table 3.17.

### 3.6.3 Electromagnet coil distance 45 mm and gap 2.34 mm while varying the magnetizing current from 1 amp to 5 amp

Tool modeled and simulated by taking coil distance from tool tip surface = 45 mm, diameter of rotating core = 25 mm, length of core = 245 mm, type of core = solid, gap = 2.34 mm, number of turns of coil = 2000 turns, diameter of abrasive = 0.19 mm, diameter of CIP = 0.23

mm and number of abrasives for two CIP chain = 3. Current density is varied from 1 amp per turn to 5 amp per turn to analysis the variation in effect of force due to variation in current

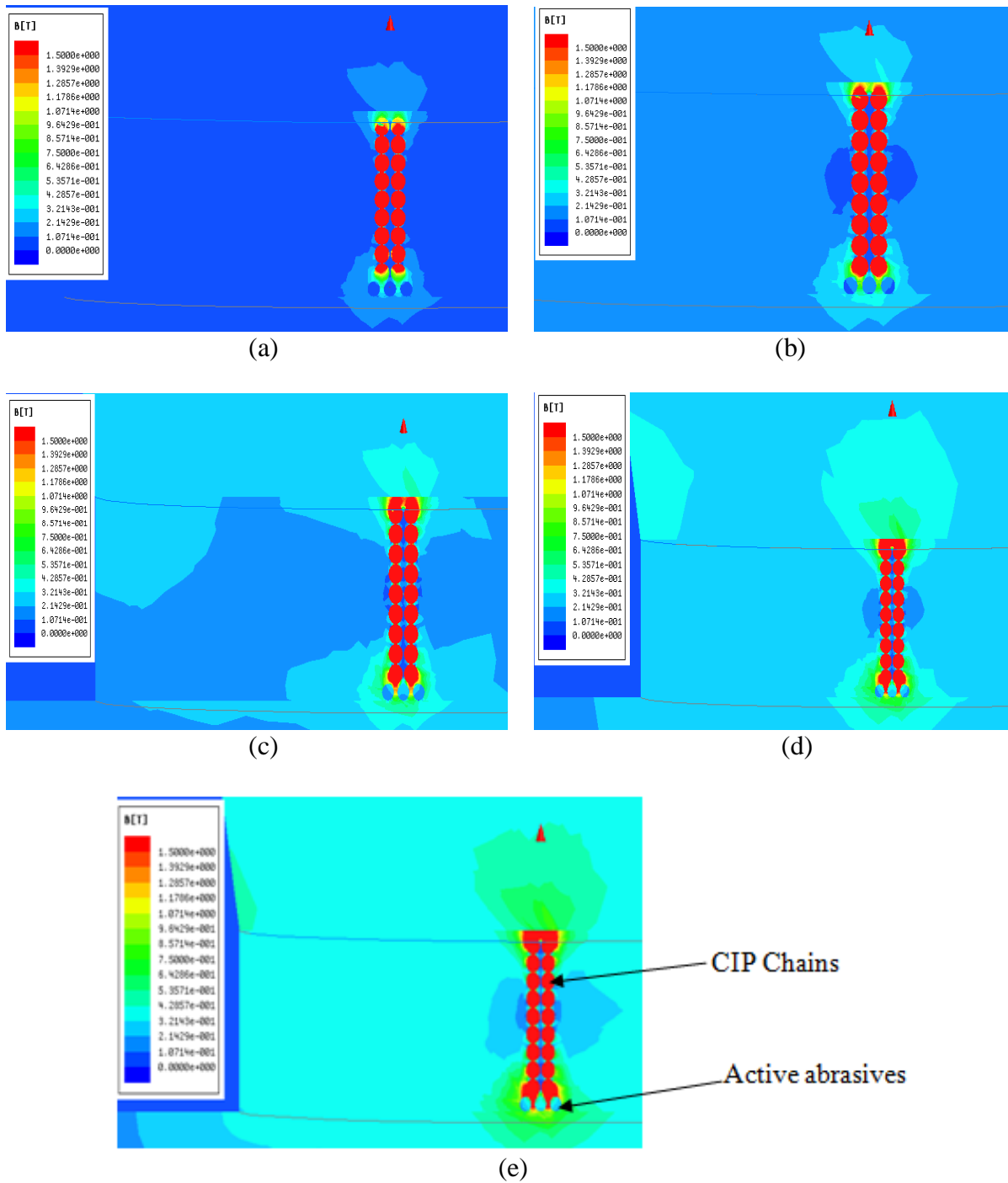


Figure 3.41 : FE simulation of the BEMRF with solid core tool of 45 mm coil distance and 2.34 mm with Current (a) 1 amp (b) 2 amp (c) 3 amp (d) 4 amp (e) 5 amp

Table 3.18 Result analysis of forces at different magnetizing current with 2.34 mm gap and 45 mm coil distance from the tool tip surface in solid core

Force	1 amp	2 amp	3 amp	4 amp	5 amp
Average Force (N)	4.56487E-05	0.000182592	0.000410837	0.000730387	0.001141203

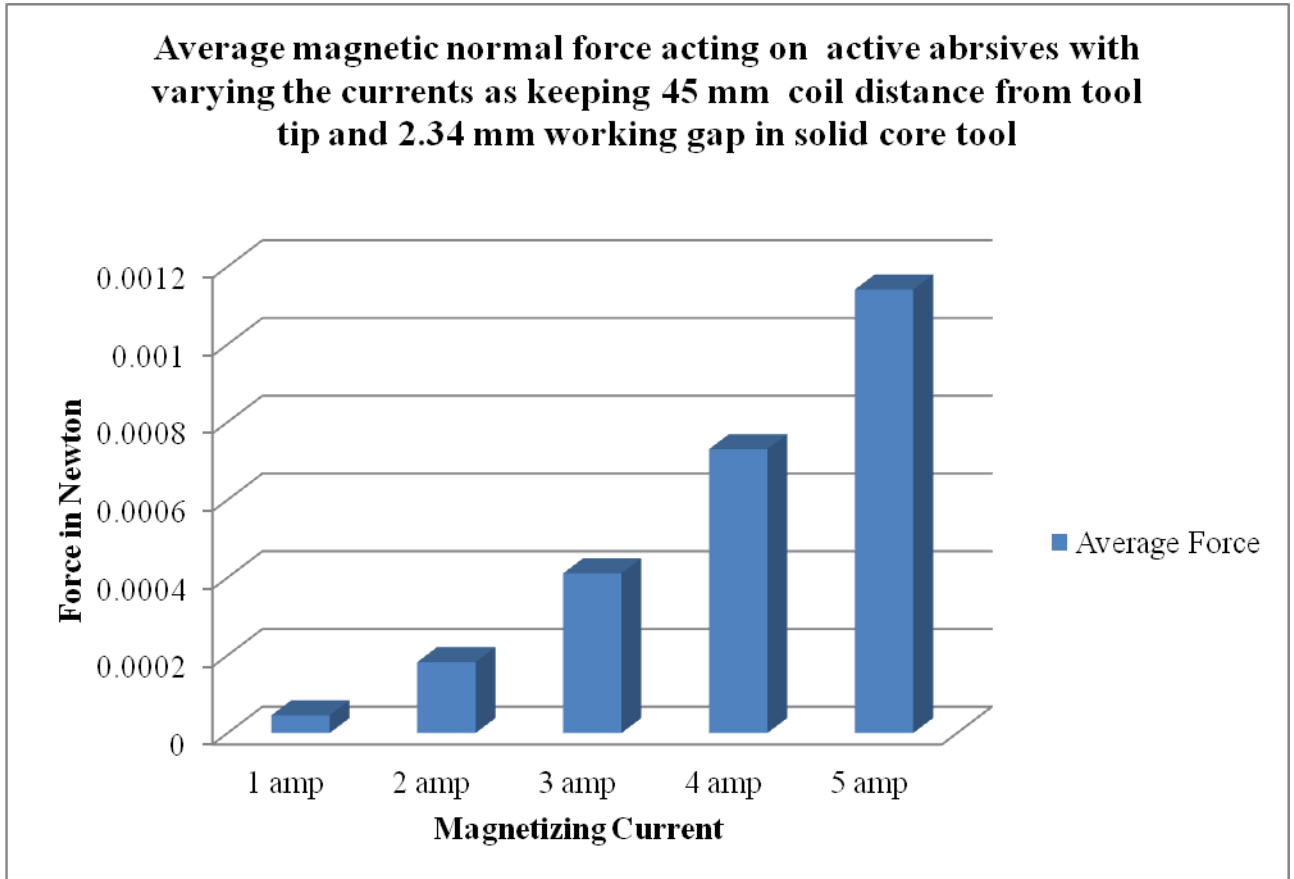


Figure 3.42 : Result analysis of force v/s current at 2.34 mm gap and 45 mm coil distance in solid core

Figure 3.42 shows the variation of magnetically induced normal force on the active abrasive particles with magnetizing current (1A to 5A) while working gap was kept as 2.34 mm and electromagnetic coil distance from the tool tip surface as 45 mm. The same result has been reported in table 3.18.

### 3.6.4 Electromagnet coil distance 50 mm and gap 0.66 mm while varying the magnetizing current from 1 amp to 5 amp

Tool modeled and simulated by taking coil distance from tool tip surface = 50 mm, diameter of rotating core = 25 mm, length of core = 245 mm, type of core = solid, gap = 0.66 mm, number of turns of coil = 2000 turns, diameter of abrasive = 0.19 mm, diameter of CIP = 0.23

mm and number of abrasives for two CIP chain = 3. Current density is varied from 1 amp per turn to 5 amp per turn to analysis the variation in effect of force due to variation in current.

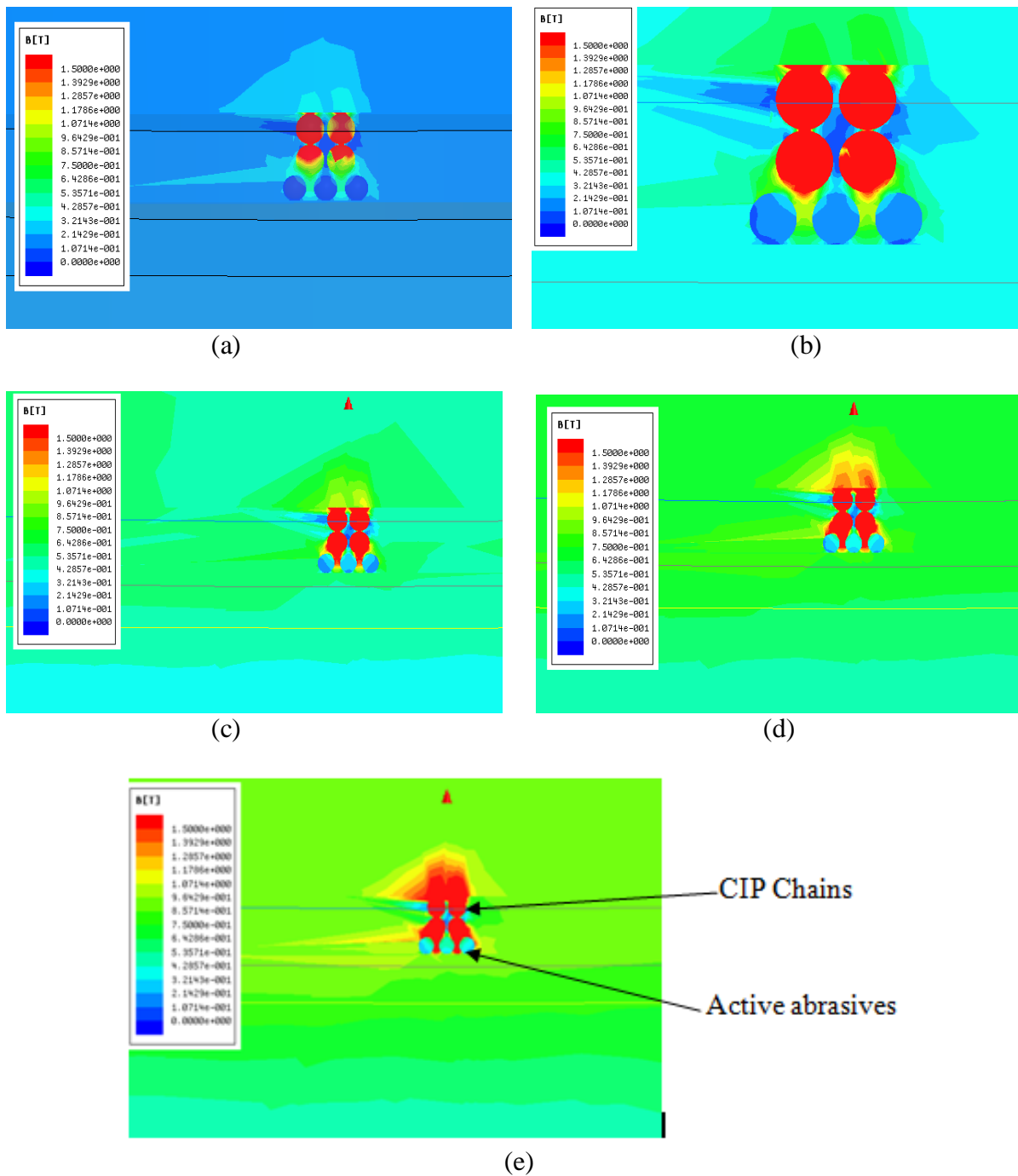


Figure 3.43 : FE simulation of the BEMRF with solid core tool of 50 mm coil distance and 0.66 mm with Current (a) 1 amp (b) 2 amp (c) 3 amp (d) 4 amp (e) 5 amp

Table 3.19 Result analysis of forces at different magnetizing current with 0.66 mm gap and 50 mm coil distance from the tool tip surface in solid core

S.No	Abrasive	1 amp	2 amp	3 amp	4 amp	5 amp
1	Average force (N)	2.61973E-05	0.0001048	0.00023578	0.00041916	0.00065493

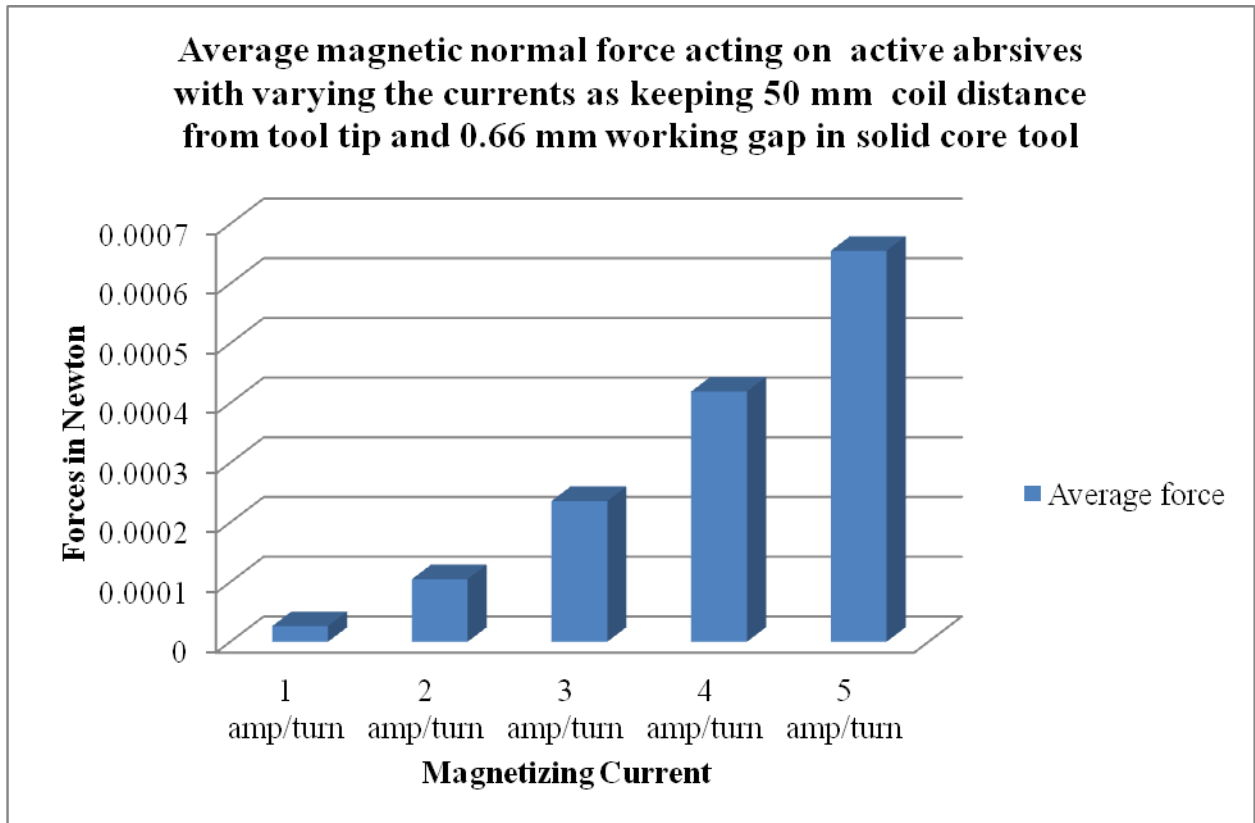


Figure 3.44 : Result analysis of force v/s current at 0.66 mm gap and 50 mm coil distance in solid core

Figure 3.44 shows the variation of magnetically induced normal force on the active abrasive particles with magnetizing current (1A to 5A) while working gap was kept as 0.66 mm and electromagnetic coil distance from the tool tip surface as 50 mm with solid core tool. The same result has been reported in table 3.19.

### 3.6.5 Electromagnet coil distance 50 mm and gap 1.5 mm while varying the magnetizing current from 1 amp to 5 amp

Tool modeled and simulated by taking coil distance from tool tip surface = 50 mm, diameter of rotating core = 25 mm, length of core = 245 mm, type of core = solid, gap = 1.5 mm,

number of turns of coil = 2000 turns, diameter of abrasive = 0.19 mm, diameter of CIP = 0.23 mm and number of abrasives for two CIP chain = 3. Current density is varied from 1 amp per turn to 5 amp per turn to analysis the variation in effect of force due to variation in current.

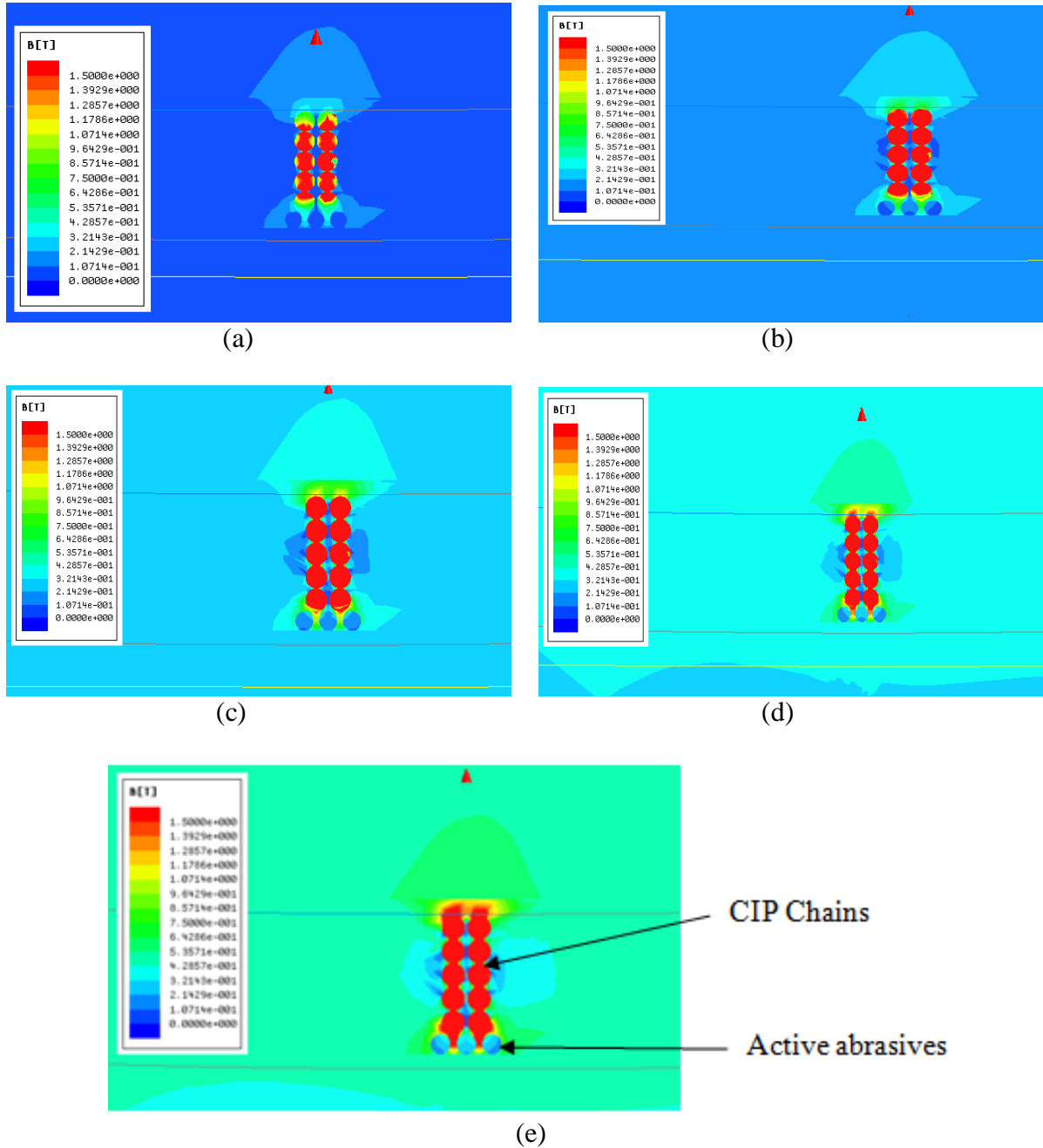


Figure 3.45 : FE simulation of the BEMRF with solid core tool of 50 mm coil distance and 1.5 mm with Current (a) 1 amp (b) 2 amp (c) 3 amp (d) 4 amp (e) 5 amp

Table 3.20 Result analysis of forces at different magnetizing current with 1.5 mm gap and 50 mm coil distance from the tool tip surface in solid core

S.No	Abrasive	1 amp	2 amp	3 amp	4 amp	5 amp
1	Average force (N)	1.07836E-05	4.313E-05	0.000097053	0.000172537	0.00026992

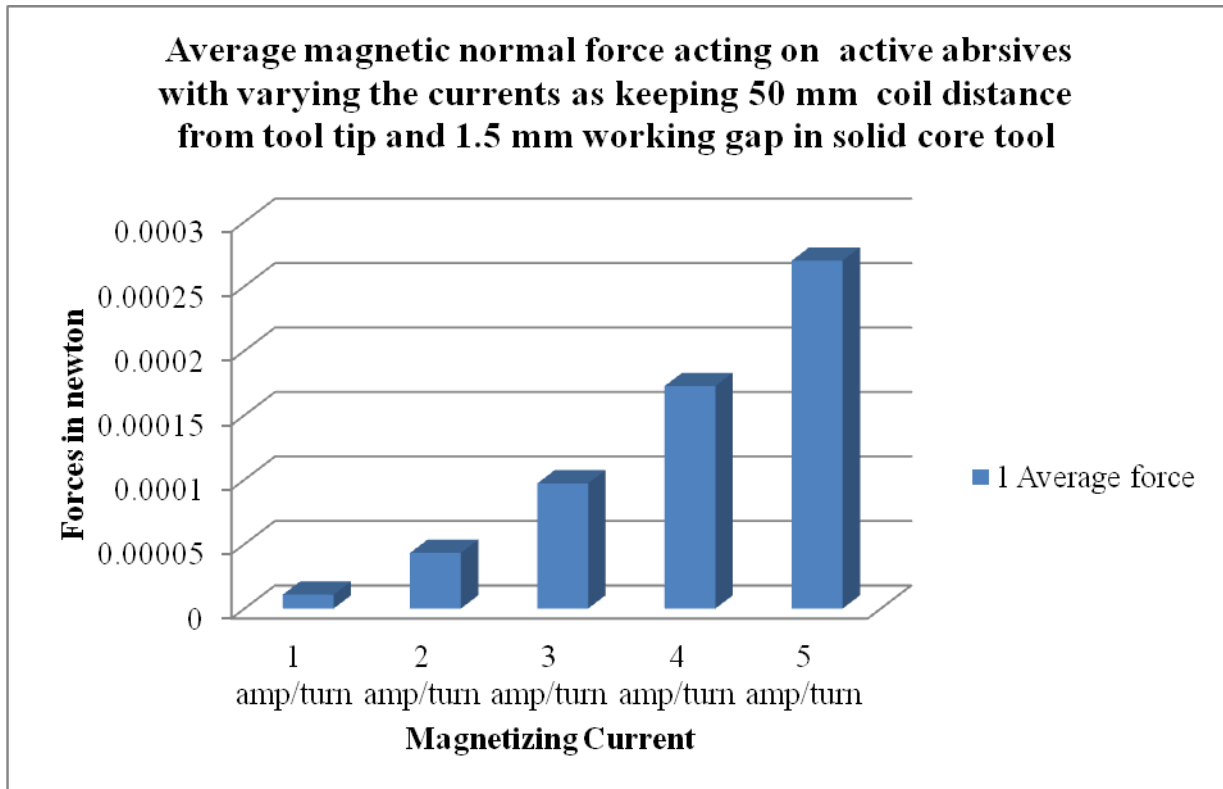


Figure 3.46 : Result analysis of force v/s current at 1.5 mm gap and 50 mm coil distance in solid core

Figure 3.46 shows the variation of magnetically induced normal force on the active abrasive particles with magnetizing current (1A to 5A) while working gap was kept as 1.5 mm and electromagnetic coil distance from the tool tip surface as 50 mm with solid core tool. The same result has been reported in table 3.20.

### 3.6.6 Electromagnet coil distance 50 mm and gap 2.34 mm while varying the magnetizing current from 1 amp to 5 amp

Tool modeled and simulated by taking coil distance from tool tip surface = 50 mm, diameter of rotating core = 25 mm, length of core = 245 mm, type of core = solid, gap = 2.34 mm,

number of turns of coil = 2000 turns, diameter of abrasive = 0.19 mm, diameter of CIP = 0.23 mm and number of abrasives for two CIP chain = 3. Current density is varied from 1 amp per turn to 5 amp per turn to analysis the variation in effect of force due to variation in current.

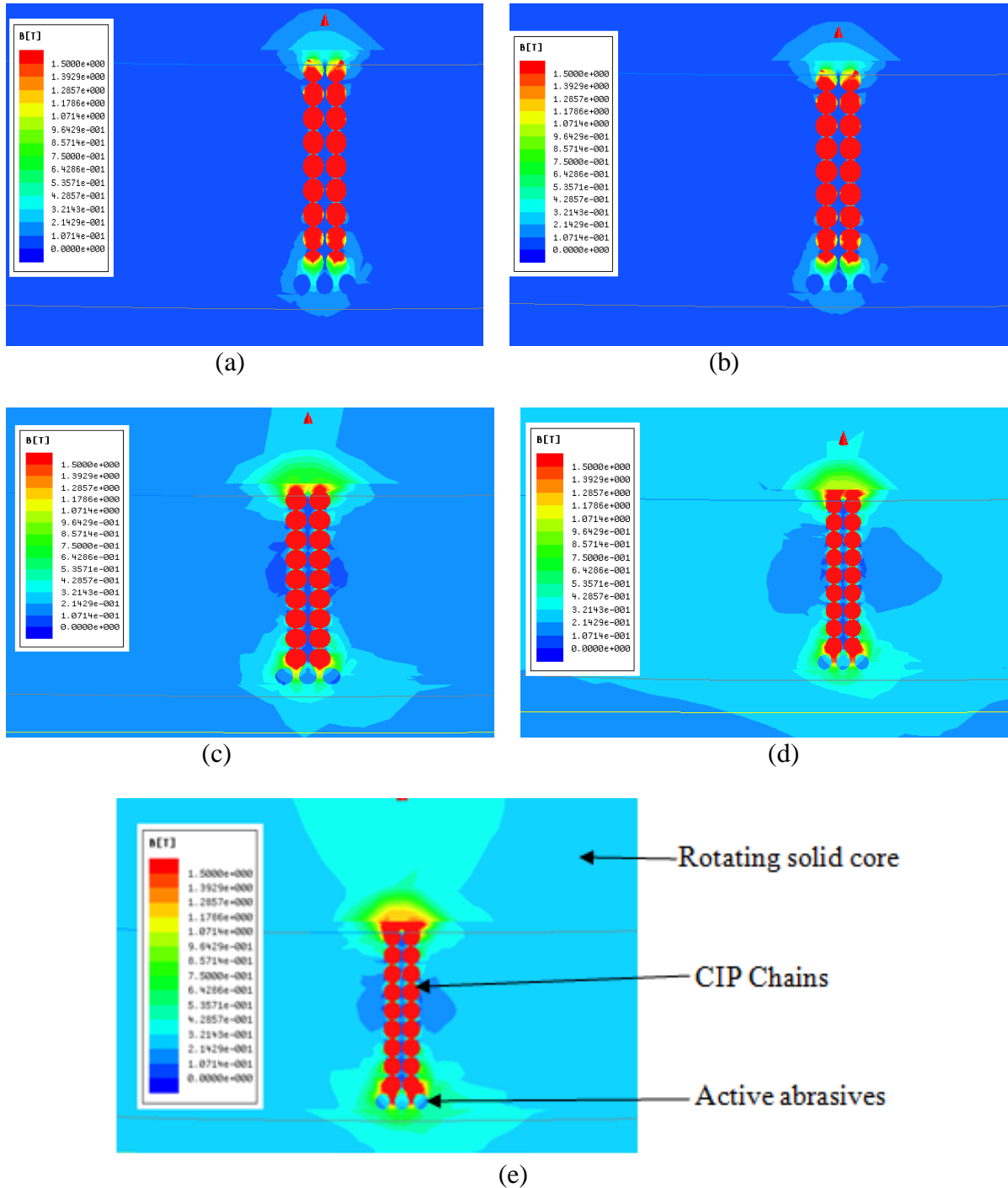


Figure 3.47 : FE simulation of the BEMRF with solid core tool of 50 mm coil distance and 2.34 mm with Current density (a) 1 amp (b) 2 amp (c) 3 amp (d) 4 amp (e) 5 amp

Table 3.21 Result analysis of forces at different magnetizing current with 2.34 mm gap and 50 mm coil distance from the tool tip surface in solid core

Force	1 amp	2 amp	3 amp	4 amp	5 amp
Average Force (N)	9.20953E-06	3.68383E-05	8.28877E-05	0.000147353	0.000230243

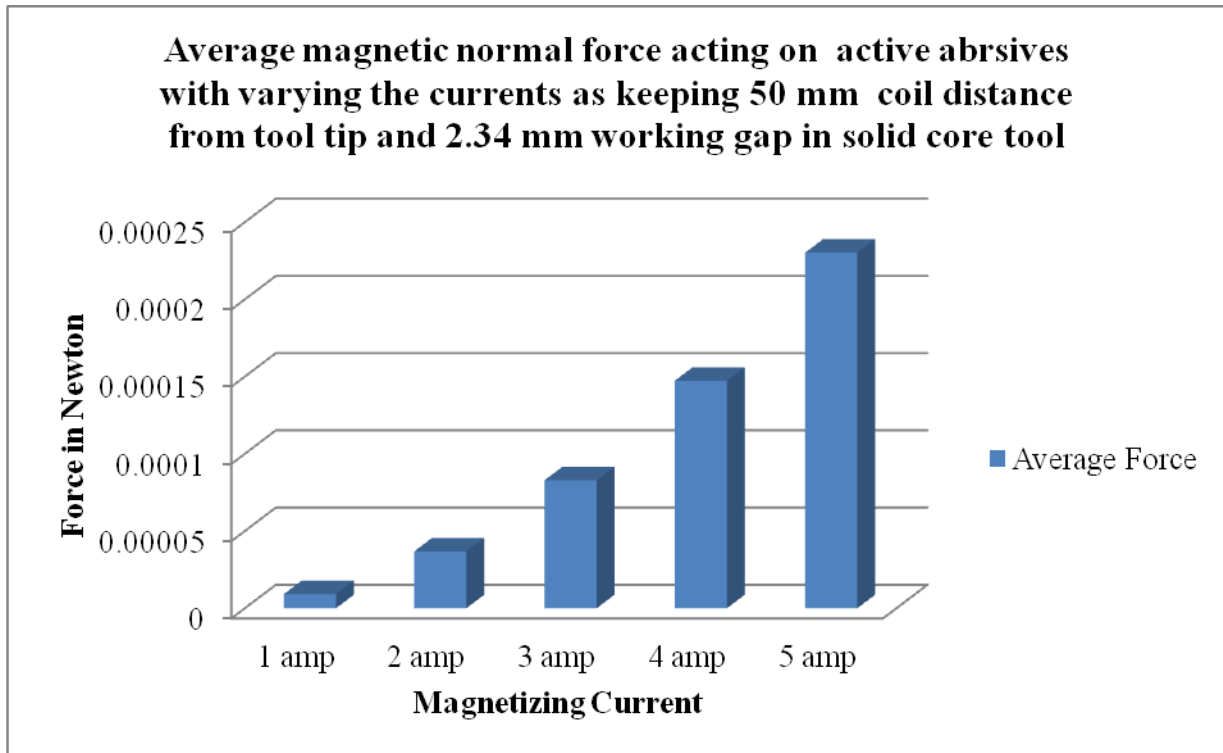


Figure 3.48 : Result analysis of force v/s current at 2.34 mm gap and 50 mm coil distance in solid core

Figure 3.48 shows the variation of magnetically induced normal force on the active abrasive particles with magnetizing current (1A to 5A) while working gap was kept as 2.34 mm and electromagnetic coil distance from the tool tip surface as 50 mm with solid core tool. The same result has been reported in table 3.21.

### 3.7 Results and discussion

Based on results of FE analysis, the results in terms of effect of working gap variation, effect of magnetizing current variation, effect of coil position variation and effect of using solid core tool instead of hollow core tool have been observed and discussed as following.

### 3.7.1 Effect of working gap variation

Table 3.22 Comparison of electromagnetic forces by variation of working gap at constant magnetizing current and coil position with hollow core BEMRF tool

Gap	1 amp	2 amp	3 amp	4 amp	5 amp
0.66 mm	1.22941E-05	0.000049177	0.000110647	0.000196707	0.000307353
1.5 mm	1.13745E-05	0.000045498	0.000102373	0.000181993	0.000284363
2.34 mm	1.08675E-05	4.34703E-05	9.78067E-05	0.00017388	0.00027169

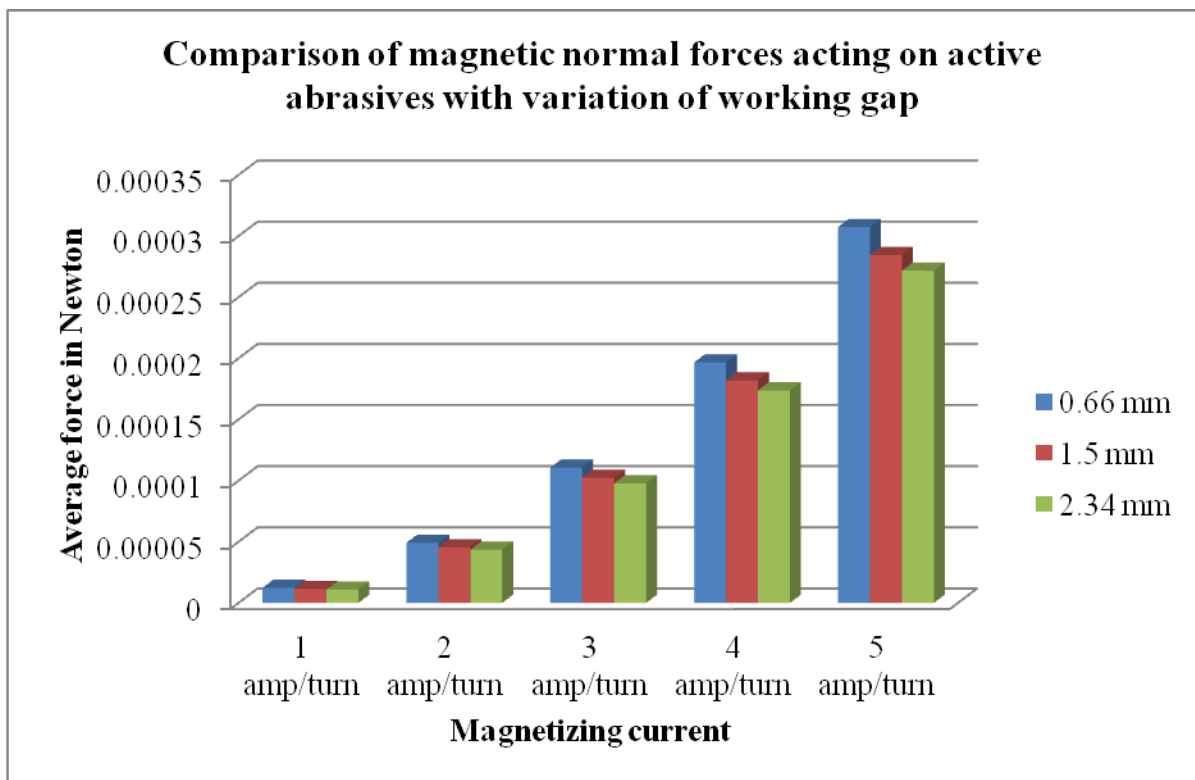


Figure 3.49 : Result analysis of force by variation in working gap at constant current and coil position

As shown in figure 3.49, it has been observed that there is decrease in magnitude of magnetically induced normal forces on active abrasive particles with increase in working gap. Material removal rate depends on magnitude of magnetically induce normal forces. Due to decrease in magnitude of magnetically induced force, material removal rate also decreases. Hence finishing rate also decreases. The results of finite element analysis of average magnetic normal force by varying working gap have been illustrated in table 3.22.

### 3.7.2 Effect of current variation

Table 3.23 Comparison of electromagnetic forces by variation of magnetizing current at constant working gap and coil position

Force	1 amp	2 amp	3 amp	4 amp	5 amp
Average Force (N)	1.13745E-05	0.000045498	0.000102373	0.000181993	0.000284363

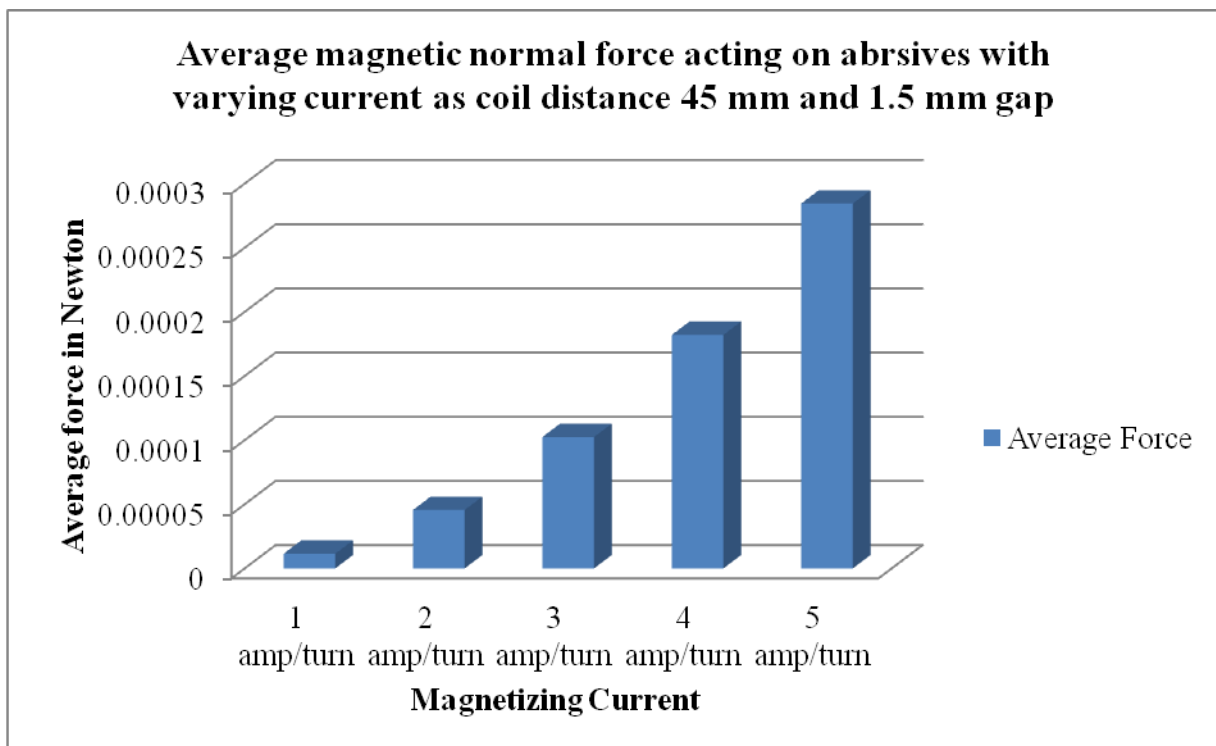


Figure 3.50 : Result analysis of force by variation in current at constant working gap and coil position

As shown in figure 3.50, it has been observed that the average magnetically induced normal force on abrasive increases with increase in magnetizing current. The results have been observed from 1A per turn to 5A per turn with 2000 number of coil turns. On 5 amp per turn, best results have been achieved. The results of finite element analysis of average magnetic normal force by varying magnetizing current have been illustrated in table 3.23.

### 3.7.3 Effect of coil position variation

The FE analysis has been performed by variation of coil position from 45 mm to 65 mm from tool tip for three work gaps. It has been observed that the value of magnetic normal force is decreased with increase in gap between tool tip and position of coil in all three cases.

### 3.7.3.1 Effect by variation of coil gap for 0.66 mm work gap

Table 3.24 Effect on electromagnetic forces by variation of coil distance at 0.66 mm working gap

Coil Distance	1 amp	2 amp	3 amp	4 amp	5 amp	Avg. Force
45 mm from tip	1.22941E-05	0.000049177	0.000110647	0.000196707	0.000307353	0.00013524
50 mm from tip	9.30663E-06	0.000037227	0.000083762	0.00014891	0.000232667	0.00010237
55 mm from tip	4.0579E-06	1.92317E-05	0.000052521	8.89263E-05	0.000126448	5.8237E-05
60 mm from tip	3.57893E-06	1.43157E-05	3.22103E-05	0.000057263	8.94733E-05	3.9368E-05
65 mm from tip	2.45217E-06	9.8088E-06	2.20697E-05	3.92347E-05	6.13047E-05	2.6974E-05
<b>% variation for 20 mm coil movement</b>						<b>-80.05</b>

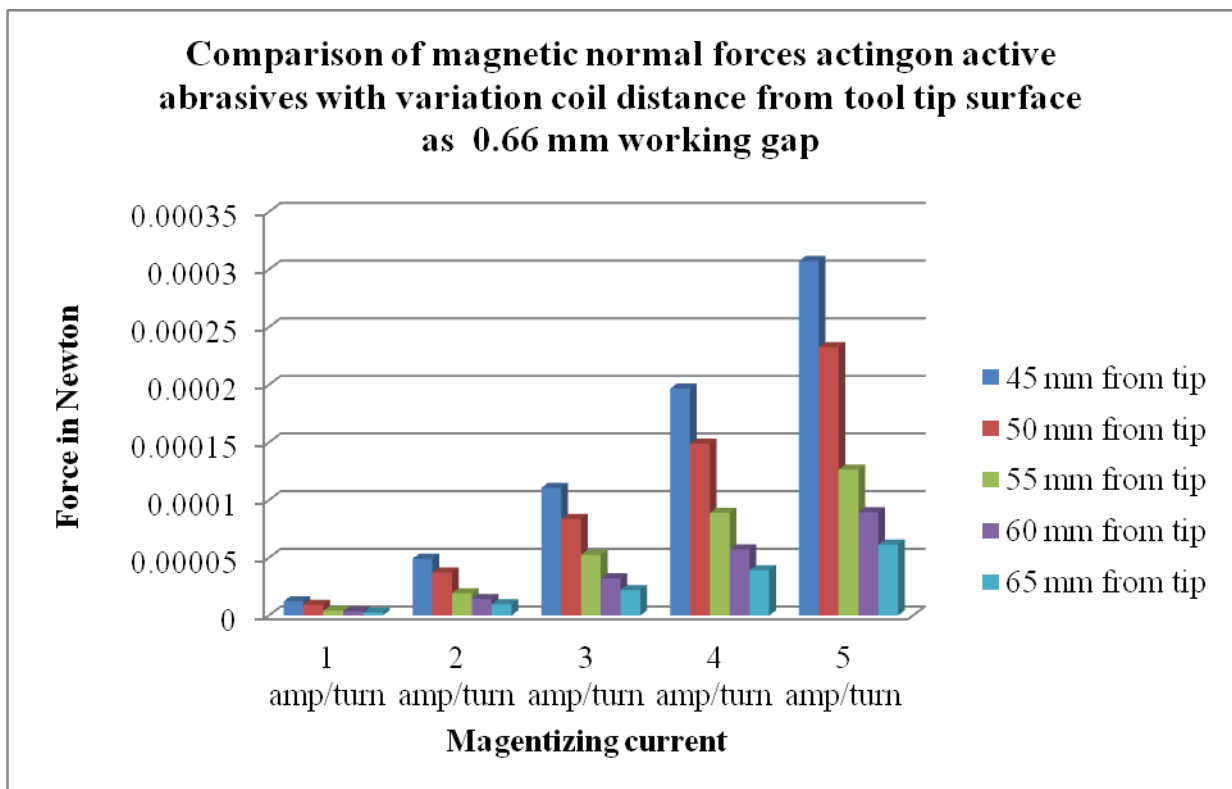


Figure 3.51 : Result analysis of force by variation in coil position at 0.66 mm working gap

As show in figure 3.51, it has been observed that the coil position plays an important role in finishing of work piece. It has been observed that the results of average electromagnetically induced normal force with 0.66 mm working gap varies 80.05 percentages by the variation of

20 mm coil position. The results of finite element analysis of average magnetic normal force by varying coil position with 0.66 mm working gap have been illustrated in table 3.24.

### 3.7.3.2 Effect by variation of coil gap for 1.5 mm work gap

Table 3.25 Effect on electromagnetic forces by variation of coil distance at 1.5 mm working gap

Coil Distance	1 amp	2 amp	3 amp	4 amp	5 amp	Avg. Force
45 mm from tip	1.13745E-05	0.000045498	0.000102373	0.000181993	0.000284363	0.00012512
50 mm from tip	5.74943E-06	2.29973E-05	5.17453E-05	9.19927E-05	0.000143739	6.3245E-05
55 mm from tip	5.28607E-06	2.05443E-05	4.89747E-05	8.41773E-05	0.000127152	5.7227E-05
60 mm from tip	0.000004742	1.89681E-05	0.000042678	7.58723E-05	0.000118551	5.2162E-05
65 mm from tip	2.9273E-06	1.17093E-05	2.63457E-05	0.000046837	0.000073184	3.2201E-05
<b>% variation for 20 mm coil movement</b>						<b>-74.26</b>

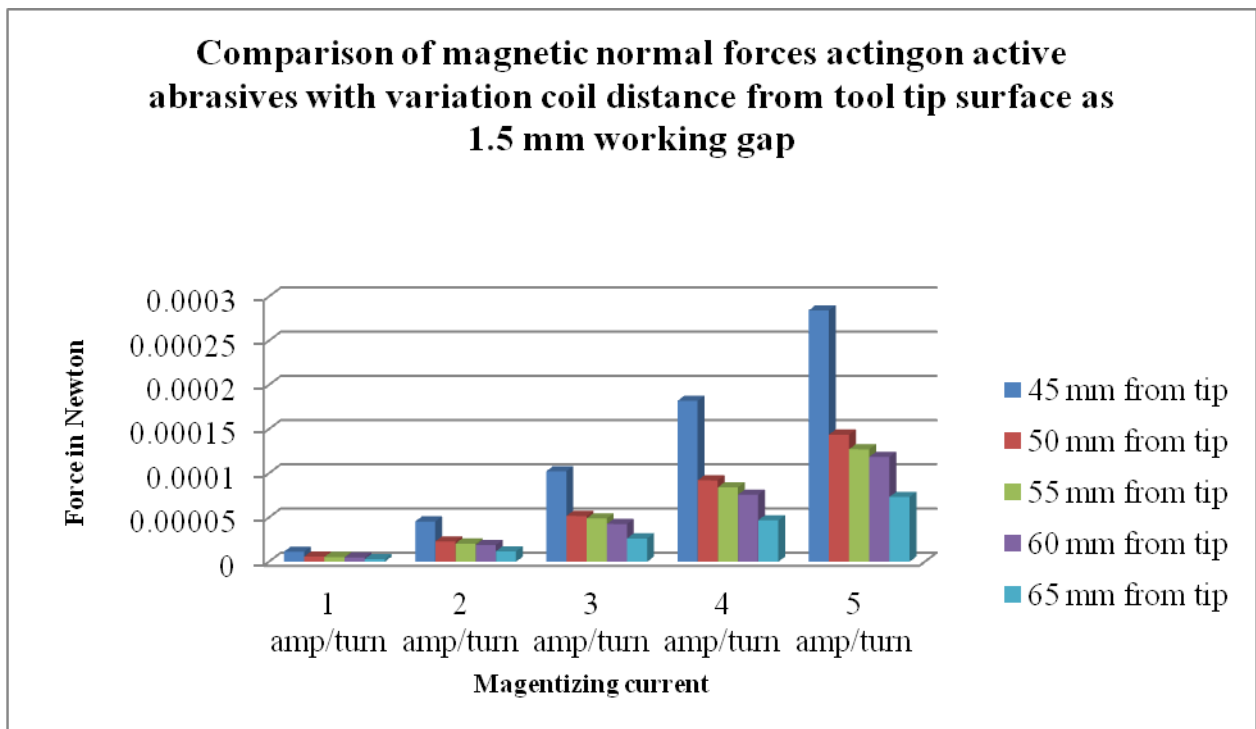


Figure 3.52 : Result analysis of force by variation in coil position at 1.5 mm working gap

As shown in figure 3.52, it has been observed that the results of average electromagnetically induced normal force with 1.5 mm working gap varies 74.26 percentages by the variation of 20 mm coil position. The results of finite element analysis of average magnetic normal force by varying coil position with 1.5 mm working gap have been illustrated in table 3.25.

### 3.7.3.3 Effect by variation of coil gap for 2.34 mm work gap

Table 3.26 Effect on electromagnetic forces by variation of coil distance at 2.34 mm working gap

Coil Distance	1 amp	2 amp	3 amp	4 amp	5 amp	Avg. Force
45 mm from tip	1.08675E-05	4.34703E-05	9.78067E-05	0.00017388	0.00027169	0.00011954
50 mm from tip	1.05228E-05	4.00917E-05	0.000090705	0.000150367	0.000243073	0.00010695
55 mm from tip	4.85433E-06	1.94173E-05	4.36893E-05	7.76687E-05	0.000121358	5.3398E-05
60 mm from tip	3.52157E-06	1.40862E-05	3.16937E-05	0.000056345	8.80397E-05	3.8737E-05
65 mm from tip	2.51724E-06	1.00691E-05	2.26552E-05	0.000040276	6.29297E-05	2.7689E-05
<b>% variation for 20 mm coil movement</b>						<b>-76.84</b>

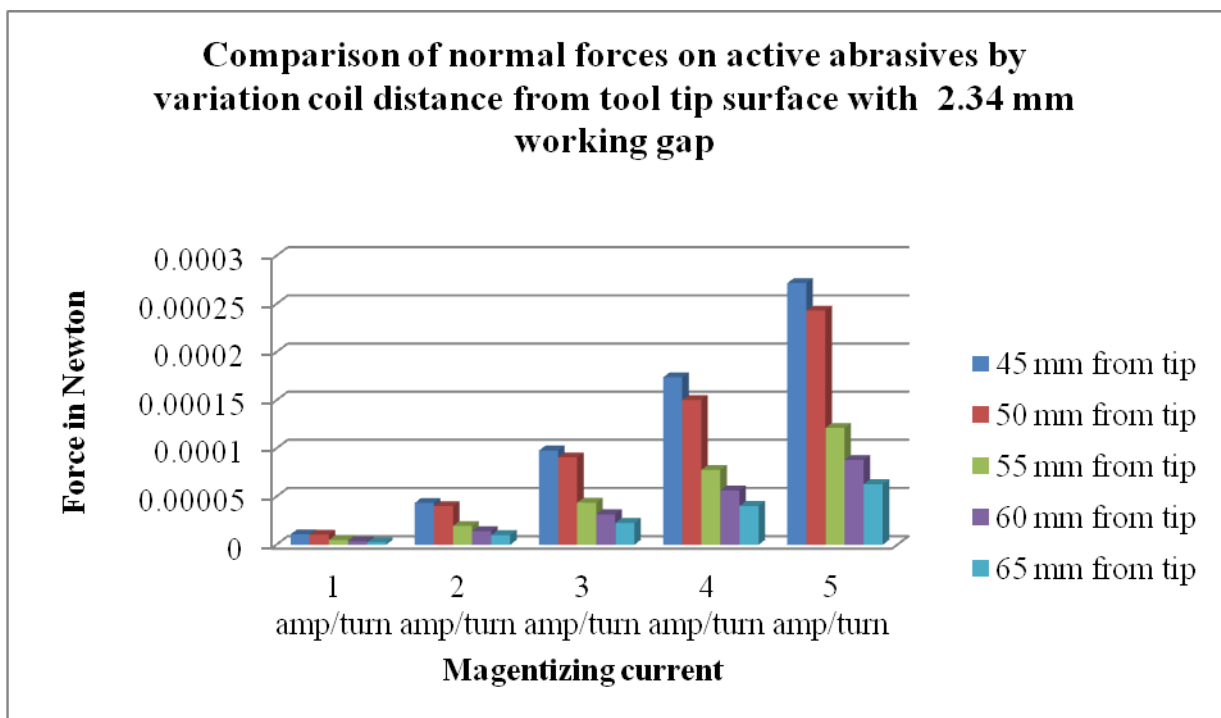


Figure 3.53 : Result analysis of force by variation in coil position at 2.34 mm working gap

As shown in figure 3.52, it has been observed that the results of average electromagnetically induced normal force with 2.34 mm working gap varies 76.84 percentages by the variation of 20 mm coil position. The results of finite element analysis of average magnetic normal force by varying coil position with 2.34 mm working gap have been illustrated in table 3.26.

### 3.7.4 Effect of using solid core tool in the replacement of hollow core tool

Table 3.27 Effect on electromagnetic forces by using solid core tool of coil distance at 0.66 mm working gap

S.No	Abrasive	1 amp	2 amp	3 amp	4 amp	5 amp	Avg. Force
1	With hole core	1.229E-05	4.9177E-05	0.000110647	0.00019671	0.000307353	0.0001352
2	Solid core	2.656E-05	0.00010624	0.000239043	0.00042496	0.00066401	0.0002922
<b>% variation by using solid core tool</b>							<b>53.71</b>

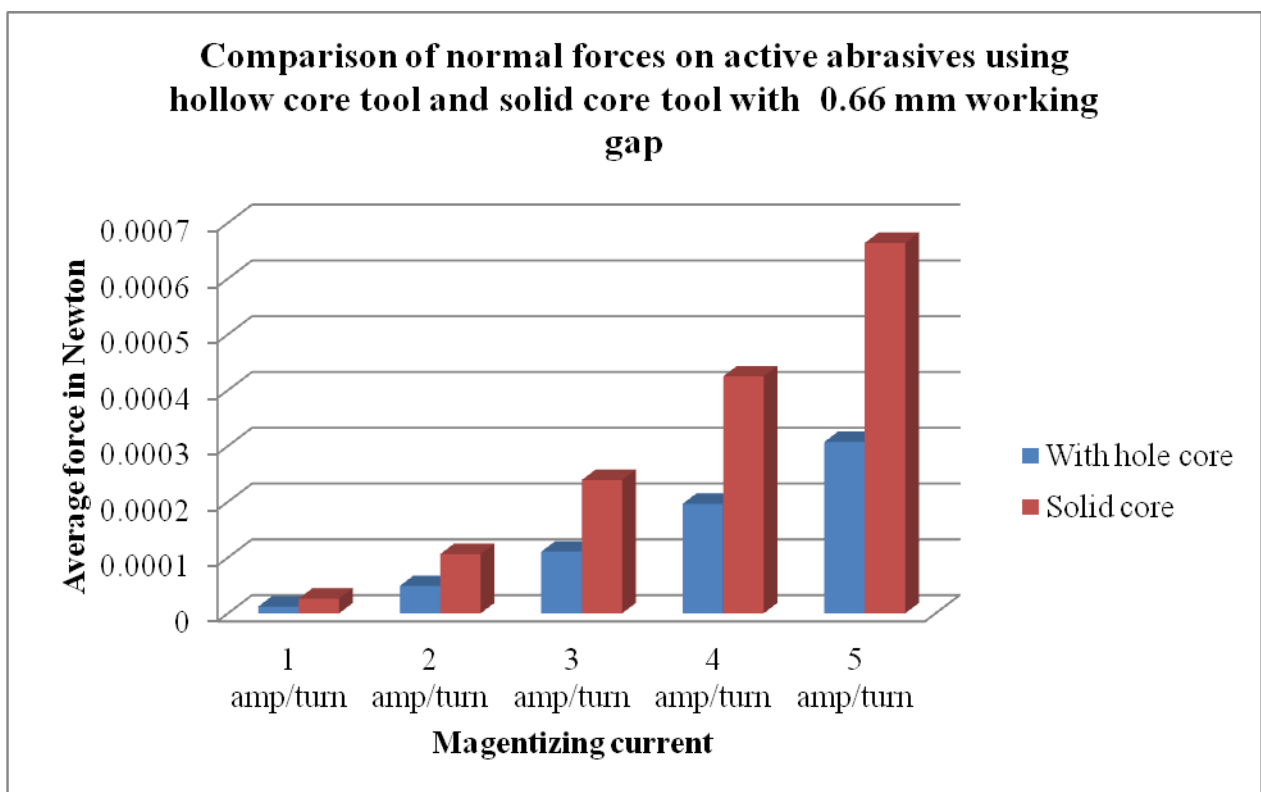


Figure 3.54 : Result analysis of force by use of solid core tool at 0.66 mm working gap

As shown in figure 3.54, it has been seen that the magnitude of average electromagnetically induced normal force is 53.71 % more in case of solid core tool. This is due to more contact area of solid tool tip and relative permeability of iron core is 600, but relative permeability of fluid is 5.

### 3.8 Validation of finite element simulated magnetic normal force with already calculated and experimentally reported magnetic normal force (Singh et. al, 2013)

The finite element magnetostatic simulation has been done at three different working gap and 4A current for hollow core tool and the results have been validated with already calculated and experimental results (Singh et. al, 2013). The comparison of present finite element magnetostatic simulated results with already calculated results for induced magnetic normal forces on the active abrasive as given in Table 3.28. Also, the comparison of present finite element magnetostatic simulated results with already experimentally reported results for induced magnetic normal forces on the active abrasive as given in Table 3.29. It has been seen that the present finite element magnetostatic simulation results of magnetic normal average force acting on active abrasives are very closer to already reported results of calculated and experimental for magnetic normal average force acting on active abrasives in ball end type of magnetorheological finishing process.

Table 3.28 Validation of magnetically induced magnetic normal forces acting on the active abrasives with already calculated magnetic normal forces

S.No.	Working gap (mm)	Current(A)	Calculated normal force $F_n/Sic$ ( $\times 10^{-4}$ N) (Singh <i>et. al</i> , 2013)	Simulation result of normal force $F_n/Sic$ ( $\times 10^{-4}$ N)	% error in $F_n$
1	0.66	4	1.927	1.96707	2.079
2	1.50	4	1.863	1.81933	-2.0344
3	2.34	4	1.803	1.7388	-3.560

Table 3.29 Validation of magnetically induced magnetic normal forces acting on the active abrasives with already reported experimentally magnetic normal forces

S.No.	Working gap (mm)	Current(A)	Experimental normal force $F_n/Sic$ ( $\times 10^{-4}$ N) (Singh <i>et. al</i> , 2013)	Simulation result of normal force $F_n/Sic$ ( $\times 10^{-4}$ N)	% error in $F_n$
1	0.66	4	1.967	1.96707	0.007
2	1.50	4	1.747	1.81933	1.715
3	2.34	4	1.6214	1.7388	1.593

# CHAPTER - 4

## Conclusions and future scope

---

### 4.1 Conclusions

The present work is done to analyze the magnetically induced normal force acting on the workpiece surfaces through active abrasives particles and CIPs chains during the finishing operation in ball end type magnetorheological process. The finite element simulated results for magnetically induced force on the active abrasives has been compared with already calculated and experimental magnetic normal forces (Singh *et. al*, 2013).

From the finite element analysis of magnetically induced normal force acting on the active abrasives in ball end type magnetorheological finishing process having tool with hollow and solid cores, the following points have been concluded:

- The magnetically induced normal force acting on active abrasives increases as current to the electromagnet per turn increased.
- Position of coil on core plays a significant role in ball end type magnetorheological tool. The magnetically induced normal force on active abrasive increases as the distance between the tool tip surface and position of coil decreased. It has been seen from the analysis, with variation of 20 mm coil distance from tool tip surface, the variation in average magnetic normal force was found as 77.05 %. The maximum magnetic normal force acting on the active abrasives has been found when electromagnet coil distance from tool tip surface was kept as 45 mm.
- The magnetically induced normal force acting on the active abrasives decreases as working gap increased.
- In ball end type magnetorheological finishing tool with solid core, the magnitude of magnetically induced normal force on the active abrasive particles was found 53.71 % more as compared to hollow core tool for the same parameters such as working gap, magnetizing current and distance of coil from tool tip surface. Therefore in case of tool with solid core, the better bonding between carbonyl iron particles along with active abrasives can be achieved even with low magnetizing current during the finishing of workpiece surfaces.
- The comparison of present finite element magnetostatic simulated results of magnetic average normal force on active abrasives with already reported results was found

within 5 % in ball end type of magnetorheological finishing process having hollow core tool.

## **4.2 Future Scope**

- The validation of finite element simulated results can be done with experimental results in case of solid core tool in ball end type magnetorheological finishing process.
- More realistic mathematical model can be done of solid core tool in ball end type magnetorheological finishing process.
- The mathematical modeling can be done for surface roughness along with the magnetically induced normal force acting on the workpiece surface through CIP chains and active abrasive particles in ball end type magnetorheological finishing process having hollow and solid tool cores.

## REFERENCES

- Gheisari, R.; Ghasemi, A.A.; Jafarkarimi, M.; Mohtaram, S. (2014) Experimental studies on the ultraprecision finishing of cylindrical surfaces using magnetorheological finishing process. *Production & Manufacturing Research*, 2:1: 550-557.
- Harris, D.C. (2011) History of Magnetorheological Finishing. *Proceedings of SPIE*, 2: 20-25.
- Hong, K.P.; Cho, Y.K.; Shin, B.C.; Cho, M.W.; Choi, S.B.; Cho, W.S.; Jae, J.J. (2012) MR fluid polishing of Alumina reinforced zirconia ceramics using diamond abrasive for dental application. *Materials and Manufacturing Processes*, 27: 1135-1138.
- Jain, V.K. (2008) Abrasive based nano finishing techniques an overview. *An International Journal of Machining Science and Technology*, 257-294
- Jain, V.K. (2009) Magnetic field assisted abrasive based micro-/nano-finishing. *Journal of Materials Processing Technology* 209: 6022-6038.
- Jha, S.; Jain, V.K. (2004) Design and development of the magnetorheological abrasive flow finishing (MRAFF) process. *International Journal of Machine Tools and Manufacturing*, 44: 1019-1029.
- Jha, S.; Jain, V.K. (2006) Modeling and simulation of surface roughness in magnetorheological abrasive flow finishing process. *Wear*, 261: 856-866.
- Jolly, M.R.; Bender, J.W.; Carlson, J.D. Properties and Applications of Commercial magnetorheological Fluids.
- Judal, K.B.; Yadava, V.; Pathak, D. (2013) Experimental investigation of vibration assisted cylindrical magnet abrasive finishing of Aluminium workpiece. *Materials and Manufacturing Processes*, 28: 1196-1202.
- Lepadatescu, B. (1998) Super finishing with abrasive stones. Doctoral thesis, Braso.
- Rhodes, L.J. (1988) Abrasive flow machining. *Manufacturing Engineering*, 75-78.
- Sadiq, A.; Shunmugam, M.S. (2009) Investigation into magnetorheological abrasive honing. *International Journal of Machine Tools and Manufacture*, 49: 554-560.
- Sadiq, A.; Shunmugam, M.S. (2009) Magnetic field analysis and roughness prediction in magnetorheological abrasive honing. *Machining Science and Technology*, 13: 246-268.
- Schey, J.A. (1987) Introduction to manufacturing process. Second edition, Mc Graw Hill Book Company

Shaw, M.C. (1996) Principles of Abrasive Processing. Clarendon press, Oxford: United Kingdom.

Sidpara, A.; Jain, V.K. (2011) Experimental investigations into forces during magnetorheological fluid based finishing process. *International Journal of Machine Tools and Manufacture*, 51 : 358-362.

Sidpara, A.; Jain, V.K. (2013) Analysis of forces on the free form surface in magnetorheological fluid based finishing process. *International Journal of Machine Tools and Manufacture*, 69: 1-10.

Singh, A.K.; Jha, S.; Pandey, P.M. (2012) Nanofinishing of a typical 3D Ferromagnetic workpiece using Ball End Magnetorheological Finishing process. *International Journal of Machine Tools and Manufacture*, 63: 21-31.

Singh, A.K.; Jha, S.; Pandey, P.M. (2013) Mechanism of material removal in ball end magnetorheological finishing process. *Wear*, 302: 1180-1191.

## **Web References**

[http://d2n4wb9orp1vta.cloudfront.net/resources/images/cdn/cms/DiamondLapping\\_a.jpg](http://d2n4wb9orp1vta.cloudfront.net/resources/images/cdn/cms/DiamondLapping_a.jpg)

[http://www.ohiotoolworks.com/upload/images/products/Horizontal\\_Machines/OTW-3000\\_Bore\\_\\_Tool\\_Grey.jpg](http://www.ohiotoolworks.com/upload/images/products/Horizontal_Machines/OTW-3000_Bore__Tool_Grey.jpg)

<http://canadianhomeworkshop.com/files/2011/10/buffingwheeldiagram.jpg>

<http://www.opticam.rochester.edu>

<http://www.wseas.us/e-library/conferences/2009/cambridge/SEPADS/SEPADS09.pdf>

